Department of Physics and Astronomy

University of Heidelberg

Master thesis

in Physics

submitted by

Anton Ivanov

born in Svishtov

2012

Bosonic transport across dot structures

This Master thesis has been carried out by Anton Ivanov

at the

Ruperto-Carola-University of Heidelberg, Germany

under the supervision of

PD Dr. Sandro Wimberger

Bosonic transport across dot structures:

In this work we study the quantum transport phenomena of bosonic particles through a chain of quantum dots with on-site particle-particle interaction. The system is driven out of equilibrium via two bosonic reservoirs that stay in equilibrium and have a continuous and nonzero density of states over a finite frequency interval. We study the behaviour of the system via two approaches.
In the first case a scalar action is constructed from which the needed nonequilibrium Green's functions can be extracted. Many-body effects are taken into account via a simple approximation of the self-energy. In the weakly interacting case, a current conserving and causality conserving approximations are derived and applied to the system. As an alternative, a flow equation of the effective action is solved in order to obtain the same observables of interest.
The second approach describes the behaviour of the system via a Master equation in Lindblad form. By using the Wigner method the problem is mapped to a set of stochastic differential equations and solved numerically. This equation can be also derived from an action, which allows us to compare directly both approaches. In addition to the numerical calculations, this connection is described in detail.

Bosonic transport across dot structures:

In dieser Arbeit wird der Quantentransport bosonischer Teilchen durch eine Kette von Quantenpunkten mit Teilchen-Teilchen Wechselwirkung untersucht. Das System wird durch zwei bosonische Reservoirs aus dem thermischen Gleichgewicht gebracht. Die Reservoirs selbst befinden sich im thermodynamischen Gleichgewicht und haben eine kontinuierliche und über einen Frequenzintervall nicht verschwindende Zustandsdichte. Das Verhalten des Systems wird durch zwei unterschiedliche Methoden beschrieben.
Im ersten Fall wird das Problem duch eine skalare Wirkung beschrieben, von der die notwendigen Nichtgleichgewichts-Green-Funktionen berechnet werden können. Die Vielteilcheneffekte werden durch eine Approximation der Selbstenergie berücksichticht. Im Fall schwacher Wechselwirkung werden zwei Näherungen hergeleitet, die den stationären Strom durch das System und die Kausalitätsbedingung erhalten. Dieselbe Observable wird zudem durch die Lösung einer simplen Flussgleichung der effektiven Wirkung hergeleitet.
Als zweite Möglichkeit kann das Verhalten des Systems durch eine Mastergleichung im Lindbladform beschrieben werden. Mit der Wigner-Methode wird das Problem auf ein System von stochastischen Differentialgleichungen abgebildet, die numerisch gelöst werden können. Das Gleichungssytem kann auch von einer skalaren Wirkung hergeleitet werden, was im Detail bescrieben wird. Dies erlaubt uns beide Methoden zu vergleichen.

Contents

Part I
Introduction

The advance in technology in the last decades has allowed the creation of smaller and smaller devices reaching the point where the realisation of logic structures on the atomic level is possible. There are few important reasons making these systems interesting. Because of their low dimensionality the dynamics of the sytem can be dominated by quantum effects, opening a large playground for experimental testing of various problems. On the other hand one can make use of the atomic structure of the particles loaded in such devices and create logic structures analogous to the known semiconductor devices [1] or create qubits.

In order to reveal the quantum properties of a system it has to operate at very low temperatures and in perfect isolation from the enviroment. Nowdays, the progress in cooling atoms allows to reach temperatures below $10^{-7}K$. If one compares the corresponding thermal energy of an alkali atom like sodium with its hyperfine splitting in the ground state one will see that the first one is by many orders of magnitude smaller than the other. The revealed atomic structure in alkali atoms, especially the interaction of the atomic dipole moment or the electonic spin with an electric/magnetic field is exploited in the creation of various magneto-optical traps and optical lattices. The main breakthrough in manipulating atoms is the creation of a Bose-Einstein condensate [2], which together with the use of optical lattices allowed the study of a large set of problems. Part of them are the one and two dimensional Anderson localisation [3], [4], tunneling and spectrum of Wannier-Stark ladders [5], [6], [7], [8], dynamics of superfluid-insulator transitions in composite bosonic gases loaded in optical lattices [9] , [10] etc.

A promising way of creating and manipulating systems of ultracold atoms is provided by microchip based magnetooptical traps. Due to the possibility of imprinting various current networks on a chip and changing the current through them, one can create, split or transport a condensate over a finite distance [11]. Creation of a quantum dot coupled to a Bose-Einstein condensate by the use of laser beams separated by a small distance is also investigated in [12], [13]. A new level of control of the particle number at a single site of an optical lattice is demonstrated in [14], [15], where due to an electronic or laser beam the position and number of the removed particles from the system can be exactly manipulated.

The advances in this field boosted the investigation into transport of ultracold atoms in systems with reduced dimensionality. In [16] the transport of fermionic and bosonic ultracold atoms in quantum wires is studied theoretically. A possible creation of such a system is given in [17]. Quantum pumping with ultracold atoms on an atomchip has also been studied in [18]. Decreasing the dimensionality of the tunneling region from one to zero, a new field is investigated - the atomtronics. The creation of bosonic analogues to the mesoscopic systems used in electronic devices like a diode or field-effect transistor is suggested in [19]. Additional studies of atomic transport in different setups can be found also in [20], [21].

In this work we will focus on a bosonic transport through a chain of quantum dots coupled to two bosonic reservoirs that keep the system far from equilibrium. In the first case the reservoir will be above the critical Bose-Einstein condensation temperature. The confinement of many thermal particles in a trap is indeed possible by the use of buffer gas cooling techniques [22], where lifetimes of more than $100s$ are achievable for particles with high magnetic moments.

The second topic is devoted to chain of quantum dots coupled to zero temperature Markovian reservoirs. Although such systems do not exist in nature they represent a good approximation of reservoirs with constant density of states over a large frequency range. Such reservoirs could be created by filling a tilted optical lattice with ultracold atoms such that every lattice site is equally occupied [19]. We also introduce an on-site particle-particle interaction in the system. The value of this parameter can in principle be tuned experimentally by making use of Feshbach resonances.

Overview

The treatment of both systems is separated into two different chapters. Each of them is supple-

mented with a brief description of the needed theory. The results are presented and discussed. A final chapter summarises the results of this work and set a future outlook of the problem. All (less) important details of the calculations can be found in the appendix.

In **Part Two**, we look at two bosonic reservoirs in thermal equilibrium ($T > T_{crit}$) but with different chemical potentials. They force the system out of equilibrium in a way that a particle flow between both reservoirs is established. The problem is described with the use of Nonequilibrium Green's functions. The idea of this formalism is explained in detail in section 1. The Green's functions (GF's) of the different building blocks of the system are calculated in section 2. Constructing the GF of a small system coupled to an infinitely large enviroment, the concept of a self-energy is introduced. It is used later to introduce the interactions in the system.
In section 4, two approaches that handle interactions systematically are presented. In both of them a certain class of Feynman diagrams contributing to the GF is summed. This is the basis for a construction of a Schwinger-Dyson equation from which an approximation of the full GF can be obtained. In the first approach the current is conserved and in the second one - the causality condition. As an alternative, in the appendix, a flow equation of the effective action is solved in order to obtain the observables of interest. In section 5, a specific realisation of the system is chosen and the results from both approximations are presented and discussed.

Part Three is devoted to the case of zero temperature reservoirs. The dynamics are described by a master equation in Lindblad form. The Lindblad superoperator $\hat{\mathcal{L}}$ is responsible for the particle gain and loss, and drives the system out of equilibrium. The equation can be mapped to a stochastic differential equation that can be solved numerically. In section 1 important stochastic processes are briefly described and a numerical method for solving them is presented. The idea of mapping a Master equation in Lindblad form to a stochastic differential equation (Wigner mapping) is explained in section 2. An alternative method to solve the master equation in Lindblad form in the limit of low occupation numbers (the Quantum Jump method) is given in the appendix. The connection between the nonequilibrium GF method and the Langevin equation is made in section 3. The origin of the noise and the memory kernels in a stochastic differential equation and their dependence on the reservoir properties is shown explicitly. This allows us to apply techniques of the previous chapter to the current problem. A motivation for the use of the Master equation in Lindblad form is given in section 4. This will complete the understanding of the underlying physics behind the equation we solve. In addition, in the end of the section a comparison of the methods in the context of a simple problem is made. The system we are interested in is presented in section 5. The results are presented and discussed in section 6.

Part Four summarises all the results from the previous two chapters and points out new relevant questions that can be investigated in the future.

Part II
Nonequilibrium Green's function approach

In this section we study the behaviour of a quantum dot coupled to two bosonic reservoirs. In contrary to the fermionic counterpart of this problem (bosonic reservoirs are replaced by semi-infinite metallic electrodes), which is widely studied, the bosonic transport in a similar to our setup is studied only in [19]. The bosonic problem differs from the fermionic one in the following points:

- The Hilbert space of the quantum dot is infinitely large.
- The density of states of the bosonic reservoir is zero below some frequency.
- Below a critical temperature the reservoir contains an additional macroscopically occupied state, that has to be additionally taken into account in the description of the sytem.

Since the system we work with is not in equilibrium, the most natural way to describe and solve the problem is by the use of nonequilibrium Green's functions (GF's). The basic definition of a GF and its physical meaning is given in section 1. A detailed explanation can be found in [25] and [26]. The way how the problem is described by the use of these GF's is given in section 2. Section 4 presents a well-known approach to handle interactions in the system by adding an approximation of an interaction self-energy to the known noninteracting Green's function. An alternative approach to solve the problem by constructing a flow equation of the effective action is described in the appendix. In section 5 we choose a concrete realisation of the system - two bosonic reservoirs coupled to a qunatum dot, and present the results from the used approximations.
This section should give answer to the following problems:

- Description of a bosonic gas condensed in energy, that is coupled to the system.
- Influence of the particle-particle interaction at the quantum dot on the system behaviour.

1 Basic definitions

1.1 Time evolution and contour ordering operator

Consider a system described by the Hamiltonian $\hat{H} = \hat{H}_0 + \hat{H}^i$. $\hat{H}_0$ will always refer to the noninteracting part quadratic in the fields and $\hat{H}^i$ to the interacting part of the Hamiltonian. In this thesis we will work only with Hamiltonians that do not depend explicitly on time. The subscript $_{H_0}$ or $_H$ of an operator should show in which picture we work ($\hat{H}_0$ for the Interaction picture and $\hat{H}$ for the Heisenberg picture). For an arbitrary operator $\mathcal{O}$ this means:

$$\begin{aligned} \hat{\mathcal{O}}_{H_0(t)} &= e^{\frac{i}{\hbar}\hat{H}_0(t-t_r)}\hat{\mathcal{O}}e^{-\frac{i}{\hbar}\hat{H}_0(t-t_r)} \\ \hat{\mathcal{O}}_{H(t)} &= \big(\hat{T}e^{-\frac{i}{\hbar}\hat{H}(t-t_r)}\big)^\dagger\hat{\mathcal{O}}\big(\hat{T}e^{-\frac{i}{\hbar}\hat{H}(t-t_r)}\big) \end{aligned} \tag{1}$$

where t_r is the reference time where all pictures coincide and $\hat{T}$ is the time ordering operator. The expectation value of an arbitrary operator $\hat{\mathcal{O}}$ at time t is given by:

$$\begin{aligned} \langle\hat{\mathcal{O}}_{(t)}\rangle &\equiv \mathrm{tr}\big[\hat{\mathcal{O}}\hat{\rho}_{(t)}\big] \\ &= \mathrm{tr}\big[\hat{\mathcal{O}}\hat{\mathcal{U}}_{(t,t_r)}\hat{\rho}\hat{\mathcal{U}}^\dagger{}_{(t,t_r)}\big] \\ &= \mathrm{tr}\big[\hat{\rho}\underbrace{\hat{\mathcal{U}}^\dagger{}_{(t,t_r)}e^{-\frac{i}{\hbar}\hat{H}_0(t-t_r)}}_{\hat{\mathcal{U}}^\dagger_{H_0(t,t_r)}}e^{\frac{i}{\hbar}\hat{H}_0(t-t_r)}\hat{\mathcal{O}}e^{-\frac{i}{\hbar}\hat{H}_0(t-t_r)}\underbrace{e^{\frac{i}{\hbar}\hat{H}_0(t-t_r)}\hat{\mathcal{U}}_{(t,t_r)}}_{\hat{\mathcal{U}}_{H_0(t,t_r)}}\big] \\ &= \mathrm{tr}\big[\hat{\rho}\hat{\mathcal{U}}^\dagger_{H_0(t,t_r)}\hat{\mathcal{O}}_{H_0(t)}\hat{\mathcal{U}}_{H_0(t,t_r)}\big] \end{aligned} \tag{2}$$

where $\hat{\mathcal{U}}_{(t,t_r)} \equiv \hat{T}e^{-\frac{i}{\hbar}\int_{t_r}^{t}\hat{H}_{(\tau)}d\tau}$ is the time evolution operator. In the last line we have also defined the form of the same operator $\hat{\mathcal{U}}_{H_0(t,t_r)}$ in the Interaction picture. From the last line of eq. (2) one can see the transformation rule from the Interaction to the Heisenberg picture:

$$\hat{\mathcal{O}}_{H(t)} = \hat{\mathcal{U}}^\dagger_{H_0(t,t_r)}\hat{\mathcal{O}}_{H_0(t)}\hat{\mathcal{U}}_{H_0(t,t_r)} \tag{3}$$

Instead of the definition of $\hat{\mathcal{U}}_{H_0(t,t_r)}$ given in eq. (2) we will use the following one [1]
:

$$\hat{\mathcal{U}}_{H_0(t,t_r)} = \hat{T} e^{-i\int_{t_r}^{t} d\tau \hat{H}^i_{H_0(\tau)}} \tag{6}$$

To simplify the notation in the last line of eq. (2) we introduce the time contour c given in fig. (1) that goes from t_r to t and back to t_r. The position on the contour is now given by the composite argument t^j ($j \in \{\leftarrow, \rightarrow\}$) where the superscript j of the time argument gives information if we are on the forward ($\rightarrow$) or backward branch of the contour. At the return point t both branches should be connected, i.e. $t \equiv t^{\rightarrow} \equiv t^{\leftarrow}$. The contour ordering operator $\hat{T}_c$ then orders the operators according to their position on the contour. They are ordered from right to left beginning with those in the beginning of the forward branch and ending with those in the end ($t^j = t_r^{\leftarrow}$) of the backward branch. After the contour ordering operator all bosonic (fermionic) operators can be treated as complex (Grassman) variables. So the expectation value of an operator $\hat{\mathcal{O}}_{(t)}$ can be written as:

$$\begin{aligned} \langle \hat{\mathcal{O}}_{(t)} \rangle &= \mathrm{tr}\big[\hat{\rho}\hat{\mathcal{U}}^{\dagger}_{H_0(t,t_r^{\leftarrow})}\hat{\mathcal{O}}_{H_0(t)}\hat{\mathcal{U}}_{H_0(t,t_r^{\rightarrow})}\big] \\ &= \mathrm{tr}\big[\hat{\rho}\hat{\mathcal{U}}_{H_0(t_r^{\leftarrow},t)}\hat{\mathcal{O}}_{H_0(t)}\hat{\mathcal{U}}_{H_0(t,t_r^{\rightarrow})}\big] \\ &= \mathrm{tr}\big[\hat{\rho}\hat{T}_c\big(\hat{\mathcal{U}}_{H_0(t,t_r)}\hat{\mathcal{O}}_{H_0(t)}\big)\big] \end{aligned} \tag{7}$$

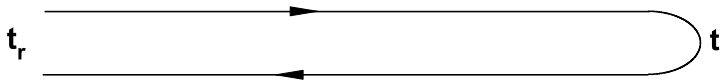

Figure 1: Contour branch on which the operator $\hat{T}_c$ acts. The forward (from t_r to t) and the backward (from t_r to t) branches will be later denoted with $(-)$ and $(+)$ instead with $(\rightarrow)$ and $(\leftarrow)$.

1.2 Green's function. Definition

Consider the problem of a single particle with the wavefunction $\psi_{(\vec{x},t)}$ that evolves according to the Schrödinger equation:

$$\big(i\hbar\frac{d}{dt} - H\big)\psi_{(\vec{x},t)} = 0 \tag{8}$$

where H is the system's Hamiltonian. If $\psi_{(\vec{x},t')}$ is known at t' one can obtain the wave-function at times $t > t'$ with the use of the formula:

$$\psi_{(\vec{x},t)} = \int G_{(\vec{x},t;\vec{x}',t')}\psi_{(\vec{x}',t')}d\vec{x}' \tag{9}$$

$G_{(\vec{x},t;\vec{x}',t')}$ is called Green's function and should be interpreted as the conditional probability amplitude for a transition of a particle to $(\vec{x},t)$ given that it was previously at $(\vec{x}',t')$. The restriction $t > t'$ is put to preserve that the wavefunction propagates only forward in time. $G_{(\vec{x},t;\vec{x}',t')}$ is defined as the solution of the equation:

$$\big(i\hbar\frac{d}{dt} - H\big)G_{(\vec{x},t;\vec{x}',t')} = i\hbar\delta_{(\vec{x}-\vec{x}')}\delta_{(t-t')} \tag{10}$$

[1] One can proof this by applying the Heisenberg equation of motion for an arbitrary operator $\hat{\mathcal{O}}_{H(t)}$:

$$i\hbar\frac{d}{dt}\hat{\mathcal{O}}_{H(t)} = [\hat{\mathcal{O}}_{H(t)}, \hat{H}] = \hat{\mathcal{U}}^{\dagger}{}_{(t,t_r)}[\hat{\mathcal{O}}, \hat{H}]\hat{\mathcal{U}}_{(t,t_r)} \tag{4}$$

Then one has to use the transformation for $\hat{\mathcal{O}}_{H(t)}$ given in eq. (3) and apply directly the time derivative:

$$\begin{aligned} i\hbar\tfrac{d}{dt}\hat{\mathcal{O}}_{H(t)} &= i\hbar\tfrac{d}{dt}(\mathcal{U}^{\dagger}_{H_0(t,t_r)}\hat{\mathcal{O}}_{H_0\,(t)}\mathcal{U}_{H_0(t,t_r)}) \\ &= ii\mathcal{U}^{\dagger}_{H_0(t,t_r)}([\hat{H}^i_{H_0}, \hat{\mathcal{O}}_{H_0\,(t)}] + [\hat{H}_0, \hat{\mathcal{O}}_{H_0\,(t)}])\mathcal{U}_{H_0(t,t_r)} \\ &= ii\underbrace{\mathcal{U}^{\dagger}_{H_0(t,t_r)}e^{\frac{i}{\hbar}\hat{H}_0(t-t_r)}}_{\mathcal{U}^{\dagger}_{(t,t_r)}}([\hat{H}^i, \hat{\mathcal{O}}] + [\hat{H}_0, \hat{\mathcal{O}}])\underbrace{e^{-\frac{i}{\hbar}\hat{H}_0(t-t_r)}\mathcal{U}_{H_0(t,t_r)}}_{\mathcal{U}_{(t,t_r)}} \\ &= \mathcal{U}^{\dagger}_{(t,t_r)}[\hat{O}, \hat{H}]\mathcal{U}_{(t,t_r)} \end{aligned} \tag{5}$$

The first term in the second line origins from the application of the time derivative at $\mathcal{U}^{\dagger}_{H_0(t,t_r)}, \mathcal{U}_{H_0(t,t_r)}$ and the second term from the application of $\frac{d}{dt}$ at $\mathcal{O}_{H_0}$.

So one can show that $\psi_{(\vec{x},t)}$ also obeys the Schrödinger equation:

$$\big(i\hbar\frac{d}{dt}-H\big)\int G_{(\vec{x},t;\vec{x}',t')}\psi_{(\vec{x}',t')}d\vec{x}'=i\hbar\int\delta_{(\vec{x}-\vec{x}')}\delta_{(t-t')}\psi_{(\vec{x}',t')}=i\hbar\delta_{(t-t')}\psi_{(\vec{x},t)}=0\quad\text{for}t>t'\qquad(11)$$

Going from single-particle to many-particle systems there is a slight change in the interpretation of the casual (time ordered) Green's function ($t_r<t,t'$; $\zeta=1$ for bosonic and $\zeta=-1$ for fermionic particles):

$$\begin{aligned}G^{--}{}_{(\vec{x},t;\vec{x}',t')} &= -i\,\mathrm{tr}\big[\hat{\rho}\hat{a}_{H(\vec{x},t)}\hat{a}^{\dagger}_{H(\vec{x}',t')}\big]\theta_{(t-t')}-i\zeta\mathrm{tr}\big[\hat{\rho}\hat{a}^{\dagger}_{H(\vec{x}',t')}\hat{a}_{H(\vec{x},t)}\big]\theta_{(t'-t)}\\ &= -i\,\mathrm{tr}\big[\hat{\rho}\hat{\mathcal{U}}^{\dagger}_{H_0(\max(t,t'),t_r)}\hat{T}\big(\mathcal{U}_{H_0(\max(t,t'),t_r)}\hat{a}_{H_0(t)}\hat{a}^{\dagger}_{H_0(t')}\big)\big]\\ &= -i\,\mathrm{tr}\big[\hat{\rho}T_c\big(\hat{a}_{H(\vec{x},t^{\rightarrow})}\hat{a}_{H(\vec{x}',t'^{\rightarrow})}\big)\big]\\ &= -i\,\mathrm{tr}\big[\hat{\rho}T_c\big(e^{-\frac{i}{\hbar}\int_c d\tau\hat{H}^i_{H_0}(\tau)}\hat{a}_{H_0(\vec{x},t^{\rightarrow})}\hat{a}^{\dagger}_{H_0(\vec{x}',t'^{\rightarrow})}\big)\big]\end{aligned}\qquad(12)$$

It describes the creation of a particle in the system at $(\vec{x}',t')$ and its destruction at $(\vec{x},t)$ for $t>t'$ or both actions in the reverse order for $t<t'$. The operators $\hat{a}^{\dagger},\hat{a}$ are responsible for the creation/annihilation of a particle and the Heaviside step function keeps the causality in the application of the operators on the system. The last three lines of eq. (12) are just different representations of the same expression. In the third line of the last equation we have introduced the contour going from t_r to $\max(t,t')$ and back to t_r. We have also set both variables t,t' to lie on the forward branch because in this case the contour ordering operator orders both operators $\hat{a},\hat{a}^{\dagger}$ in the same way as the time ordering operator $\hat{T}$ does. In the second and last line we have used eq. (3) and the fact that after the contour ordering operator all operators can be commuted as complex/Grassman variables. One can always extend the return point of contour from $\max(t,t')$ to infinity since the phase collected from the propagation in the forward direction after $\max(t,t')$ is cancelled by the propagation in the backward direction, i.e:

$$\hat{\mathcal{U}}^{\dagger}_{H_0}(\infty,\max(t,t'))\hat{\mathcal{U}}_{H_0}(\infty,\max(t,t'))=\hat{\mathbb{I}}$$

1.3 Schwinger-Keldysh formalism. Short introduction

The Schwinger-Keldysh theory is a natural way to extend the equilibrium perturbation theory to interacting systems in nonequilibrium steady state. Doing this we get also rid of some constraints like that the interaction should be switched on and off adiabatically [25] and that the ground state should be nondegenerate. The price we have to pay is that instead of one Green's function we have to work with four different types of them. The theory can also be easily extended to systems at finite temperature.

We work in the interaction picture representation since we can easily obtain the explicit time dependence of the creation and annihilation operators of the system. On the other hand this picture is also appropriate to do perturbation theory of the expectation value of a given observable if some nonquadratic interaction term is added to the Hamiltonian. We can just expand the exponential function of the nonquadratic part of the Hamiltonian (of $\hat{\mathcal{U}_{H_0}}$), apply the Wick's theorem[2] and express everything in terms of noninteracting Green's functions, which are known, in order to derive some useful approximations.

The need for the use of the Schwinger-Keldysh method can be seen explicitly if one writes down the definition of the time ordered Green's function given in eq. (12) ($t_r\to-\infty$):

$$G_{(\vec{x},t;\vec{x}',t')}=-i\,\mathrm{tr}\big[\hat{\mathcal{U}}^{\dagger}_{H_0(\infty,-\infty)}\hat{T}\big(\hat{\mathcal{U}}_{H_0(\infty,-\infty)}\hat{a}_{H_0(\vec{x},t)}\hat{a}^{\dagger}_{H_0(\vec{x}',t')}\big)\big].\qquad(13)$$

Only in the case where the temperature is equal to zero and the ground state of the system is nondegenerate one can show (Gell-Mann and Low theorem [23]) that after adiabatically switching on and off

[2]The Wick's theorem gives a way to decompose Gaussian averages of strings of operators. If $\hat{\rho}$ is the density matrix of the noninteracting system, i.e. $\hat{\rho}=\exp[-\beta\hat{H}_0/\mathrm{tr}[\exp[-\beta\hat{H}_0]]$ then the expectation value of a string of contour ordered operators is equal to the sum of all possible pairwise products (a.p.p.):

$$\begin{aligned}\langle\ldots\rangle &= \mathrm{tr}[\ldots\hat{\rho}]\\ \langle\hat{T}_c(\hat{\alpha}_{(\tau_n)}\hat{\alpha}_{(\tau_{n-1})}\ldots\hat{\alpha}_{(\tau_1)})\rangle &= \textstyle\sum_{a.p.p.}\prod_{jj'}\langle\hat{T}_c(\hat{\alpha}_{(\tau_j)}\hat{\alpha}_{(\tau_{j'})})\rangle\end{aligned}$$

where $\hat{\alpha}_{(\tau_n)}$ can be $\hat{a}_{(\tau_n)}$ or $\hat{a}^{\dagger}_{(\tau_n)}$. In the case that one works with fermionic fields one has to count explicitly the number of operator permutations (l) and multiply the expression with $(-1)^l$.

the interactions, the system remains in its ground state and only the phase of the state is changed. This allows one to decouple eq. (13) at $t = \infty$ and do only an integration on the forward contour. However, this simplification is not possible in the nonequilibrium case and one has to perform an integration following the path from $-\infty$ to ∞ and back to $-\infty$. So instead of the time-ordered GF one has to work with the more general one:

$$G_{(\vec{x},t;\vec{x}',t')} = -i \operatorname{tr}\big[\hat{\rho}_0 \hat{T}_c \big(e^{-\frac{i}{\hbar}\int_c d\tau \hat{H}^{i}_{H_0(\tau)}} \hat{a}_{H_0(\vec{x},t)} \hat{a}^{\dagger}_{H_0(\vec{x}',t')}\big)\big]. \tag{14}$$

In the derivation of the last equation we have already assumed that we are not interested in transient time phenomena but in the steady state properties of the system. The density matrix $\hat{\rho}_0$ we use at $t_r = -\infty$ is the density matrix of the noninteracting system. Unlike eq. (12) where both operators act only on the forward branch, in eq. (14) they can act on both branches. The four possible combinations are accounted by introducing the following matrix notation for the Green's function ($\zeta = 1$ for bosons and $\zeta = -1$ for fermions):

$$G_{(\vec{x},t;\vec{x}',t')} = \begin{bmatrix} G^{--}_{(\vec{x},t;\vec{x}',t')} & G^{-+}_{(\vec{x},t;\vec{x}',t')} \\ G^{+-}_{(\vec{x},t;\vec{x}',t')} & G^{++}_{(\vec{x},t;\vec{x}',t')} \end{bmatrix} \tag{15}$$

$$\begin{aligned}
G^{--}_{(\vec{x},t;\vec{x}',t')} &= -i \operatorname{tr}\big[\hat{T}\hat{a}_{H(x,t)}\hat{a}^{\dagger}_{H(x',t')}\big] && t,t' \in C^- \\
G^{++}_{(\vec{x},t;\vec{x}',t')} &= -i \operatorname{tr}\big[\hat{\tilde{T}}\hat{a}_{H(x,t)}\hat{a}^{\dagger}_{H(x',t')}\big] && t,t' \in C^+ \\
G^{-+}_{(\vec{x},t;\vec{x}',t')} &= -\zeta i \operatorname{tr}\big[\hat{a}^{\dagger}_{H(x',t')}\hat{a}_{H(x,t)}\big] && t \in C^-, t' \in C^+ \\
G^{+-}_{(\vec{x},t;\vec{x}',t')} &= -i \operatorname{tr}\big[\hat{a}_{H(x,t)}\hat{a}^{\dagger}_{H(x',t')}\big] && t \in C^+, t' \in C^- \\
G^{R}_{(\vec{x},t;\vec{x}',t')} &= \theta_{(t-t')}\big(G^{+-}_{(\vec{x},t;\vec{x}',t')} - G^{-+}_{(\vec{x},t;\vec{x}',t')}\big) \\
G^{A}_{(\vec{x},t;\vec{x}',t')} &= -\theta_{(t'-t)}\big(G^{+-}_{(\vec{x},t;\vec{x}',t')} - G^{-+}_{(\vec{x},t;\vec{x}',t')}\big) \\
G^{K}_{(\vec{x},t;\vec{x}',t')} &= G^{+-}_{(\vec{x},t;\vec{x}',t')} + G^{-+}_{(\vec{x},t;\vec{x}',t')}
\end{aligned}$$

The superscripts j, j' of $G^{j,j'}_{(\vec{x},t;\vec{x}',t')}$ now refer to the branch on which the operators $\hat{a}_{H(\vec{x},t^j)}, \hat{a}^{\dagger}_{H(\vec{x}',t'^{j'})}$ are applied. For example $G^{-+}_{(\vec{x},t;\vec{x}',t')}$ means that $\hat{a}_{H(\vec{x},t)}$ is applied on the forward contour and $\hat{a}^{\dagger}_{H(\vec{x}',t')}$ on the backward, so the annihilation operator acts always before the creation one. Because of the definition of the four Green's functions in eq. (15) they always fulfill the causality condition:

$$G^{--}_{(\vec{x},t;\vec{x}',t')} + G^{++}_{(\vec{x},t;\vec{x}',t')} = G^{-+}_{(\vec{x},t;\vec{x}',t')} + G^{+-}_{(\vec{x},t;\vec{x}',t')} \tag{16}$$

and one can eliminate one of them and work with the rest three GF's. Instead of the first four GF's one often prefers to work with the retarded G^R, the advanced G^A and the Keldysh G^K Green's functions since they have a more transparent physical interpretation: G^A and G^R carry information about the spectral properties of the system and the last one, G^K, contain information about the quantum statistics of the concerned particles (examples are given in the next section).

2 Some important Green's functions

In this section all GF's that are needed will be derived. The GF of an isolated noninteracting bosonic reservoir is calculated in sec. 2.1 and that of a chain of two quanum dots is derived in sec. 2.2. With this knowledge one will be able to write down the action of a system of a chain of quantum dots connected with two reservoirs and then extract from it the GF's one need (sec. 2.3). The addition of a self-energy term into the Green's function and the description of a bosonic gas, condensed in energy, are given in sec. 2.4, 2.5.

2.1 Calculation of the Green's function of a noninteracting bosonic reservoir

The Hamiltonian of the system can always be diagonalised and given in the form (set $\hbar \equiv 1$):

$$\hat{H} = \sum_k \varepsilon_k \hat{L}^{\dagger}_k \hat{L}_k \tag{17}$$

where ε_k are the eigenenergies of the Hamiltonian. The index k comprises all relevant quantum numbers that describe fully a state and $\hat{L}_k, \hat{L}^{\dagger}_k$ are the usual ladder operators. The density matrix of the system

at temperature T is given by $\hat{\rho}_0 = \exp[-\beta(\hat{H}-\mu\hat{N})]/\mathrm{tr}\{\exp[-\beta(\hat{H}-\mu\hat{N})]\}$ with μ, $\hat{N}$ defined as the chemical potential and the particle number operator respectively and $\beta = (k_B T)^{-1}$. In the Interaction picture representation the ladder operators are given by ($t_r = 0$):

$$\begin{array}{rcl} \hat{L}_{k,H_0(t)} & = & e^{\frac{i}{\hbar}\hat{H}_0(t-t_r)}\hat{L}_k e^{-\frac{i}{\hbar}\hat{H}_0(t-t_r)} = e^{-\frac{i}{\hbar}\varepsilon_k(t-t_r)}\hat{L}_k \\ \hat{L}^\dagger_{k,H_0(t)} & = & e^{\frac{i}{\hbar}\hat{H}_0(t-t_r)}\hat{L}^\dagger_k e^{-\frac{i}{\hbar}\hat{H}_0(t-t_r)} = e^{\frac{i}{\hbar}\varepsilon_k(t-t_r)}\hat{L}^\dagger_k \end{array} \tag{18}$$

From the four components of the reservoir Green's function $g_{kk';L(t,t')} = -i\,\mathrm{tr}\big[\hat{T}_c\big(\hat{L}_{k,H(t)}\hat{L}^\dagger_{k',H(t')}\big)\big]$ we will calculate only the $(--)$ one since the rest of the GF's can be obtained in a similar way. We also use the fact that we are in a steady state and only the time difference between the application of both operators matters. So we use the short notation $g_{kk';L(t,t')} = g_{kk';L(t-t')}$. The Fourier transform of $g^{--}_{kk';L(t-t')}$ is given by (see sec. 5 of appendix):

$$\begin{array}{rcl} g^{--}_{kk';L(w)} & = & \int_{-\infty}^{\infty} dt e^{iwt} g^{--}_{kk';L(t)} \\ & = & \int_{-\infty}^{\infty} dt e^{iwt}(-i)\Big(\mathrm{tr}\big[\hat{\rho}_0\hat{L}_{k,H(t)}\hat{L}^\dagger_{k',H(0)}\big]\theta_{(t)} + \mathrm{tr}\big[\hat{\rho}\hat{L}^\dagger_{k',H(0)}\hat{L}_{k,H(t)}\big]\theta_{(-t)}\Big) \\ & = & -i\,\lim_{\delta\to 0^+}\Big(\int_0^\infty dt e^{i(w-\varepsilon_k+i\delta)t}\delta_{kk'}(n_{\varepsilon_k-\mu}+1) + \int_{-\infty}^0 dt e^{i(w-\varepsilon_k-i\delta)t}\delta_{kk'}n_{\varepsilon_k-\mu}\Big) \\ & = & \lim_{\delta\to 0^+}\delta_{kk'}(n_{\varepsilon_k-\mu}+1)\frac{1}{(w-\varepsilon_k)+i\delta} - \delta_{kk'}(n_{\varepsilon_k-\mu})\frac{1}{(w-\varepsilon_k)-i\delta} \\ & = & (-2\pi i)\delta_{kk'}\delta_{(w-\varepsilon_k)}(n_{\varepsilon_k-\mu}+\frac{1}{2}) + \mathcal{P}\frac{1}{w-\varepsilon_k} \end{array} \tag{19}$$

where $n_{\varepsilon_k-\mu} = 1/[e^{(\varepsilon_k-\mu)\beta}-1] = \mathrm{tr}\big[\hat{a}^\dagger\hat{a}\hat{\rho}_0\big]$. In the third line we have added a small convergence factor δ and in the last line we have used the Sokhotsky-Plemelj-theorem (see appendix sec. 4). Similarly, we obtain the other three components of the matrix $g_{kk';L(w)}$:

$$g_{kk';L(w)} = -2\pi i\delta_{kk'}\delta_{(w-\varepsilon_k)}\begin{bmatrix} n_{\varepsilon_k-\mu}+\frac{1}{2} & n_{\varepsilon_k-\mu} \\ n_{\varepsilon_k-\mu}+1 & n_{\varepsilon_k-\mu}+\frac{1}{2}\end{bmatrix} + \sigma_z\mathcal{P}\frac{1}{w-\varepsilon_k} \tag{20}$$

with σ_z - the Pauli z-matrix. From the last equation one can obtain useful information like the mean occupation number of a single mode and its spectral function. Both are defined as:

$$\begin{array}{rcccccc} n_k & \equiv & \mathrm{tr}\big[\hat{\rho}_0\hat{L}^\dagger_k\hat{L}_k\big] & = & ig^{-+}_{kk;L(t=0)} = i\int\frac{dw}{2\pi}g^{-+}_{kk;L(w)} & = & n_{\varepsilon_k-\mu} \\ S_{(w)} & \equiv & -2\Im\big(g^R_{kk;L(w)}\big) & = & -2\Im\big(g^{--}_{kk;L(w)} - g^{-+}_{kk;L(w)}\big) & = & 2\pi\delta_{(w-\varepsilon_k)} \end{array} \tag{21}$$

The spectral function $S_{(w)}$ gives information about the response of the system after applying a slight perturbation at the frequency w. $S_{(w)}$ fulfills always the condition $\int\frac{dw}{2\pi}S_{(w)} = 1$.

2.2 Green's funtion for a chain of one or two quantum dots

Consider the system of two quantum dots at energy levels Δ_1, Δ_2 that are connected via a hopping term proportional to η:

$$\hat{H} = \Delta_1\hat{a}^{1\dagger}\hat{a}^1 + \Delta_2\hat{a}^{2\dagger}\hat{a}^2 - \eta\hat{a}^{1\dagger}\hat{a}^2 - \eta^*\hat{a}^{2\dagger}\hat{a}^1 \tag{22}$$

The superscript of $\hat{a}$ refers to the position in the lattice. In the following we rewrite the Keldysh partition function in a path integral form, then from this expression we extract the action $\mathcal{S}$ and the Green's function of the isolated quantum dots. The Keldysh partition function is defined as:

$$\mathcal{Z} = \frac{\mathrm{tr}\big[\hat{\rho}_0\hat{T}_C\big(e^{-\frac{i}{\hbar}\int_c d\tau\hat{H}(\tau)}\big)\big]}{\mathrm{tr}\big[\hat{\rho}\big]} \tag{23}$$

It is equal to one since the time evolution operator is not interrupted by any other operator during its evolution on the forward and backward contour. We rewrite the trace in basis of coherent states $\{|\vec{a}_j\rangle\}$ with $|\vec{a}_j\rangle \equiv |a^1_j\ \ a^2_j\rangle$ (the index j refers to the time) which have the properties:

$$\begin{array}{rcll} \langle\vec{b}_{j'}|\vec{a}_j\rangle & = & e^{\vec{b}^*_{j'}\cdot\vec{a}_j} = e^{b^{1*}_{j'}a^1_j + b^{2*}_{j'}a^2_j} & \diamondsuit \\ \hat{a}^m|\vec{a}_j\rangle & = & a^m_j|\vec{a}_j\rangle & \diamondsuit\diamondsuit \\ \hat{1} & = & \int\prod_{m=1}^2\big(\frac{da^{m*}_j da^m_j}{\pi}\big)e^{-\vec{a}^*_j\cdot\vec{a}_j} & \diamondsuit\diamondsuit\diamondsuit \end{array}$$

By dividing the forward and backward contour into infinitely many parts and inserting ($\diamondsuit\diamondsuit\diamondsuit$) between them one can derive (see sec. 7 of appendix) the path integral representation of the Keldysh partition function:

$$\mathcal{Z} = \int D[\vec{\alpha}^*_{(\tau)}, \vec{\alpha}_{(\tau)}] e^{i\mathcal{S}[\vec{\alpha},\vec{\alpha}^*]} \tag{24}$$

where $D[\vec{\alpha}^*_{(\tau)}, \vec{\alpha}_{(\tau)}]$ should be interpreted as the integral over all functions $a^{m*}_{l,j}, a^m_{l,j}$ ($m \in \{1,2\}$, $l \in \{+,-\}$, j - discretised time index that in the limit of infinitely many partitions of the contour becomes continuous [3]). The action $\mathcal{S}$ is defined as:

$$\begin{array}{rcl} \mathcal{S}[\vec{\alpha}^*, \vec{\alpha}] & = & \int d\tau_1 d\tau_2 \vec{\alpha}_{(\tau_1)} \mathcal{G}^{-1}_{(\tau_1-\tau_2)} \vec{\alpha}_{(\tau_2)} = \int \frac{dw}{2\pi} \vec{\alpha}^\dagger_{(w)} \mathcal{G}^{-1}_{(w)} \vec{\alpha}_{(w)} \\ \vec{\alpha}^T_{(w)} & = & \begin{pmatrix} a^1_{-(w)} & a^1_{+(w)} & a^2_{-(w)} & a^2_{+(w)} \end{pmatrix}. \end{array} \tag{25}$$

The Green's function $\mathcal{G}$ is given by the 4x4 matrix (σ_z - Pauli z-matrix):

$$\mathcal{G}^{-1}_{(w)} = \begin{bmatrix} g^{-1}_{11\,(w)} & \eta\sigma_z \\ \eta^*\sigma_z & g^{-1}_{22\,(w)} \end{bmatrix} \tag{26}$$

and the GF for an isolated singe quantum dot is $g^{-1}_{jj\,(w)} = (w - \Delta_j)\sigma_z \quad (jj \in \{11, 22\})$.

2.3 Addition of reservoirs to a chain of one or two quantum dots

Single quantum dot

We modify the system from the last subsection by an addition of two reservoirs and removal of one of the quantum dots. The system is described by the Hamiltonian:

$$\hat{H} = \Delta \hat{a}^\dagger \hat{a} + \sum_k \varepsilon_k \hat{L}^\dagger_k \hat{L}_k + \sum_{k'} \varepsilon_{k'} \hat{R}^\dagger_{k'} \hat{R}_{k'} - \sum_k \left(\gamma_{kL} \hat{L}^\dagger_k \hat{a} + \gamma^*_{kL} \hat{a}^\dagger \hat{L}_k\right) - \sum_{k'} \left(\gamma_{k'R} \hat{a}^\dagger \hat{R}_{k'} + \gamma^*_{k'R} \hat{R}^\dagger_{k'} \hat{a}\right) \tag{27}$$

Here k, k' are indices that contain all quantum numbers, $\hat{L}^\dagger_k, \hat{R}^\dagger_{k'}$ create particle with the set of quantum numbers k/k' in the left/right reservoir. Both reservoirs are connected with the quantum dot via the coupling γ. From the derivation of the action in the last subsection one can deduce the form of the new action (w dependence dropped for legibility):

$$\begin{array}{rcl} i\mathcal{S} & = & \int \frac{dw}{2\pi} \left[i\vec{a}^* g^{-1}_{11} \vec{a} + \sum_k i\vec{L}^*_k g^{-1}_{kk;L} \vec{L}_k + \sum_{k'} i\vec{R}^*_{k'} g^{-1}_{k'k';R} \vec{R}_{k'} \right] + \\ & & \int \frac{dw}{2\pi} \left[\sum_k \vec{L}^*_k \left(i\gamma_{kL}\sigma_z \vec{a}\right) + \sum_k \left(\vec{a}^* i\gamma^*_{kL}\sigma_z\right) \vec{L}_k + \sum_{k'} \vec{R}^*_{k'} \left(i\gamma^*_{k'R}\sigma_z \vec{a}\right) + \sum_{k'} \left(\vec{a}^* i\gamma_{k'R}\sigma_z\right) \vec{R}_{k'} \right] \end{array} \tag{28}$$

The vectors $\vec{L}_k, \vec{R}_{k'}$ are of the same form as $\vec{a} = (a_{-(w)} \;\; a_{+(w)})^T$. Because the reservoirs are noninteracting $g_{kk';L/R} = \delta_{kk'} g_{kk;L/R}$, which is already taken into account. The Keldysh partition function is of the form:

$$\mathcal{Z} = \int D[\vec{a}^*, \vec{a}, \vec{L}^*, \vec{L}, \vec{R}^*, \vec{R}] e^{i\mathcal{S}[\vec{a}^*, \vec{a}, \vec{L}^*, \vec{L}, \vec{R}^*, \vec{R}]} \tag{29}$$

Since the action is quadratic in the L, R fields they can be integrated out[4]. The result is:

$$\begin{array}{rcl} \mathcal{Z} & = & \int D[\vec{a}^*, \vec{a}] e^{i\mathcal{S}'[\vec{a}^*, \vec{a}]} \\ i\mathcal{S}' & = & i \int \frac{dw}{2\pi} \vec{a}^* \left[g^{-1}_{11} - \sum_k |\gamma_{kL}|^2 \sigma_z g_{kk;L} \sigma_z - \sum_{k'} |\gamma_{k'R}|^2 \sigma_z g_{k'k';R} \sigma_z \right] \vec{a} = i \int \frac{dw}{2\pi} \vec{a}^*_{(w)} \mathcal{G}^{-1}_{(w)} \vec{a}_{(w)} \end{array} \tag{30}$$

$\mathcal{G}_{(w)}$ is the Green's function of a noninteracting quantum dot connected to two reservoirs that are in thermal equilibrium. For the terms $\sum_k |\gamma_{k,L/R}|^2 \sigma_z g_{kk;L/R} \sigma_z$ one can go from summation to integration $\left(\sum_k \to \int d\varepsilon D_{L/R(\varepsilon)}\right)$ where $D_{L(w)}$, $D_{R(w)}$ is the density of states of the left, right reservoir. With the substitution:

$$\begin{array}{rcl} \Gamma_{L/R\;(\varepsilon)} & \equiv & \pi D_{L/R\;(\varepsilon)} |\gamma_{L/R(\varepsilon)}|^2 \\ \tilde{\Lambda}_{L/R(w)} & = & \lim\limits_{|w-\varepsilon|>\delta} \int d\varepsilon \frac{D_{L/R(\varepsilon)} |\gamma_{L/R\,\varepsilon}|^2}{w-\varepsilon} \\ \tilde{\Lambda}_{(w)} & = & \tilde{\Lambda}_{L(w)} + \tilde{\Lambda}_{R(w)} \end{array} \tag{31}$$

[3] Since we have inserted ($\diamondsuit\diamondsuit\diamondsuit$) in both directions of the contour C we have added again an additional variable $l = \pm$ to denote the position of the field a^m_j on the contour.

[4] One has to apply the formula for a Gaussian integral.

one gets:

$$\sum_k |\gamma_{k,L}|^2 \sigma_z g_{kk;L(w)} \sigma_z = \begin{bmatrix} -i\Gamma_{L(w)}\big(2n_{w-\mu_L}+1\big) & +i\Gamma_{L(w)} 2n_{w-\mu_L} \\ i\Gamma_{L(w)}\big(2n_{w-\mu_L}+2\big) & -i\Gamma_{L(w)}\big(2n_{w-\mu_L}+1\big) \end{bmatrix} + \begin{bmatrix} \tilde{\Lambda}_{L(w)} & 0 \\ 0 & -\tilde{\Lambda}_{L(w)} \end{bmatrix}. \tag{32}$$

The Green's function $\mathcal{G}_{(w)}$ is then given by (w-dependence dropped; $n_L \equiv n_{w-\mu_L}$):

$$\begin{aligned} \mathcal{G}_{(w)} &= -\tfrac{1}{(w-\Delta-\tilde{\Lambda})^2+(\Gamma_L+\Gamma_R)^2} \\ &\times \begin{bmatrix} -(w-\Delta-\tilde{\Lambda}) + i(\Gamma_L(2n_L+1)+\Gamma_R(2n_R+1)) & i(\Gamma_L 2n_L + \Gamma_R 2n_R) \\ i(\Gamma_L(2n_L+2)+\Gamma_R(2n_R+2)) & i(\Gamma_L(2n_L+1)+\Gamma_R(2n_R+1)) + (w-\Delta-\tilde{\Lambda}) \end{bmatrix}. \end{aligned} \tag{33}$$

The matrix fulfills the relations $\big(\Re\mathcal{G}^{-+}_{(w)} = 0 = \Re\mathcal{G}^{+-}_{(w)},\ \mathcal{G}^{--}_{(w)} = -\big(\mathcal{G}^{++}_{(w)}\big)^*\big)$ They will come in hand in sec. 4.

Two quantum dots

We construct the Green's function in the same way as in the last subsection. For the Hamiltonian:

$$\begin{aligned} \hat{H} &= \Delta_1 \hat{a}^{1\dagger}\hat{a}^1 + \Delta_2 \hat{a}^{2\dagger}\hat{a}^2 + \textstyle\sum_k \varepsilon_k \hat{L}^\dagger_k \hat{L}_k + \sum_{k'} \varepsilon_{k'} \hat{R}^\dagger_{k'} \hat{R}_{k'} \\ &\quad - \textstyle\sum_k \left(\gamma_{kL} \hat{L}^\dagger_k \hat{a}^1 + \gamma^*_{kL} \hat{a}^{1\dagger} \hat{L}_k\right) - \left(\eta \hat{a}^{1\dagger}\hat{a}^2 + \eta^* \hat{a}^{2\dagger}\hat{a}^1\right) - \textstyle\sum_{k'} \left(\gamma_{k'R} \hat{a}^{2\dagger} \hat{R}_{k'} + \gamma^*_{k'R} \hat{R}^\dagger_{k'} \hat{a}^2\right) \end{aligned} \tag{34}$$

we have the following action:

$$\begin{aligned} i\mathcal{S} &= i \textstyle\int \frac{dw}{2\pi} \vec{\alpha}^\dagger \mathcal{G}^{-1} \vec{\alpha} \\ \vec{\alpha} &= \begin{pmatrix} a^1_{-(w)} & a^1_{+(w)} & a^2_{-(w)} & a^2_{+(w)} \end{pmatrix}^T \end{aligned} \tag{35}$$

The inverse Green's fuction is a 4x4 matrix which in a block matrix form looks like:

$$\mathcal{G}^{-1}_{(w)} = \begin{bmatrix} g_{11}^{-1} - \sum_k |\gamma_{kL}|^2 \sigma_z g_{kk;L} \sigma_z & \eta\sigma_z \\ \eta^*\sigma_z & g_{22}^{-1} - \sum_{k'} |\gamma_{k'R}|^2 \sigma_z g_{k'k';R} \sigma_z \end{bmatrix} \tag{36}$$

where $g_{jj} = (w-\Delta_j)^{-1}\sigma_z$, $jj \in \{(11),(22)\}$ is the Green's function of an isolated quantum dot and $g_{kk;L/R}$ are the GF's of both reservoirs.

2.4 Addition of an interaction term. Self-energy.

In the last two subsections we have dealt with systems consisting of a chain of quantum dots coupled to bosonic reservoirs with infinite number of degrees of freedom. Since we were interested only in the properties of the chain of quantum dots (which we call system) but not of the reservoirs (which we call enviroment) we have integrated out the reservoir degrees of freedom in the Keldysh partition function. Doing this we have modified the system GF with terms of the form $\sum_k |\gamma_k|^2 \sigma_z g_{k;} \sigma_z$, e.g. in the case of a single dot coupled to two bosonic reservoirs we had:

$$g^{-1}_{11\,(w)} \longrightarrow G^{-1}_{11\,(w)} = g^{-1}_{11\,(w)} - \underbrace{\sum_k |\gamma_{kL}|^2 \sigma_z g_{k;LL(w)} \sigma_z}_{\Sigma_{res,L}(w)} - \underbrace{\sum_k |\gamma_{kR}|^2 \sigma_z g_{k;RR(w)} \sigma_z}_{\Sigma_{res,R}(w)}. \tag{37}$$

These objects, called self-energies, contain the complete information about system-enviroment scattering processes.

Their effect can be seen by comparing the spectral function of a single isolated quantum dot $\mathcal{A}_0(w)$ and quantum dot coupled to one (ore more) bosonic reservoir(s) $\mathcal{A}_1(w)$:

$$\begin{aligned} \mathcal{A}_0(w) &= 2\pi\delta(w-\Delta) \\ \mathcal{A}_1(w) &= \tfrac{2\Gamma_{L(w)}}{(w-\Delta-\tilde{\Lambda}_L(w))^2+\Gamma^2_{L(w)}} \end{aligned} \tag{38}$$

The self-energy renormalises the energy level of the quantum dot by $\tilde{\Lambda}_L(w)$. Since $\Sigma_{res,L}(w)$ is not Hermitian the eigenvalues of the system matrix get an additional imaginary part which accounts for the finite lifetime of the corresponding eigenstates. This results in a broadening of the spectral function. The strength of broadening $\Gamma_{L(w)}$ is proportional to the sum of the particle escape and entry rates:

$$\Gamma_{L(w)} = -\tfrac{i}{2}\big(\Sigma^{+-}_{res,L}(w) - \Sigma^{-+}_{res,L}(w)\big) \tag{39}$$

The idea of an addition of a self-energy term to the GF can also be extended to the case of a particle-particle interaction process inside the system (Σ_{int}). If we denote the sum of all self-energy contributions to the isolated sytem GF $g(w)$ by Σ then the full system GF $G(w)$ should have the following form:

$$G^{-1}_{(w)} = \left[g^{-1}{}_{(w)} - \Sigma_{int(w)}\right] \tag{40}$$

If all processes (particle-particle interaction, system-reservoir tunneling, etc..) are properly taken into account the system GF G should again fulfill the causality condition (eq. (16)) and it follows that:

$$\Sigma^{--}_{int\,(w)} + \Sigma^{++}_{int\,(w)} = -\Sigma^{-+}_{int\,(w)} - \Sigma^{+-}_{int\,(w)} \tag{41}$$

In the time domain eq. (40) is also equivalent to the Schwinger-Dyson equation [5] :

$$\begin{array}{rcl} G_{(t,t')} & = & g_{(t,t')} + \int_c d\tau_1 \int_c d\tau_2 g_{(t,\tau_1)} \Sigma'_{int(\tau_1,\tau_2)} G_{(\tau_2,t')} \\ G_{(t,t')} & = & g_{(t,t')} + \int_{-\infty}^{\infty} d\tau_1 \int_{-\infty}^{\infty} d\tau_2 g_{(t,\tau_1)} \sigma_z \Sigma'_{int(\tau_1,\tau_2)} \sigma_z G_{(\tau_2,t')} \end{array} \tag{42}$$

with $\Sigma_{int} = \sigma_z \Sigma'_{int} \sigma_z$. In the second line of the last equation we used the matrix notation of a Green's function given in eq. (15). One can also express both sides of the last equation in terms of retarded, advanced and Keldysh Green's functions (RAK-notation). In this case the equation has the same matrix form as before but g, G, Σ_{int} are triangular matrices:

$$g_{(t,t')} = \begin{bmatrix} 0 & g^A_{(t,t')} \\ g^R_{(t,t')} & g^K_{(t,t')} \end{bmatrix} \qquad G_{(t,t')} = \begin{bmatrix} 0 & G^A_{(t,t')} \\ G^R_{(t,t')} & G^K_{(t,t')} \end{bmatrix} \qquad \Sigma_{int(t,t')} = \begin{bmatrix} \Sigma^K_{(t,t')} & \Sigma^R_{(t,t')} \\ \Sigma^A_{(t,t')} & 0 \end{bmatrix} \tag{43}$$

In this work we will use the on-site interaction given by $\hat{H}_{int} = \frac{U}{2} \hat{a}^\dagger \hat{a}^\dagger \hat{a} \hat{a}$. In practice Σ_{int} can never be calculated exactly and approximations have to be used. This means that the self-energy will not always fulfill some important relations like the causality condition or the conservation of the current in steady state.

2.5 Addition of a BEC

In general, the time evolution of any closed system is periodic, the period τ being proportional to the inverse of the smallest difference of the eigenenergies. By the addition of bosonic reservoirs with continuous density of states $\tau \to \infty$, and the time evolution of the system becomes irreversible. Now, consider the case of two noninteracting bose gases at $T = 0$ that are condensed in energy and coupled to both ends of a chain of $\mathcal{N}$ quantum dots. The system can be described by the Hamiltonian:

$$\begin{array}{rcl} \hat{H} & = & \varepsilon_{0,L} \hat{L}^\dagger_0 \hat{L}_0 + \sum_{j=0}^{\mathcal{N}-1} \Delta_j \hat{a}^\dagger_j \hat{a}_j + \varepsilon_{0,R} \hat{R}^\dagger_0 \hat{R}_0 \\ & & + \gamma(\hat{L}^\dagger_0 \hat{a}_0 + \hat{a}^\dagger_0 \hat{L}_0 + \hat{R}^\dagger_0 \hat{a}_{\mathcal{N}-1} + \hat{a}^\dagger_{\mathcal{N}-1} \hat{R}_0) + \sum_{j=0}^{\mathcal{N}-2} \eta(\hat{a}^\dagger_{j+1} \hat{a}_j + \hat{a}^\dagger_j \hat{a}_{j+1}) \end{array} \tag{44}$$

where $\varepsilon_{0,L}, \varepsilon_{0,R}$ are the lowest energy levels of the left,right reservoirs. In this case the time evolution is reversible and has a finite periodicity in time τ. So the average particle flow through the chain of dots is for times $t \gg \tau$ approximately zero. In order to have a steady state one has to include a reservoir with continuous and nonzero over some frequency intervall density of states. Now assume that the mean particle occupation of these states follows a Bose-Einstein distribution ($n_{B(w)} = \left(\exp[\beta(w-\mu)] - 1\right)^{-1}$). At $T = 0$ $n_B(w) \neq 0$ only for $w = \varepsilon_0 = \mu$. One can calculate the mean particle occupation of every dot and of the zero modes of the reservoir and find out that it is zero. In this case the reservoir modes provide escape channels for the particles in the lattice chain but do not feed it with new particles.
We list some important aspects of adding a condensate to the system:

- If the reservoir contains a discrete set of states, the discrete set has to be added explicitly to the action and not integrated out.
- The inclusion of a noninteracting bosonic gas condensed in energy (ε_0) does not modify the steady state of the system. The system is modified only by the existence of the energy level ε_0.
- In the limit of very weak coupling between the system (the chain of quantum dots) and the discrete energy levels of the reservoir, i.e. γ is the smallest energy scale in the system, one can neglect the discret set completely in the action of the system (see fig. 2). One can not do the same for the ocntinuous density of states of the reservoir, since they provide the existence of a steady state.

[5] Multiply eq. (40) with G on the right and with g on the left side, then perform a Fourier transformation.

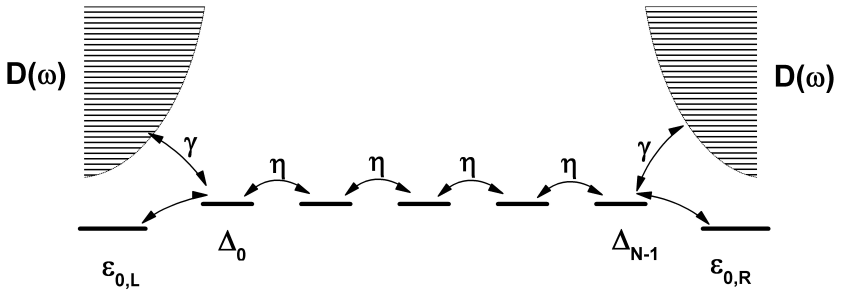

Figure 2: Chain of quantum dots with energy levels $\Delta_0 \dots \Delta_{N-1}$ coupled to two reservoirs with continuous density of states $D(\omega)$. The strength of the coupling is γ. In the case that for the lowest energy level of the reservoir, ε_0, the equation $D(\varepsilon_0) = 0$ is fulfilled, we add this level explicitly to the system. If the coupling between the reservoir and the chain of dots is the smallest scale of the system and $\Gamma(w) = \pi D(w)\gamma^2 \gg \gamma$ one can completely neglect the $\varepsilon_{0,L/R}$ levels in the Hamiltonian.

3 Calculation of the steady state current

Consider a chain of quantum dots coupled to two reservoirs. The system is described by[6]

$$\begin{aligned}\hat{H} &= \sum_k \varepsilon_k \hat{L}_k^\dagger \hat{L}_k + \sum_{k'} \varepsilon_{k'} \hat{R}_{k'}^\dagger \hat{R}_{k'} + \sum_{j=1}^{N} \Delta_j \hat{a}_j^\dagger \hat{a}_j + \\ &\sum_k \left(\gamma_{kL} \hat{L}_k^\dagger \hat{a}_1 + \gamma_{kL}^* \hat{a}_1^\dagger \hat{L}_k\right) + \sum_{k'} \left(\gamma_{k'R} \hat{a}_N^\dagger \hat{R}_{k'} + \gamma_{k'R}^* \hat{R}_{k'}^\dagger \hat{a}_N\right) + \sum_{j=1}^{N-1} \left(\eta_j \hat{a}_j^\dagger \hat{a}_{j+1} + \eta_j^* \hat{a}_{j+1}^\dagger \hat{a}_j\right)\end{aligned} \tag{45}$$

The operator for the particle flow between the j-th and the (j+1)-th quantum dots is derived in [27] and is given by:

$$\hat{I} = \tfrac{1}{i\hbar}\left(\eta_j^* \hat{a}_{j+1}^\dagger \hat{a}_j - \eta_j \hat{a}_j^\dagger \hat{a}_{j+1}\right) \tag{46}$$

It is positive if the flow on average is from site j to site $j+1$. The average steady state current at arbitrary time t is given by:

$$\langle \hat{I} \rangle = \tfrac{\eta_j^*}{\hbar}(-i)\mathrm{tr}\left[\hat{\rho}_0 \hat{a}_{j+1,H(t)}^\dagger \hat{a}_{j,H(t)}\right] - \tfrac{\eta_j}{\hbar}(-i)\mathrm{tr}\left[\hat{\rho}_0 \hat{a}_{j,H(t)}^\dagger \hat{a}_{j+1,H(t)}\right] = \tfrac{\eta_j^*}{\hbar} G_{j,j+1(0)}^{-+} - \tfrac{\eta_j}{\hbar} G_{j+1,j(0)}^{-+} \tag{47}$$

If we are interested in the current between the bosonic reservoir and the first dot of the chain we have to apply the formula above for all tunneling channels labelled with k ($\hbar = 1$):

$$\langle \hat{I} \rangle = \textstyle\sum_k \left[\gamma_{kL} G_{k1\,(t=0)}^{-+} - \gamma_{kL}^* G_{1k\,(t=0)}^{-+}\right] \tag{48}$$

Because of the fact that there is a linear coupling between the reservoir and the lattice chain one can express G_{1k}, G_{k1} in terms of known GF's like g_{kk}, G_{11} (a proof for a simpler Hamiltonian is given in sec. 6 in the appendix):

$$\begin{aligned} G_{k1(t,0)} &= \gamma_k \textstyle\int_c d\tau\, g_{kk;L(t,\tau)} G_{11(\tau,0)} \\ G_{1k(t,0)} &= \gamma_k^* \textstyle\int_c d\tau\, G_{11(t,\tau)} g_{kk;L(\tau,0)} \end{aligned} \tag{49}$$

Because $\int_c d\tau = \int_{-\infty}^{\infty} d\tau + \int_{\infty}^{-\infty} d\tau$ both GF's can be rewritten as:

$$\begin{aligned} G_{k1\,(t,0)}^{-+} &= \gamma_k \textstyle\int_{-\infty}^{\infty} d\tau \left(g_{kk;L(t,\tau)}^{--} G_{11\,(\tau,0)}^{-+} - g_{kk;L(t,\tau)}^{-+} G_{11\,(\tau,0)}^{++}\right) \\ G_{1k\,(t,0)}^{-+} &= \gamma_k^* \textstyle\int_{-\infty}^{\infty} d\tau \left(G_{11\,(t,\tau)}^{--} g_{kk;L(\tau,0)}^{-+} - G_{11\,(t,\tau)}^{-+} g_{kk;L(\tau,0)}^{++}\right) \end{aligned} \tag{50}$$

The steady-state current is then:

$$\begin{aligned} \langle \hat{I} \rangle &= \textstyle\sum_k \left[\gamma_k^* G_{k1\,(t=0)}^{-+} - \gamma_k G_{1k\,(t=0)}^{-+}\right] \\ &= \textstyle\int_{-\infty}^{\infty} d\tau \sum_k |\gamma_k|^2 \left[g_{kk;L(\tau)}^{+-} G_{11\,(-\tau)}^{-+} - g_{kk;L(-\tau)}^{-+} G_{11\,(\tau)}^{+-}\right] \\ &= \textstyle\int \frac{dw}{2\pi} \sum_k |\gamma_k|^2 \left[g_{kk;L(w)}^{+-} G_{11\,(w)}^{-+} - g_{kk;L(w)}^{-+} G_{11\,(w)}^{+-}\right] \end{aligned} \tag{51}$$

[6] In this section we have changed the sign of all tunneling terms because we do not want to count additional minus signs in the derivation of some important formulas. In the end one can always resubsitute $\gamma \to -\gamma$, $\eta \to -\eta$, etc...

In the derivation we have used the Causality condition $\left(G^{++} = G^{-+} + G^{+-} - G^{--}\right)$.
This formula express the current in terms of already known Green's functions $G_{11}(w)$, $g_{kk;L}(w)$. The result for the special case of a quantum dot coupled to two bosonic reservoirs will be discussed briefly:

$$\langle \hat{I} \rangle = \int \frac{dw}{2\pi} \underbrace{\frac{4\Gamma_L \Gamma_R}{(w - \Delta - \tilde{\Lambda})^2 + (\Gamma_L + \Gamma_R)^2}}_{\mathcal{T}} (n_L - n_R) \tag{52}$$

The result coincides with the one for the fermionic case if the Bose-Einstein distribution n_L, n_R is replaced by the Fermi-Dirac one. Despite this similarity there is a difference in the transport properties. In the fermionic case in the low temperature regime the fermionic distribution function can always be approximated with a Heaviside step function with a step at μ and it follows that the difference $n_L - n_R$ is nonzero only in the interval $[\mu_R, \mu_L]$ $(\mu_R < \mu_L)$; the current depends only on the values of $\mathcal{T}$ in this range. If the reservoirs are bosonic the difference $n_L - n_R$ is well defined and non-zero over the whole positive axis ($\mu \leq 0$ for bosons). If the bosonic reservoirs have a density of states $D(w) = \mathcal{D} w^2 \theta(w) \theta(\varepsilon_{cut} - w)$ $(\varepsilon_{cut} > 0, \mathcal{D} > 0)$ then modes in the range $w \in [0, \varepsilon_{cut}]$ contribute to the current. Since n_L, n_R (and also their difference) drop rapidly with increasing w one expects that the main contribution to the current comes from the energies close to zero.

4 Approximations for interacting quantm dots

Consider the Hamiltonian:

$$\begin{aligned} \hat{H} = & \Delta \hat{a}^\dagger \hat{a} + \textstyle\sum_k \varepsilon_k \hat{L}_k^\dagger \hat{L}_k + \sum_{k'} \varepsilon_{k'} \hat{R}_{k'}^\dagger \hat{R}_{k'} \\ & - \textstyle\sum_k \left(\gamma_{kL} \hat{L}_k^\dagger \hat{a} + \gamma_{kL}^* \hat{a}^\dagger \hat{L}_k \right) - \sum_{k'} \left(\tilde{\gamma}_{k'R} \hat{a}^\dagger \hat{R}_{k'} + \tilde{\gamma}_{k'R}^* \hat{R}_{k'}^\dagger \hat{a} \right) + \frac{U}{2} \hat{a}^\dagger \hat{a}^\dagger \hat{a} \hat{a} \end{aligned} \tag{53}$$

In this subsection two possible approximations of the self-energy Σ_{int} coming from the on-site interaction term $\frac{U}{2} \hat{a}^\dagger \hat{a}^\dagger \hat{a} \hat{a}$ will be discussed.

4.1 Self-consistent approximations for the interacting case

4.1.1 Approximation that conserves the current

In order to do an approximation for the interacting contribution to the self-energy we expand the dot Green's function as a sum of Feynman diagrams, sum part of them and neglect the rest in order to build a Schwinger-Dyson equation (eq. 42) for the full Green's function. All diagrams that do not include interaction terms are summed exactly. From the interaction diagrams we take only those which have the form of chain of Tadpole and/or Sunset diagrams (see fig. 3). They have the advantage that their symmetry factor factorises into a product of symmetry factors of the single Tadpole/Sunset diagrams. All calculations of the symmetry factors and the derivation of the Schwinger-Dyson equation for the case of a single quantum dot or a chain of quantum dots coupled to two bosonic reservoirs can be found in sec. 8 of the appendix, 9. In the following g denotes the Green's function of an isolated quantum dot or a bosonic reservoir, $\mathcal{G}$ - the GF of the dot with $U = 0, \gamma_{L/R} \neq 0$ and G - the complete GF with $U, \gamma_{L/R} \neq 0$.
The contribution of all diagrams that have a form of a chain of Sunset and/or Tadpole diagrams is given by:

$$\begin{aligned} \Sigma_{(w)} &= \Sigma_1 + \Sigma_{2(w)} \\ \Sigma_{tad} &= \textstyle\int \frac{dw}{2\pi} \tilde{M}_{(w)} \\ \Sigma_{sun(w)} &= \textstyle\int \frac{dw dw'}{(2\pi)^2} \sigma_z M_{(w', w'', w' + w'' - w)} \sigma_z \end{aligned} \tag{54}$$

with:

$$\begin{aligned}
\tilde{M}^{--}_{(w)} &= +4\big(i\tfrac{U}{2}\big)\mathcal{G}^{--}_{(w)} \\
\tilde{M}^{++}_{(w)} &= -4\big(i\tfrac{U}{2}\big)\mathcal{G}^{++}_{(w)} \\
\tilde{M}^{-+}_{(w)} &= 0 = \tilde{M}^{+-}_{(w)} \\
M^{--}_{(w',w'',w''')} &= \big(i\tfrac{U}{2}\big)^2 8\mathcal{G}^{--}_{(w')}\mathcal{G}^{--}_{(w'')}\mathcal{G}^{--}_{(w''')} \\
M^{-+}_{(w',w'',w''')} &= \big(i\tfrac{U}{2}\big)^2 8\mathcal{G}^{-+}_{(w')}\mathcal{G}^{-+}_{(w'')}\mathcal{G}^{+-}_{(w''')} \\
M^{+-}_{(w',w'',w''')} &= \big(i\tfrac{U}{2}\big)^2 8\mathcal{G}^{+-}_{(w')}\mathcal{G}^{+-}_{(w'')}\mathcal{G}^{-+}_{(w''')} \\
M^{++}_{(w',w'',w''')} &= \big(i\tfrac{U}{2}\big)^2 8\mathcal{G}^{++}_{(w')}\mathcal{G}^{++}_{(w'')}\mathcal{G}^{++}_{(w''')}
\end{aligned} \tag{55}$$

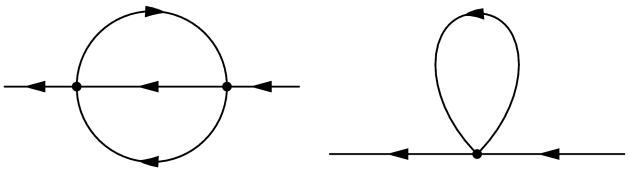

Figure 3: Sunset (left) and Tadpole (right) diagrams.

Properties of the approximation
Since we do not sum over all diagrams we can not expect that the approximated Σ fulfills all symmetries that the true self-energy should have. We show that Σ does not fulfill the causality condition but it still gives real quantities for the average current and the mean ocupation number of the dot.

Causality condition
In order to show the statements above we recall again the result from sec. 2.3 for the full Green's function of the noninteracting system (eq. (33)). Since $\mathcal{G}^{--}_{(w)} = -\big(\mathcal{G}^{++}_{(w)}\big)^*$ it follows that $\Sigma^{--}_{(w)} = -\big(\Sigma^{++}_{(w)}\big)^*$ for the Sunset and Tadpole contributions. From $\Re\big(\mathcal{G}^{-+}_{(w)}\big) = 0 = \Re\big(\mathcal{G}^{+-}_{(w)}\big)$ one obtains that $\Re\big(\Sigma^{-+}_{(w)}\big) = 0 = \Re\big(\Sigma^{+-}_{(w)}\big)$. In order to fulfill the causality condition $\big(\Sigma^{--}_{(w)} + \Sigma^{++}_{(w)} + \Sigma^{-+}_{(w)} + \Sigma^{+-}_{(w)} = 0\big)$ the approximated Σ has to fulfill the equation:

$$\begin{aligned}
\iff \quad \Im\big(\Sigma^{--}_{sun\,(w)} + \Sigma^{++}_{sun\,(w)} + \Sigma^{-+}_{sun\,(w)} + \Sigma^{+-}_{sun\,(w)} + \Sigma^{--}_{tad} + \Sigma^{++}_{tad}\big) &= 0 \\
2\Im\big(\Sigma^{--}_{sun\,(w)}\big) + \Im\big(\Sigma^{-+}_{sun\,(w)}\big) + \Im\big(\Sigma^{+-}_{sun\,(w)}\big) + 2\Im\big(\Sigma^{--}_{tad}\big) &= 0
\end{aligned} \tag{56}$$

This is in general not the case.

Current
The determinant of the matrix $G^{-1}_{(w)} = \big[\mathcal{G}^{-1}_{(w)} - \Sigma_{(w)}\big]$ is given by:

$$\begin{aligned}
\mathrm{Det} &\equiv \mathrm{Det}\big[\mathcal{G}^{-1}_{(w)} - \Sigma_{(w)}\big] \\
&= -\big[\big(w - \Delta - \tilde{\Lambda} - \Re\Sigma^{--}\big)^2 + \big(\Gamma_L + \Gamma_R + \Im\Sigma^{--} + \Im\Sigma^{+-}\big)^2\big] \\
&\quad + \big[2\Im\Sigma^{--} + \Im\Sigma^{-+} + \Im\Sigma^{+-}\big]\big[2\Gamma_L(n_L+1) + 2\Gamma_R(n_R+1) + \Im\Sigma^{+-}\big]
\end{aligned} \tag{57}$$

and the Green's function of the interacting system is given by:

$$\begin{aligned}
&G_{(w)} = \tfrac{1}{\mathrm{Det}} \\
&\times \begin{bmatrix} i\big(\Gamma_L(2n_L+1) + \Gamma_R(2n_R+1) - \Im\Sigma^{--}\big) & i\big(\Gamma_L 2n_L + \Gamma_R 2n_R + \Im\Sigma^{-+}\big) \\ -\big(w - \Delta - \tilde{\Lambda} - \Re\Sigma^{--}\big) & \\ & \big(w - \Delta - \tilde{\Lambda} - \Re\Sigma^{--}\big) \\ i\big(\Gamma_L(2n_L+2) + \Gamma_R(2n_R+2) + \Im\Sigma^{+-}\big) & +i\big(\Gamma_L(2n_L+1) + \Gamma_R(2n_R+1) + \Im\Sigma^{--}\big) \end{bmatrix}
\end{aligned} \tag{58}$$

Because the causality condition for $\Sigma_{(w)}$ is not fulfilled the same statement follows for $G_{(w)}$. Looking again at the formula for the determinant (eq. (57)) one can see that the last line is nonzero only because of the violation of the causality condition (the left expression in the square brackets is equivalent to the LHS of eq. (56)). We assume that neglecting this term should improve the approximation.

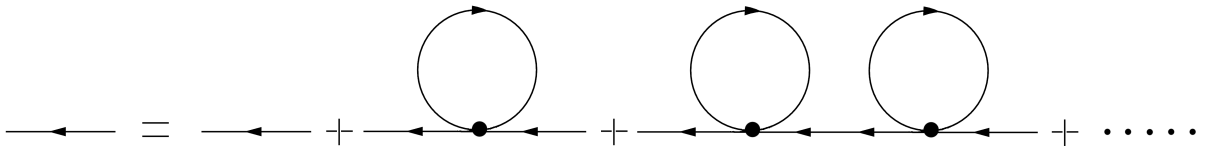

Figure 4: The solid line in the figure corresponds to the noninteracting Green's function $\mathcal{G}_{(w)}$.

The average currents between the left reservoir and the dot $\langle \hat{I}_{L1} \rangle$, between the dot and the right reservoir $\langle \hat{I}_{1R} \rangle$ are given by [7]:

$$\begin{aligned} \langle \hat{I}_{L1} \rangle &= \sum_k \left[\gamma_k^* G^{-+}_{k1\,(t=0)} - \gamma_k G^{-+}_{1k\,(t=0)} \right] \\ &= \int \tfrac{dw}{2\pi} \tfrac{2\Gamma_L}{-\mathrm{Det}} \left[2\Gamma_R(n_L - n_R) + n_L(\Im\Sigma^{+-} - \Im\Sigma^{-+}) - \Im\Sigma^{-+} \right] \\ \langle \hat{I}_{1R} \rangle &= \int \tfrac{dw}{2\pi} \tfrac{2\Gamma_R}{-\mathrm{Det}} \left[2\Gamma_L(n_L - n_R) - n_R(\Im\Sigma^{+-} - \Im\Sigma^{-+}) + \Im\Sigma^{-+} \right] \end{aligned} \tag{59}$$

Since that are the main observables we are interested in, we have to be sure that they are equal. We consider first the case where only the Tadpole approximation is applied. From eq. (54) we see that $\Sigma^{-+}_{tad} = 0 = \Sigma^{+-}_{tad}$, it follows that both currents are equal. For the following discussion we have to define the full Green's function obtained by this approximation:

$$\begin{aligned} G_{tad\,(w)} = & \underbrace{-\left[(w - \Delta - \tilde{\Lambda} - \Re\Sigma^{--}_{tad})^2 + (\Gamma_L + \Gamma_R + \Im\Sigma^{--}_{tad})^2 \right]}_{\mathrm{Det}_{2(w)}}{}^{-1} \\ & \times \begin{bmatrix} i(\Gamma_L(2n_L+1) + \Gamma_R(2n_R+1) - \Im\Sigma^{--}_{tad}) & i(\Gamma_L 2n_L + \Gamma_R 2n_R) \\ -(w - \Delta - \tilde{\Lambda} - \Re\Sigma^{--}_{tad}) & \\ & (w - \Delta - \tilde{\Lambda} - \Re\Sigma^{--}_{tad}) + \\ i(\Gamma_L(2n_L+2) + \Gamma_R(2n_R+2)) & i(\Gamma_L(2n_L+1) + \Gamma_R(2n_R+1) - \Im\Sigma^{--}_{tad}) \end{bmatrix} \end{aligned} \tag{60}$$

Next, we calculate the Sunset contribution but instead of $\mathcal{G}_{(w)}$ given in eq. (54),(55) we use $G_{tad\,(w)}$. This means that every line of the left diagram in fig. 3 has the form given in fig. 4. The full GF has the form:

$$\begin{aligned} G_{(w)} = & \underbrace{-\left[(w - \Delta - \tilde{\Lambda} - \Re\Sigma^{--}_{tad} - \Re\Sigma^{--}_{sun})^2 + (\Gamma_L + \Gamma_R + \Im\Sigma^{--}_{tad} + \Im\Sigma^{--}_{sun} + \Im\Sigma^{+-}_{sun})^2 \right]}_{\mathrm{Det}_{3(w)}}{}^{-1} \\ & \times \begin{bmatrix} i(\Gamma_L(2n_L+1) + \Gamma_R(2n_R+1) - \Im\Sigma^{--}_{tad} - \Im\Sigma^{--}_{sun}) - & i(\Gamma_L 2n_L + \Gamma_R 2n_R - \Im\Sigma^{-+}_{sun}) \\ (w - \Delta - \tilde{\Lambda} - \Re\Sigma^{--}_{tad} - \Re\Sigma^{--}_{sun}) & \\ & (w - \Delta - \tilde{\Lambda} - \Re\Sigma^{--}_{tad} - \Re\Sigma^{--}_{sun}) + \\ i(\Gamma_L(2n_L+2) + \Gamma_R(2n_R+2) + \Im\Sigma^{+-}_{sun}) & i(\Gamma_L(2n_L+1) + \Gamma_R(2n_R+1) - \Im\Sigma^{--}_{tad} - \Im\Sigma^{--}_{sun}) \end{bmatrix}. \end{aligned} \tag{61}$$

In the ideal case the difference between $\langle \hat{I}_{L1} \rangle$ and $\langle \hat{I}_{1R} \rangle$ has to be equal to zero. In this approximation it is equal to:

$$\langle \hat{I}_{L1} - \hat{I}_{1R} \rangle = \int \tfrac{dw}{2\pi} \left[\tfrac{2(\Gamma_L n_L + \Gamma_R n_R)}{-\mathrm{Det}_3} \Im\Sigma^{+-}_{sun} - \tfrac{2(\Gamma_L(n_L+1) + \Gamma_R(n_R+1))}{-\mathrm{Det}_3} \Im\Sigma^{-+}_{sun} \right] \tag{62}$$

Using the fact that $\Sigma_{sun} \sim U^2$ and $\Sigma_{tad} \sim U$ we can assume that for small enough U we can neglect Σ_{sun} from Det_3. In this case $\mathrm{Det}_3 \approx \mathrm{Det}_2$ and one can express the terms in the last equation completely with G^{-+}_{tad}, G^{+-}_{tad}:

$$\begin{aligned} \langle \hat{I}_{L1} - \hat{I}_{1R} \rangle &\approx \int \tfrac{dw}{2\pi} \left[G^{-+}_{tad} \Sigma^{+-}_{sun} - G^{+-}_{tad} \Sigma^{-+}_{sun} \right] \\ &= +8\left(\tfrac{iU}{2}\right)^2 \int \tfrac{dw dw' dw''}{8\pi^3} \left[G^{-+}_{tad\,(w)} G^{+-}_{tad\,(w')} G^{+-}_{tad\,(w'')} G^{-+}_{tad\,(w'+w''-w)} \right] \\ &\quad -8\left(\tfrac{iU}{2}\right)^2 \int \tfrac{dw dw' dw''}{8\pi^3} \left[G^{+-}_{tad\,(w)} G^{-+}_{tad\,(w')} G^{-+}_{tad\,(w'')} G^{+-}_{tad\,(w'+w''-w)} \right] \\ &= 0. \end{aligned} \tag{63}$$

In the next to last line we have performed a variable transformation to get the desired result. So in the case of weak interactions the steady state current is approximately conserved.
In the for us relevant case $\Gamma = \Gamma_L = \Gamma_R$ we will work with the symmetrised current:

$$\begin{aligned} \langle \hat{\tilde{I}} \rangle = \tfrac{1}{2} \langle \hat{I}_{L1} + \hat{I}_{1R} \rangle &= \int \tfrac{dw}{2\pi} \tfrac{1}{-\mathrm{Det}_3} \left[4\Gamma^2 + \Gamma(\Im\Sigma^{+-} - \Im\Sigma^{-+}) \right] (n_L - n_R) \\ &\approx \int \tfrac{dw}{2\pi} \tfrac{1}{-\mathrm{Det}_2} \left[4\Gamma^2 + \Gamma(\Im\Sigma^{+-} - \Im\Sigma^{-+}) \right] (n_L - n_R) \end{aligned} \tag{64}$$

[7] We do not use the result from eq. (51) since there we have already used that $G_{(w)}$ fulfills the causality condition.

4.1.2 Approximation that conserves the causality condition

Instead of working with four GF's we can rewrite the action of the system entirely in terms of retarded (**R**), advanced (**A**) and Keldysh (**K**) Green's functions and approximate the corresponding Self-energies again with Tadpole and Sunset diagrams as before:

$$\begin{array}{lcl}
\Sigma^{R/A/K}_{(w)} & = & \Sigma^{R/A/K}_{tad} + \Sigma^{R/A/K}_{sun\ (w)} \\
\Sigma^{R/A}_{tad} & = & \frac{iU}{2} 2 \int \frac{dw}{2\pi} \mathcal{G}^{K}_{(w)} \\
\Sigma^{K}_{tad} & = & 0 \\
\Sigma^{R/A/K}_{sun\ (w)} & = & \int \frac{dw' dw''}{4\pi^2} M^{R/A/K}_{(w',w'',w'+w''-w)} \\
M^{R}_{(w',w'',w''')} & = & \left(\frac{iU}{2}\right)^2 \left[2\mathcal{G}^{R}_{(w')}\mathcal{G}^{R}_{(w'')}\mathcal{G}^{A}_{(w''')} + 4\mathcal{G}^{R}_{(w')}\mathcal{G}^{K}_{(w'')}\mathcal{G}^{K}_{(w''')} + 2\mathcal{G}^{K}_{(w')}\mathcal{G}^{K}_{(w'')}\mathcal{G}^{A}_{(w''')}\right] \\
M^{A}_{(w',w'',w''')} & = & \left(\frac{iU}{2}\right)^2 \left[2\mathcal{G}^{A}_{(w')}\mathcal{G}^{A}_{(w'')}\mathcal{G}^{R}_{(w''')} + 4\mathcal{G}^{A}_{(w')}\mathcal{G}^{K}_{(w'')}\mathcal{G}^{K}_{(w''')} + 2\mathcal{G}^{K}_{(w')}\mathcal{G}^{K}_{(w'')}\mathcal{G}^{R}_{(w''')}\right] \\
M^{K}_{(w',w'',w''')} & = & \left(\frac{iU}{2}\right)^2 \left[2\mathcal{G}^{K}_{(w')}\mathcal{G}^{K}_{(w'')}\mathcal{G}^{K}_{(w''')} + 2(\mathcal{G}^{R}_{(w')}\mathcal{G}^{R}_{(w'')} + \mathcal{G}^{A}_{(w')}\mathcal{G}^{A}_{(w'')})\mathcal{G}^{K}_{(w''')}\right] + \\
 & & \left(\frac{iU}{2}\right)^2 \left[4\mathcal{G}^{K}_{(w')}(\mathcal{G}^{R}_{(w'')}\mathcal{G}^{A}_{(w''')} + \mathcal{G}^{A}_{(w'')}\mathcal{G}^{R}_{(w''')})\right]
\end{array} \tag{65}$$

Using that $\mathcal{G}^{R}_{(w)} = \left(\mathcal{G}^{A}_{(w)}\right)^*$, $\Re\mathcal{G}^{K}_{(w)} = 0$ it follows $\Sigma^{R}_{(w)} = \left(\Sigma^{A}_{(w)}\right)^*$, $\Re\Sigma^{K}_{(w)} = 0$ which is also fulfilled for the full Self-energy. This approximation will be appropriate to calculate the spectral function of an interacting quantum dot coupled to two reservoirs:

$$\begin{array}{lcl}
\mathcal{S}_{(w)} & = & -2\Im G^{R}_{(w)} \\
 & = & \frac{2(\Gamma_L + \Gamma_R - \Im\Sigma^R)}{(w - \Delta - \tilde{\Lambda} - \Re\Sigma^R)^2 + (\Gamma_L + \Gamma_R - \Im\Sigma^R)^2}.
\end{array} \tag{66}$$

The symmetrised current in the for us relevant case $\Gamma_L = \Gamma_R = \Gamma$ is given by:

$$\langle \hat{\bar{I}} \rangle = \tfrac{1}{2}\langle \hat{I}_{L1} + \hat{I}_{1R} \rangle = -\int \frac{dw}{2\pi} 2\Gamma \Im G^R (n_L - n_R) \tag{67}$$

5 Quantum dot coupled to two bosonic reservoirs

In the last section we have derived the general form of the Green's function of a system consisting of a chain of quantum dots coupled to two bosonic resrvoirs. We have also presented a simple way to approximate the interaction effects of the system coming from an on-site interaction term in the Hamiltonian. Now we apply this theory to bosonic reservoirs above the critical temperature. First we start with the calculation of the density of states of the bosonic resrvoir and the reservoir-quantum dot transparency (sec. 5.1) followed by short description of the system parameters (sec. 5.2). In the end, the observables we are interested in (current, spectral function, mean particle occupation of the quantum dot) are calculated and presented (sec. 5.3).

5.1 Reservoir density of states and reservoir-dot transparency calculation

Consider the case of noninteracting particles with mass m in a 3D-harmonic potential $V_{(\vec{r})} = \frac{1}{2}m\big(w_x^2 x^2 + w_y^2 y^2 + w_z^2 z^2\big)$ ($w_i = \sqrt{K_i/m}$; K_i-stiffness coefficient). The Hamiltonian describing the system is given by:

$$\hat{H} = \frac{\hat{p}^2}{2m} + \hat{V}_{(\vec{r})} \tag{68}$$

Since it is quadratic in its operators it can be diagonalised and rewritten in the form:

$$\hat{H} = \big(\tfrac{1}{2} + \hat{a}_x^\dagger \hat{a}_x\big)\hbar w_x + \big(\tfrac{1}{2} + \hat{a}_y^\dagger \hat{a}_y\big)\hbar w_y + \big(\tfrac{1}{2} + \hat{a}_z^\dagger \hat{a}_z\big)\hbar w_z \tag{69}$$

The single particle eigenenergies are given by:

$$\varepsilon_{\vec{n}} \equiv \varepsilon_{(n_x,n_y,n_z)} = \big(\tfrac{1}{2} + n_x\big)\hbar w_x + \big(\tfrac{1}{2} + n_y\big)\hbar w_y + \big(\tfrac{1}{2} + n_z\big)\hbar w_z \qquad n_i \in \mathbb{N}_0 \quad (i = x, y, z) \tag{70}$$

The ladder operators $\hat{a}_i^\dagger, \hat{a}_i$ with $[\hat{a}_i, \hat{a}_j^\dagger] = \delta_{ij}$ are responsible for the creation of an excitation with energy $\hbar w_i$ $(i = x, y, z)$. In order to calculate the density of states we treat n_i as a continuous variable. The

number of configurations $N_{(\varepsilon)}$ that fulfill the condition $\hbar(w_x n_x + w_y n_y + w_z n_z) \leq \varepsilon - \frac{1}{2}\hbar(w_x + w_y + w_z)$ is given by ($\varepsilon' = \varepsilon - \frac{1}{2}\hbar(w_x + w_y + w_z)$):

$$N_{(\varepsilon)} = \int_0^{\frac{\varepsilon'}{\hbar w_x}} dn_x \int_0^{\frac{\varepsilon' - \hbar w_x n_x}{\hbar w_y}} dn_y \int_0^{\frac{\varepsilon' - \hbar w_x n_x - \hbar w_y n_y}{\hbar w_z}} dn_z = \frac{\varepsilon'^3}{6\hbar^3 w_x w_y w_z} = \frac{[\varepsilon - \frac{1}{2}\hbar(w_x + w_y + w_z)]^3}{6\hbar^3 w_x w_y w_z} \tag{71}$$

The density of states is given by:

$$D_{(\varepsilon)} = \frac{dN_{(\varepsilon)}}{d\varepsilon} = \frac{[\varepsilon - \frac{1}{2}\hbar(w_x + w_y + w_z)]^2}{2\hbar^3 w_x w_y w_z} \theta_{(\varepsilon - \frac{1}{2}\hbar(w_x + w_y + w_z))} = \mathcal{D}(\varepsilon - c)^2 \theta_{(\varepsilon - c)} \tag{72}$$

with $c = \frac{1}{2}\hbar(w_x + w_y + w_z)$, $\mathcal{D} = \frac{1}{2\hbar^3 w_x w_y w_z}$. We have also multiplied the result with a Heaviside step function in order to keep in mind that the density of states is zero for negative energies. Now we take the many-particle Hamiltonian:

$$\hat{H} = \textstyle\sum_{\vec{n}} \varepsilon_{\vec{n}} \hat{a}^\dagger_{\vec{n}} \hat{a}_{\vec{n}} \tag{73}$$

The operators $\hat{a}^\dagger_{\vec{n}}, \hat{a}_{\vec{n}}$ create/annihilate a particle with energy $\varepsilon_{\vec{n}}$[8]. In order to calculate the action of the system of a chain of quantum dots connected to two bosonic reservoirs (eq. (30),(35)) we have to calcualte terms of the form $\sum_{\vec{n}} |\gamma_{\vec{n}}|^2 \sigma_z g_{\vec{n}\vec{n}'(w)} \sigma_z$. The resrvoir GF $g_{\vec{n}\vec{n}'(w)}$ is given in eq. (19). We show only the calculation of the $(--)$ component of this matrix. It consists of two terms. The first one is:

$$\begin{aligned} \textstyle\sum_{\vec{n}} |\gamma_{\vec{n}}|^2 (-2\pi i) \delta_{(w - \varepsilon_{\vec{n}})} (n_{(w-\mu)} + \tfrac{1}{2}) &= \int_0^\infty d\varepsilon D_{(\varepsilon)} |\gamma_\varepsilon|^2 (-2\pi i) \delta_{(w-\varepsilon)} (n_{(w-\mu)} + \tfrac{1}{2}) \\ &= -2i\pi D_{(w)} |\gamma_{(w)}|^2 (n_{(w-\mu)} + \tfrac{1}{2}) \\ &\equiv -2i\Gamma_{(w)} (n_{(w-\mu)} + \tfrac{1}{2}) \end{aligned} \tag{74}$$

The left(right) reservoir-quantum dot contact transparency is $\Gamma_{L(w)}$ $\big(\Gamma_{R(w)}\big)$. Since the left and right reservoirs are the same but with different chemical potetntials the contact transparencies are the same $\big(\Gamma_{L(w)} = \Gamma_{R(w)} = \Gamma_{(w)}\big)$.
The second summand of the $(--)$ component of $\sum_{\vec{n}} |\gamma_{\vec{n}}|^2 \sigma_z g_{\vec{n}\vec{n}'(w)} \sigma_z$ is:

$$\tilde{\Lambda}_{L/R\ (w)} = \sum_{\vec{n}} |\gamma_{\vec{n}}|^2 \mathcal{P} \tfrac{1}{w - \varepsilon_{\vec{n}}} = \lim_{\delta \to 0^+} \int\limits_{|w-\varepsilon| > \delta} d\varepsilon \tfrac{D_{(\varepsilon)} |\gamma_{(\varepsilon)}|^2}{w - \varepsilon_{\vec{n}}}. \tag{75}$$

At this point one should take into account that a physical harmonic trap should have a finite depth and particles with energies larger than this depth should be lost from the system. This constraint is implemented by multiplying the density of states with a sharp (smooth) cut-off function $\mathcal{F}_{1\ (w)}$ $\big(\mathcal{F}_{2\ (w)}\big)$ that damps all contributions with energies larger than some cut-off value ε_{cut}:

$$\begin{aligned} \mathcal{F}_{1\ (w)} &= \theta_{(\varepsilon_{cut} + c - w)} \\ \mathcal{F}_{2\ (w)} &= \big[\exp\big(\tfrac{(w - (\varepsilon_{cut} + c))}{\kappa}\big) + 1\big]^{-1} \end{aligned} \tag{76}$$

The degree of smoothness of the cut-off is controlled by κ (small κ corresponds to a sharper cut-off). Because of the cut-off functions the integral in eq. (75) is now well-defined [9]. For the case of a sharp cut-off the expression in eq. (75) can be calculated explicitly ($\gamma_{(w)} = \gamma = \text{const}$):

$$\tilde{\Lambda}_{L/R\ (w)} = -\mathcal{D}\gamma^2 \tfrac{1}{2}\big[\varepsilon_{cut}^2 + \varepsilon_{cut}(w - c)\big] + \begin{cases} -\mathcal{D}\gamma^2 (w-c)^2 \ln\big(\frac{\varepsilon_{cut}}{c-w} + 1\big) & w < c \\ -\mathcal{D}\gamma^2 (w-c)^2 \ln\big(\frac{\varepsilon_{cut}}{w-c} - 1\big) & c < w < \varepsilon_{cut} + c \\ -\mathcal{D}\gamma^2 (w-c)^2 \ln\big(1 - \frac{\varepsilon_{cut}}{w-c}\big) & \varepsilon_{cut} + c < w \end{cases} \tag{77}$$

We substitute $\tilde{\Lambda}_{(w)} = \tilde{\Lambda}_{L\ (w)} + \tilde{\Lambda}_{R\ (w)}$.
We can now calculate the Green's function in eq. (30):

$$\begin{aligned} \mathcal{G}_{(w)} &= -\tfrac{1}{(w - \Delta - \tilde{\Lambda}_{(w)})^2 + 4\Gamma^2_{(w)}} \\ &\quad \times \begin{bmatrix} -(w - \Delta - \tilde{\Lambda}_{(w)}) + i2\Gamma(n_L + n_R + 1) & i2\Gamma(n_L + n_R) \\ i2\Gamma(n_L + n_R + 2) & (w - \Delta - \tilde{\Lambda}_{(w)}) + i2\Gamma(n_L + n_R + 1) \end{bmatrix} \end{aligned} \tag{78}$$

[8] They fulfill also the relation $[\hat{a}_{\vec{n}}, \hat{a}^\dagger_{\vec{n}'}] = \delta^{(3)}_{\vec{n}\vec{n}'}$, $[\hat{a}_{\vec{n}}, \hat{a}_{\vec{n}'}] = 0 = [\hat{a}^\dagger_{\vec{n}}, \hat{a}^\dagger_{\vec{n}'}]$; $\delta^{(3)} = \delta_{n_x n'_x} \delta_{n_y n'_y} \delta_{n_z n'_z}$.

[9] Another possibility could be to use an energy-dependent coupling $\gamma_{(\varepsilon)}$ but this does not change anything in the final result, since the action of the system depends on the product $\mathcal{D}\gamma^2$.

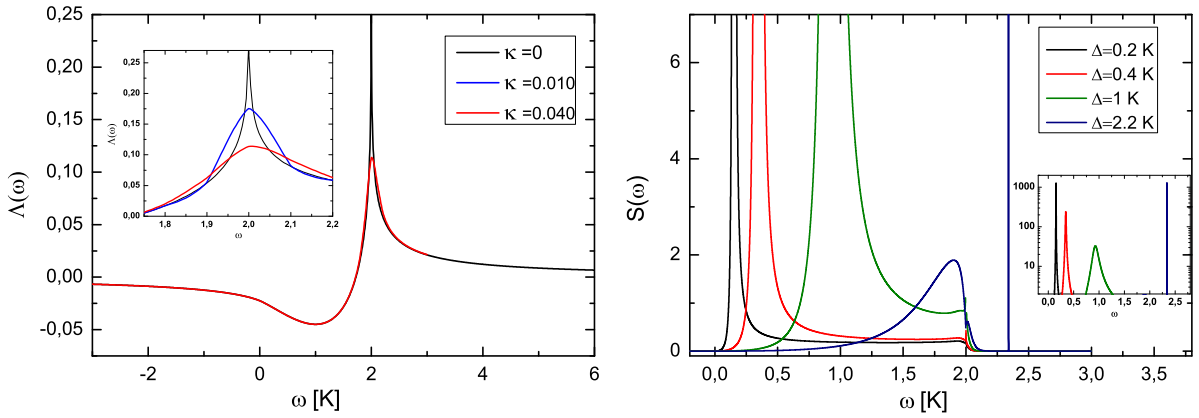

Figure 5: Left panel: $\tilde{\Lambda}_{(w)}$ defined in eq. (75) in dependence of the chosen cut-off. Larger cut-off parameter κ corresponds to smoother cut-off of the density of states of the reservoir. The function defined in eq. (77) is obtained in the limit $\kappa \to 0$.
Right panel: Spectral function. The peak depends clearly on the energy level Δ of the quantum dot. The peak at $\omega = \varepsilon_{cut} = 2K$ for $\Delta = 1K$ is due to the cut-off of the density of states of both reservoirs. For $\Delta = 2.2K$ the peak lies outside the intervall, where the density of states of the reservoir is non-zero. The peak is very sharp since it is barely influenced by the reservoir.

In fig. 5 one can see that $\tilde{\Lambda}_{(w)}$ has a a removable singularity at $w = c$ and singularity at $w = \varepsilon_{cut} + c$. The nature of the singularity is due to the cut-off function have we used. For a smooth coutoff it is absent. The second important feature of $\tilde{\Lambda}_{(w)}$ is that it is negative for $w < 0$ and converges to zero for $w \to -\infty$ which means that the equation $\left(w - \Delta - \tilde{\Lambda}_{(w)} = 0\right)$ can have solutions for negative w and thus $\mathcal{G}_{(w)}$ can have poles. Since $\tilde{\Lambda}_{(w)}$ is proportional to $\mathcal{D}\gamma^2$ it follows that an increase of $\mathcal{D}\gamma^2$ moves one of the solutions of $\left(w - \Delta - \tilde{\Lambda}_{(w)} = 0\right)$ to the left towards zero. For strong enough $\mathcal{D}\gamma^2$ the line $w - \Delta$ can cross $\tilde{\Lambda}$ at two points around ε_{cut}. The first crossing is for $w < \varepsilon_{cut}$ and does not produce any singularities in $\mathcal{G}_{(w)}$ since $\Gamma_{(w)}$ is nonzero, the second crossing at $w > \varepsilon_{cut}$ leads to a singularity or a very strong peak in dependece of the chosen cut-off.

5.2 Parameters

Using the fact that atoms of a thermal gas can be trapped via buffer gas cooling tecniques [22] with maximal depth of few Kelvin we choose the value of the cut-off to be $\varepsilon_{cut} = 2K$. The temperature of the reservoir is set to be 0.2K. The trapping frequency ω is set to $\omega = 10^7 Hz$. With this value the order of extension of the particles in the potential is of the order of $10^{-6}m$ if one assumes that the gas obeys classical statistics. The chemical potential μ is varied in the range $[-1.8K, -0.6K]$. With these parameters the mean particle number in the reservoir $N = \int d\varepsilon D(\varepsilon) n(\varepsilon)$ varies in the range $[2.10^8,\ 10^{11}]$. The critical temperature at which Bose-Einstein condensation occurs is given by [31]:

$$T_c \approx 4.5 \left(\frac{\omega}{2\pi 100 Hz}\right) N^{1/3} nK. \tag{79}$$

This value is smaller or equal to the temperature we work with, so no extra care of the condensate fraction is needed. In the following all quantities will be given in units of Kelvin. For the coupling between reservoir and lattice we choose $\gamma = 10^{-9}K$; the transparancy $\Gamma(w)$ and $\tilde{\Lambda}(w)$ will be of order $0.1K, 0.4K$ in the range $w \in [0, 2K]$.

5.3 Results. Quantum dot coupled to two bosonic reservoirs

In the following graphs the interaction strength will be measured in units of $\bar{\Gamma}$. The quantity is defined as

$$\bar{\Gamma} = \frac{1}{\varepsilon_{cut}} \int_0^{\varepsilon_{cut}} \Gamma_{(w)} dw \tag{80}$$

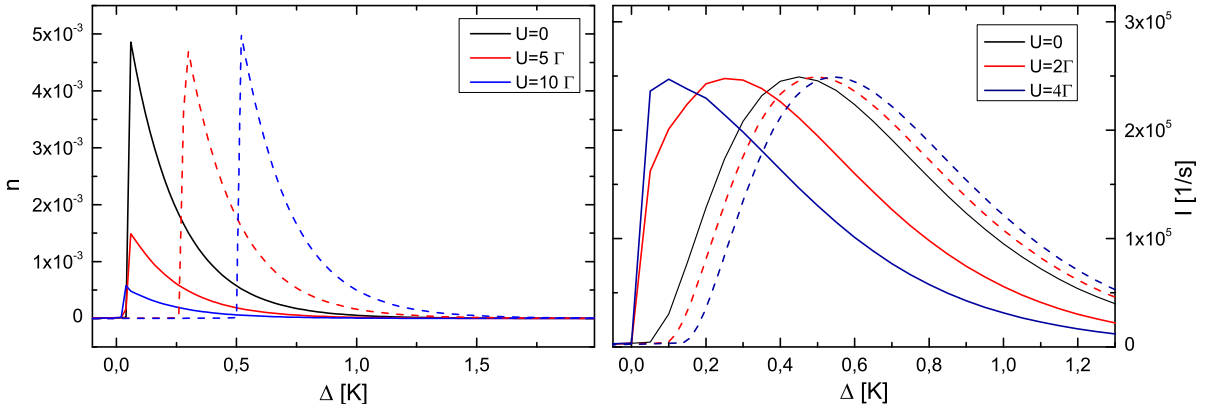

Figure 6: Left panel: Mean particle occupation of the quantum dot. Tadpole (solid line) and mean field (dashed line) approximation. Additional parameters: $\mu_L = -1.1K$, $\mu_R = -1K$, $T = 0.2K$.
Right panel: Steady state current. Tadpole (solid line) and mean field (dashed line) approximation. Additional parameters: $\mu_L = -1.1K$, $\mu_R = -1K$, $T = 0.2K$.

and is to be intepreted as the average transparency.
We discuss the behaviour of the current, mean particle occupation and spectral function of the quantum dot obtained by the approximations introduced in the previous section.

5.3.1 Current

First, we apply only the Tadpole approximation. It has two effects on the behaviour of the system: it shifts the position of the energy level of the quantum dot (the shift being in the same direction as the sign of U) and it introduces a positive additive contribution to Γ in the denominator of the formula for the current (64). The second effect leads to a decrease of the current but this can not be seen because the system is dominated by the shift of the energy level (see fig. 6). Including the Sunset contribution to the Self-energy in the way described in sec. 4.1.1, leads to an insignificant decrease of the current. So this correction does not introduce any additional effects into the system.

5.3.2 Spectral function

Looking at the definition of the Tadpole approximation (eq. 65), we see that it is entirely real, so the on-site interaction leads only to a shift of the energy level of the quantum dot. In fig. 9 one can see a decrease of the peak of the spectral function and an increase of its width for an increasing interaction

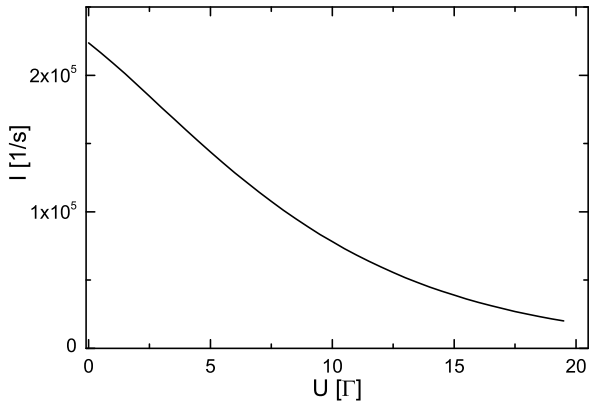

Figure 7: Steady state current, Tadpole approximation (solid line). Parameters: $\mu_L = -1K$, $\mu_R = -1.1K$, $\Delta = 0.6K$, $T = 0.2K$. One sees that changing the interaction strength U is effectively the same as changing the energy level of the quantum dot since the shape of the curve is the same as in the right panel of fig. 6.

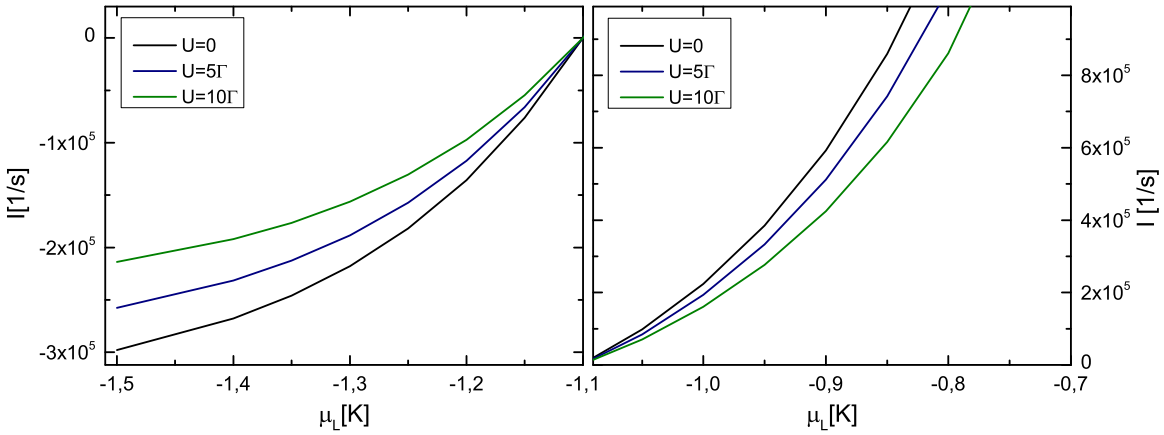

Figure 8: Steady state current in dependence of the chemical potential μ_L of the left reservoir; Tadpole approximation (solid line). Parameters: $\mu_R = -1.1K$, $\Delta = 0.6K$, $T = 0.2K$. The interaction strength is given in units of $\bar{\Gamma}$ defined in eq. (80).

strength. This is due to the fact that the spectral density of the reservoirs increases for higher frequencies and so the denominator of eq. (66) is larger for higher frequencies. In addition we have also added the Sunset contribution to the self-energy, but this approximation fails in giving physical results since we have obtained a spectral funciton that has negative values and that does not fulfill the normalisation condition $\int \frac{dw}{2\pi} \mathcal{S}(w) = 1$.
One should note that by shifting the position of Δ towards zero the point is reached, where the peak of the spectral function reaches $w = 0$. A further decrease of Δ leads to the appearance of an additional δ-peak of $\mathcal{S}(w)$ at $w < 0$. The exact position should be at the negative solution of the equation $(w - \Delta - 2\tilde{\Lambda}(w)) = 0$ and the strength of the δ-peak should be chosen such that the normalisation condition $\int \frac{dw}{2\pi} S(w) = 1$ is fulfilled. In the parameter regime we work with, such a δ-peak appears for $\Delta < 0.05K$.

5.3.3 Mean particle occupation

In the Tadpole approximation one sees that instead of a shift of the graph for the mean particle occupation (n) to the left for higher interaction strengths there is always a rapid drop for values of $\Delta < 0.05K$. The reason is that the particle self-interaction contribution (Tadpole contribution) rapidly drops to zero, meaning that n is approximately given by:

$$n \approx \int_0^\infty \frac{dw}{2\pi} \mathcal{S}_{(w)} \frac{n_{L(w)} + n_{R(w)}}{2} \tag{81}$$

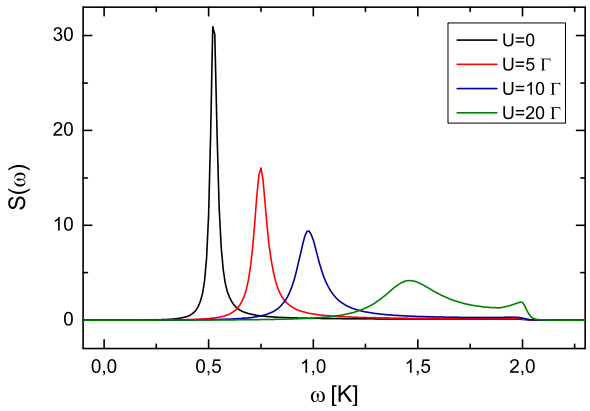

Figure 9: Spectral function of a quantum dot. Tadpole approximation (solid line). Parameters: $\mu_L = -1K$, $\mu_R = -1.1K$, $\Delta = 0.6K$, $T = 0.2K$.

where $\mathcal{S}_{(w)}$ is the spectral function in the noninteracting case. Since for $\Delta < 0.05K$ almost the whole weight of $\mathcal{S}(w)$ is included in the new δ-peak at $w < 0$, we observe a rapid decrease of n.

In addition to the Tadpole approximation we have added also the results from a mean-field approximation[10]. Since we investigate a zero-dimensional system, we can not expect that this approximation should give reliable results. Although this approximation modifies only the energy level of the quantum dot similarly to the Tadpole approximation, the results are qualitatively different (see fig. 6). This can be explained with the fact that the mean occupation number at the dot is smaller than one and the energy correction $\Delta \to \Delta + U(\langle n\rangle - 1/2)$ is negative for positive interaction strengths ($\langle n\rangle$-mean particle occupation of the dot).

[10]Mean field approximation:
Approximate $\hat{a}^\dagger\hat{a}\hat{a}^\dagger\hat{a} \approx 2\hat{a}^\dagger\hat{a}\langle\hat{a}^\dagger\hat{a}\rangle - \langle\hat{a}^\dagger\hat{a}\rangle^2$ (substitute $\hat{a}^\dagger\hat{a} \equiv \hat{n}$). It follows that the interaction term $\frac{U}{2}\hat{a}^\dagger\hat{a}^\dagger\hat{a}\hat{a}$ only modifies the energy level of the dot:

$$\Delta\hat{a}^\dagger\hat{a} \to \big(\Delta + U(\langle\hat{n}\rangle - 1/2)\big)\hat{a}^\dagger\hat{a}. \tag{82}$$

The expectation value of the dot occupation $\langle n\rangle$ is still unknown. One can get it by solving the equation:

$$N(\Delta + U(\langle n\rangle - 1/2)) \quad = \quad \langle n\rangle \tag{83a}$$

$$N(\Delta) \quad \equiv \quad \int \tfrac{dw}{2\pi} \tfrac{2\Gamma_{(w)}(n_{L(w)}+n_{R(w)})}{(w-\Delta-2\tilde{\Lambda}_{(2)})^2+4\Gamma^2_{(w)}}, \tag{83b}$$

where the last function is the mean occupation number of the quantum dot.
Since the typical values of $\langle n\rangle$ in our case are less than 10^{-3} the left hand side of the eq. (83a) is in a good approximation constant for $\langle n\rangle \in [0, 10^{-3}]$, so the equation has always a solution.

Part III
Master equation approach

In this section an alternative approach to the nonequilibrium Green's function method is presented that allows us to calculate the expectation values of the observables we are interested in, like mean occupation number, current, equal-time first and second order coherence. We start from a Hamiltonian $\hat{H}$ of a lattice chain of quantum dots (which we call system), but instead of an action we construct a Master equation in Lindblad form for the density matrix $\hat{\rho}$ of the system. We should note that the $\hat{H}$ we use does not contain information about the bosonic reservoirs (denoted also as enviroment). Their effect is simulated via addition of a particle loss and gain terms at specific lattice sites in the equation. One can expect that this approximation is worse than the nonequilibrium GF method because of the crude description of the effect of the particle reservoirs on the system. These aspects are also discussed in this chapter.
There are two methods to solve the Master equation which work in different regimes. In the case that the particle number in every lattice site is small, we cut the system Hilbert-space and apply the Quantum jump method [43]. In the case of average and large occupation numbers in the lattice sites, we use the Truncated Wigner method [32] to map the Master equation in Lindblad form for the density matrix to a Fokker-Planck equation for a probability density funciton. Under certain conditions the latter equation is equivalent to a Langevin equation for the conditional probability density function and can be solved numerically via the Euler-Maruyama or a higher order method. We also show a connection between the nonequilibrium GF formalism and the Truncated Wigner approximation. This allows us to apply the approximation methods from the previous chapter and apply them for the current problem.

This section starts with some basic definitons of stochastic processes (sec. 1), followed by an explanation of the Wigner mapping and the Quantum jump method (sec. 2, 3). A connection between the formalism in the previous chapter and the Wigner method is made (sec. 3). The master equation in Lindblad form is then physically motivated, using a simple system as an example. All methods discussed in this chapter are applied to this particular system and compared (sec. 4). Details to the numerical application of the method to the system we are interested in are given (sec. 5). In the end the results are presented and discussed (sec. 6).

1 Stochastic processes. Basics.

We first recall some basic definitions. A **random variable** is formally described by the following map:

$$\begin{array}{rccc} X: & S & \longrightarrow & Z \\ & s & \longmapsto & X(s)=x \end{array} \tag{84}$$

The domain S is the set of events of the system and the image Z can be interpreted as the set of events of the measuring system. The map should fulfill the condition that every event of the measuring system Z corresponds to an event of the system S. A family of random variables $\{X_t\}_{t\in T}$ (with $X: T\times S\to Z;\ \ (t,s)\mapsto X_t(s)$) that describe the time evolution of a random value along some time intervall $T=[t_0,t_{max}]$ is called a **stochastic process**. The **Path** or **trajectory** of a process is defined by the following map:

$$\forall s\in S \qquad \begin{array}{rccc} X(\cdot,s): & T & \longrightarrow & Z \\ & t & \longmapsto & X_t(s)=x(t) \end{array} \tag{85}$$

In addition if we take a set of points t_k from T and the corresponding random variables X_{t_k} we can describe their properties completely by their **joint probability distribution**:

$$\rho_{X_{t_n},\dots X_{t_1}}(x_n,\dots x_1)\equiv\rho(x_n,t_n;\dots;x_1,t_1). \tag{86}$$

In the definiton we always order the times such that $t_n\geq t_{n-1}\geq\ldots\geq t_1$. The conditional probability that the event x_n occurs at t_n given that the events $x_{n-1},x_{n-2}\dots x_1$ have occured is denoted by $\rho(x_n,t_n|x_{n-1},t_{n-1}\dots x_1,t_1)$. The **conditional translation probability** refers to the special case $\rho(x_1t_1|x_0t_0)$. The short notation for the expectation value of a random variable is $\langle X_t\rangle=\int dx\rho(x,t)x$.

A Gaussian distribution with mean μ and variance σ^2 is denoted by $\mathcal{N}(\mu, \sigma^2)$.

All processes used in this chapter are presented in the following paragraphs:

1.1 White Gaussian noise

This is a process whose joint probability density function always factorises into a product of density functions for a single random variable, i.e:

$$\rho(x_n, t_n; x_{n-1}, t_{n-1} \ldots; x_1, t_1) = \prod_{i=1}^{n} \rho^i(x_i, t_i) \quad \forall n \in \mathbb{N} \quad \textit{and} \quad t_1, \ldots t_n \in T \tag{87}$$

where $\rho^i(x_i, t_i)$ is a Gaussian distribution function with mean $\langle X_i \rangle = 0$. The random variables at different times are completely uncorrelated. This is expressed by the autocovariance:

$$\Big\langle \Big(X_t - \langle X_t \rangle \Big) \Big(X_{t'} - \langle X_{t'} \rangle \Big) \Big\rangle = \langle X_t X_{t'} \rangle = \sigma^2(\vec{x}, t_i)\delta(t - t') \tag{88}$$

If σ^2 does not depend on $\vec{X}$ then the process is called additive. Since $\delta(0) = \infty$ it follows that the probability density function of the random variable can not be defined, i.e. no trajectory of the process actually exist. In the following we denote a white Gaussian noise with ξ_t.

1.2 Wiener process

A Wiener process $(W_t)_{t \in I}$, $I = [t_0, T]$ is defined by the following conditions:

1. $W_{t_0} > 0$.
2. For $t_0 < t_1 < \ldots < t_N$ the increments of the process $W_{t_{n+1}} - W_{t_n}$ are stochastically independent.
3. For every pair $(t, t') \in I \times I$ with $t > t'$ the increments $W_t - W_{t'}$ are normally distributed with variance equal to $(t - t')$.
4. The paths of W_t are almost surely continuous.

For simplicity the process can be formally defined as:

$$W_t = \textstyle\int_{t_0}^{t} d\tau \xi_\tau \tag{89}$$

where ξ_t is a white Gaussian noise. This allows us to show many of the properties of a Wiener process like:

$$\begin{array}{rcl} \langle W_t \rangle & = & \int_{t_0}^{t} d\tau \langle \xi_\tau \rangle = 0 \\ \langle W_t W_t \rangle & = & \int_{t_0}^{t} d\tau \int_{t_0}^{t} d\tau' \langle \xi_\tau \xi_{\tau'} \rangle = \int_{t_0}^{t} d\tau \int_{t_0}^{t} d\tau' \delta(\tau - \tau') = (t - t_0) \\ \langle W_t W_{t'} \rangle & = & \min(t, t') - t_0 \end{array} \tag{90}$$

Next, if we want to calculate an integral of a function over such a process we have to use the definition of an Ito integral. For an arbitrary nonanticipating function $G(t)$ it is given by:

$$\int_{t_0}^{t} G(s) dW_s = \lim_{N \to \infty} \sum_{n=0}^{N-1} G(t_n)(W_{t_{n+1}} - W_{t_n}) = \lim_{N \to \infty} \sum_{n=0}^{N-1} G(t_n) \Delta W_{t_n} = \lim_{N \to \infty} \sum_{n=0}^{N-1} G(t_n) \sqrt{\Delta_n} \zeta_{t_n} \tag{91}$$

where $t_0 < t_1 < \ldots < t_N$, $\Delta_n = t_{n+1} - t_n$, $\Delta W_{t_n} = W_{t_n + \Delta_n} - W_{t_n}$ and $\{\zeta_{t_n}\}_{n=0 \ldots N-1}$ is a set of uncorrelated random variables with $\mathcal{N}(0, 1)$. The limit $N \to \infty$ means that we divide the time intervall into N parts and let $N \to \infty$. The last equality follows from the third line of the definition of a Wiener process and the fact that $\sqrt{\Delta_n}\zeta_{t_n}$ is $\mathcal{N}(0, \Delta_n)$. There are two important things that one has to note. The first is that the result in eq. (91) differs from the one obtained by the simple replacement $dW_t = dt\xi_t$ from eq. (89). The second is that for every interval in the sum of eq. (91) we evaluate $G(t)$ at the beginning of the interval, which is important since in the limit $N \to \infty$ the result depends on the point where we take $G(t)$. This is the main difference from the case of Riemann integration.

1.3 Markov process

This process is characterised with a short memory that can be expressed by the following condition:

$$\rho(x_n, t_n|x_{n-1}, t_{n-1}; \ldots; x_0, t_0) = \rho(x_n, t_n|x_{n-1}, t_{n-1}) \qquad \forall n \in \mathbb{N} \;\; \forall t_0, \ldots, t_n \in T \tag{92}$$

This means that the conditional probability that the event x_n occurs at t_n given that the events $x_{n-1} \ldots x_0$ have occured at $t_{n-1} \ldots t_0$, depends only on the last event but not on any of the previous ones. The conditional translation probability describes the process almost completely since every joint probability density function can be rewritten as a product of conditional translational probabilities and the initial density function of a single random variable $\rho(x_0, t_0)$:

$$\begin{aligned} \rho(x_n, t_n; \ldots; x_0, t_0) &= \rho(x_n, t_n|x_{n-1}, t_{n-1} \ldots x_0, t_0)\rho(x_{n-1}, t_{n-1}; \ldots; x_0, t_0) \\ &= \rho(x_n, t_n|x_{n-1}, t_{n-1})\rho(x_{n-1}, t_{n-1}; \ldots; x_0, t_0) \\ &\vdots \\ &= \rho(x_n, t_n|x_{n-1}, t_{n-1})\rho(x_{n-1}, t_{n-1}|x_{n-2}, t_{n-2}) \ldots \rho(x_1, t_1|x_0, t_0)\rho(x_0, t_0) \end{aligned} \tag{93}$$

With this relation one can derive the Chapman-Kolmogorov equation for the conditional translation probability:

$$\rho(x_1, t_1|x_3, t_3) = \int dx_2 \rho(x_1, t_1|x_2, t_2)\rho(x_2, t_2|x_3, t_3) \tag{94}$$

There are three basic types of Markov processes: the Deterministic -, Jump - and Diffusion process. In the first one the sample paths are smooth solutions of a deterministic equation of motion and only the intial conditions are taken to be random. The second one is characterised with discontinuous sample paths broken by instantaneous jumps. The last one has still continuous but not differentiable sample paths. It will be analysed more carefully.

A process that has continuous but nowhere differentiable sample paths fulfills the following equation:

$$d\vec{X}_t = \vec{f}(\vec{X}_t, t)dt + \sigma(\vec{X}_t, t)d\vec{W}_t \qquad \vec{X}_t, \vec{f}(\vec{X}, t) \in \mathbb{R}^n \;\; \sigma(\vec{X}_t, t) \in \mathbb{R}^{n\times m} \;\; \vec{W}_t \in \mathbb{R}^m \tag{95}$$

where $\vec{f}(\vec{X}, t)$ is a continuous differentiable function responsible for the deterministic drift of the trajectories of $\vec{X}_t$ and $\vec{W}_t$ is a Wiener process (called also Brownian motion). If one looks at a single trajectory $x(t)$ and differentiates formally with respect to t one gets the Langevin equation:

$$\dot{\vec{x}}(t) = \vec{f}(\vec{x}(t), t) + \sigma(\vec{x}(t), t)\vec{\xi}(t) \tag{96}$$

with $\langle \xi_{i,t}\xi_{j,t'} \rangle = \delta_{ij}\delta(t - t')$, $i, j = 1, \ldots n$. It can be solved analytically only in few special cases, so we need an appropriate method to calculate it. If we use the Euler-Maruyama method the increments of a single trajectory have the following form:

$$\Delta\vec{x}(t) = \int_t^{t+dt} d\vec{x} = \int_t^{t+dt} \vec{f}(\vec{x}(\tau), \tau)d\tau + \int_t^{t+dt} \sigma(\vec{x}(\tau), \tau)d\vec{w}(\tau) \approx \vec{f}(\vec{x}(t), t)dt + \sigma(\vec{x}(t), t)\vec{\zeta}(t)\sqrt{dt} \tag{97}$$

with $\zeta_t \sim \mathcal{N}(0, 1)$. The discretisation of the first term should be familiar since $f(\vec{x}(t), t)$ is a continuous function and we have a Riemann integral. The discretisation of the second term is already discussed. A trajectory is calculated via the prescription:

$$\begin{aligned} \vec{x}(t_{n+1}) &= \vec{x}(t_n) + \vec{f}(\vec{x}(t_n), t_n)\Delta_n + \sigma(\vec{x}(t_n), t_n).\vec{\zeta}(t_n)\sqrt{\Delta_n} \\ \Delta_n &= t_{n+1} - t_n \qquad\qquad t_0 \le t_1 \le \ldots t_{n-1} \le t_n \ldots \le T \end{aligned} \tag{98}$$

If the functions f, σ fulfill the conditions for an existence of a solution of the stochastic differential equation (see sec. 2 of the appendix), then the method has a strong order of convergence of $1/2$ in the sense that the difference of the exact trajectories $\vec{x}'(t)$ of a process starting at $t_0 = 0$ and its Euler approximation $\vec{x}(t)$ for a special mesh of the time axis fulfills the following relation:

$$\langle \|\vec{X}'_t - \vec{X}_t\|^2 \rangle \le K(T)\Delta^{1/2} \qquad \Delta = \max\{\Delta_1, \Delta_2 \ldots\} \tag{99}$$

where $\| \ldots \|$ is an arbitrary norm and $K(T)$ is some real positive funciton. In this work we use methods with a higher strong order of convergence. Their exact form and the basic idea of their derivation is

given in sec. 1 of the appendix.

In the end one can show (Kramers-Moyal expansion) that the equation of motion for the trajectories of the process defined in eq. (96) with probability density function $\rho(\vec{x},t)$ is equivalent to a Fokker-Planck equation for the conditional translation probability $\rho(\vec{x},t|\vec{x}',t')$:

$$\partial_t\rho(\vec{x},t|\vec{x}',t') = -\partial_{x_j}\left[f_j(\vec{x}(t),t)\rho(\vec{x},t|\vec{x}'t')\right] + \tfrac{1}{2}\partial_{x_i}\partial_{x_j}\left[\mathcal{D}_{ij}\rho(\vec{x},t|\vec{x}',t')\right] \qquad \mathcal{D}_{ij} = \sigma_{il}\sigma_{jl} \tag{100}$$

This relation will be used in the next section.

2 The Wigner formalism

There is a great effort made to represent quantum mechanics using entirely the language of phase space variables like in the classical mechanics. From the Heisenberg uncertainity principle it is clear that the evolution of the system can not be described by a single trajectory in the phase space. One can suggest that instead of a δ-function the state of a quantum mechanical system can be described by some probability density function $p(\{x_i\})$ (x_i are arbitrary variables). In order to describe completely the dynamics of a QM-system one has to define a transformation that maps a density operator $\hat{\rho}$ to a quasi-probability density function $p(\{x_i\})$ and a normal ordered operator $\hat{\Omega}(\{\hat{a_i}^\dagger\hat{a_i}\}_{i\in I})$ to a function of real variables $\Omega(\{x_i\}_{i\in I})$. The expectation value of an observable is then naturally defined as : $\langle\hat{\Omega}\rangle \to \int dx_i p(\{x_i\})\Omega(\{x_i\})$. This map is not uniquely defined. In practice one uses the Q-, P- and Wigner representations [52]. We will concentrate on the last one.

The expression that assigns a quasiprobability density function to a density matrix is the Wigner transform of the density matrix. It is convenient to define it with the use of coherent states:

$$\hat{\rho} \longmapsto \rho_{\mathcal{W}}(\psi,\psi^*) = \int d\eta^* d\eta \; {}_c\langle\psi-\eta/2|\hat{\rho}|\psi+\eta/2\rangle_c e^{-|\psi|^2-1/4|\eta|^2+1/2(\eta^*\psi-\eta\psi^*)} \tag{101}$$

The field ψ can be interpreted as the center of mass coordinate or as a classical trajectory of the system and η as the quantum fluctation around ψ.

The second expression that maps a normal ordered operator to a function of complex variables is:

$$\hat{\Omega}(\hat{a},\hat{a}^\dagger) \longmapsto \Omega_{\mathcal{W}}(\psi,\psi^*) \quad = \quad \int d\eta^* d\eta \; e^{-|\eta|^2/2}\hat{\Omega}(\psi-\eta/2,\psi^*+\eta^*/2), \tag{102}$$

where $\Omega(\psi-\eta/2,\psi^*+\eta^*/2)$ is the normal ordered operator with quantum operators $\hat{a},\hat{a}^\dagger$ replaced by complex numbers $(\psi-\eta/2),(\psi^*+\eta^*/2)$. $\Omega_{\mathcal{W}}$ is called the Weyl symbol of $\hat{\Omega}$. This map is equivalent to representing the normal ordered operator as a function of symmetrically ordered operators and then replacing $\hat{a},\hat{a}^\dagger$ by ψ,ψ^*.

2.1 Truncated Wigner approximation (TWA)

Our aim is to describe the time evolution of an interacting quantum system for which we expect that it evolves closely to a corresponding classical system. We are not interested in the time evolution of the full density matrix but only in the expectation values of some operators. In order to be more concrete consider that the system is described by the Hamiltonian $\hat{H} = \hat{H}_0 + \hat{H}^i$. Then for an arbitrary operator $\hat{\Omega}$ in the Heisenberg picture we have to calculate (notation as in the previous chapter):

$$\langle\hat{\Omega}(t)\rangle = \mathrm{tr}\left[\hat{\rho}(t_0)\left(\hat{T}_c e^{\imath\int_c \hat{H}^i_{H_0}(\tau)d\tau}\hat{\Omega}_{H_0}(t)\right)\right] \tag{103}$$

where c denotes time ordering along the Keldysh contour (see fig. 10) and t_0 is the time where the Schrödinger and Heisenberg pictures coincide.

For this operator one can develop a perturbation theory in quantum fluctuations around the classical path [32]. The zeroth order approximation gives a discrete nonlinear Schrödinger equation (DNSE) and the first order - the TWA. In the latter approximation the evolution of the system still obeys the DNSE

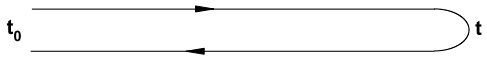

Figure 10: Keldysch contour used in eq. (103).

but one has to average the time dependent expectation values over the initial conditions of the system and over the initial distribution of a set of random variables. The advantage of this formalism is that one can increase the accuracy of the estimated expectation value by including higher order quantum corrections. Here we will not repeat the steps in the derivation of the formalism in [32] since the idea is the same as in the derivation of the path integral in sec. 7 of the appendix, but just briefly discuss the main result of it:

$$\langle\hat{\Omega}(t)\rangle = \int D[\eta,\eta^*]D[\psi,\psi^*]\rho_{\mathcal{W}}(\psi_{t_0},\psi^*_{t_0})\Omega_{\mathcal{W}}\left(\psi_t,\psi^*_t\right)$$
$$\exp\left(\int_{t_0}^{t} d\tau\{\eta^*_\tau\mathcal{L}[\psi_\tau,\psi^*_\tau,\tau]-\eta_\tau\mathcal{L}^*[\psi_\tau,\psi^*_\tau,\tau]\}\right)$$
$$\times\exp\left(\imath\int_{t_0}^{t} d\tau\sum_{n\geq 1}\sum_{m=0}^{2n+1}\frac{\partial^{2n+1}H(\psi_\tau,\psi^*_\tau,\tau)}{\partial\psi^m_\tau\psi^{*2n+1-m}_\tau}\frac{\eta^m_\tau\eta^{*2n+1-m}_\tau}{2^{2n}m!(2n+1-m)!}\right) \tag{104}$$

The fields ψ_t,η_t refer to the classical trajectory and the quantum fluctuations around it and the index t to the time. $D[\eta,\eta^*]=\Pi_{\tau\neq 0,t}d\eta_\tau d\eta^*_\tau$, $D[\psi,\psi^*]=\Pi_\tau d\psi_\tau d\psi^*_\tau$, $\rho_{\mathcal{W}}$, $\Omega_{\mathcal{W}}$ are the Wigner transform of the density matrix and the Weyl symbol of $\hat{\Omega}$ respectively, and $\mathcal{L}_j[\psi_\tau,\psi^*_\tau,\tau]$ stands for the classical differential operator acting on the field ψ_τ [11] :

$$\mathcal{L}_j[\psi_\tau,\psi^*_\tau,\tau]\equiv\frac{d\psi_{j,\tau}}{d\tau}+\imath\frac{\delta H(\psi_\tau,\psi^*_\tau)}{\delta\psi^*_{j,\tau}} \tag{105}$$

If one takes for H the normal ordered Bose-Hubbard Hamiltonian (eq. (156)) and replaces $\hat{a}_j,\hat{a}^\dagger_j$ with ψ_j,ψ^*_j respectively then the equation $\mathcal{L}_j[\psi_\tau,\psi^*_\tau,\tau]$ is equivalent to the DNSE equation:

$$\imath\frac{d\psi_j}{d\tau}=-J\left(\psi_{j+1}+\psi_{j-1}\right)+U|\psi_j|^2\psi_j \tag{106}$$

The last exponent of eq. (104) which contains all higher orders of η in its argument represents the quantum corrections to the classical equation of motion. Neglecting this term we get[12]:

$$\langle\hat{\Omega(t)}\rangle\approx\int d\psi^*_{t_0}d\psi_{t_0}\rho_{\mathcal{W}}(\psi_{t_0},\psi^*_{t_0})\Omega_{\mathcal{W}}(t,\psi_t,\psi^*_t)\delta\big(\mathcal{L}[\psi_\tau,\psi^*_\tau,\tau]\big)\delta\big(\mathcal{L}^*[\psi_\tau,\psi^*_\tau,\tau]\big) \tag{107}$$

[11] One can compare the action given in eq. (104) with the action we used in the last chapter. There are only two significant differences between them. In eq. (104) the path extends only in the range between t_0 and t and in the previous chapter its extension is from $-\infty$ to ∞. In the derivation of the action from the last chapter (see sec. 7 of the appendix) we have argued that the boundary terms appearing at $\pm\infty$ are correctly absorbed in the nonequilibrium GF's. The Keldysh partition function was then of the form:

$$\mathcal{Z}=\int D[\vec{\varphi},\vec{\varphi}^*]e^{i\mathcal{S}}=\int D[\eta,\eta^*]D[\psi,\psi^*]e^{i\mathcal{S}}$$

where in the second step we have performed the transformation

$$\psi=\frac{1}{2}(\varphi^-+\varphi^+)\qquad\qquad\eta=\varphi^--\varphi^+$$

In equation (104) the path has finite extension and going from summation to functional integration the boundary terms at $\tau=t_0$ and $\tau=t$ are kept explicitly. The terms at t_0 are absorbed in the definition of $\rho_{\mathcal{W}}$ and the terms at t are absorbed in the definiton of the Weyl symbol of $\hat{\Omega}$. That is why $D[\eta,\eta^*]=\prod\limits_{\tau\neq 0,t}d\eta_\tau d\eta^*_\tau$, i.e. the boundary terms have been already integrated out.

[12] Use the formula $\delta(f(\psi_{(t)},\psi^*_{(t)}))=\int D[\eta]e^{i2\int d\tau\eta f(\psi_{(\tau)},\psi^*_{(\tau)})}$. The action can in general also contain terms that are quadratic in the quantum fields. These terms can be eliminated with the use of a Hubbard-Stratonovich transformation

$$e^{\frac{1}{2}\alpha\eta^2_{(t)}}=\int D[\xi]e^{-\frac{\xi^2_{(t)}}{2\alpha}+i\eta_{(t)}\xi_{(t)}}.$$

The condition $\mathcal{L}=0$ then corresponds to a Langevin equation (eq.(96)).

where $\psi(0) = \psi_0$. This approximation is called the Truncated Wigner approximation.
In practice this integral is evaluated by sampling a finite number N_T of points from the pdf $\rho_{\mathcal{W}}(\psi(t_0), \psi^*(t_0))$, letting them evolve according to the DNSE's given in the argument of both δ-functions and taking the average of Ω evaluated as follows[13]:

$$\langle \hat{\Omega}(t) \rangle = \frac{1}{N_T} \sum_{i \in I} \Omega_{cl}(t, \psi_i(t), \psi_i^*(t)). \tag{108}$$

The TWA is exact only for harmonic systems. In all other cases, one can improve the approximation by expressing the quantum corrections in the form of stochastic quantum jumps of the trajectories one calculates [42]. Since each jump carries a factor of $\hbar^2$, an expansion in the number of jumps is equivalent to an expansion in powers of the Planck's constant.

In [32, 33] one can see how these corrections are implemented in practice for closed quantum systems. From the results one sees that the TWA is asymptotically correct at short times. However, both the TWA and higher order quantum corrections, fail to reproduce the purely quantum mechanical effects of the system. In [32] the author compares the exact, the TWA and the first quantum correction for a condensate loaded in an optical lattice where the tunneling is completely switched off (J=0) and the initial state is a product of coherent states ($|0\rangle = |\sqrt{N}\rangle_{1c}|\sqrt{N}\rangle_{2c} \ldots$, N - particle number per well). Here both approximations fail to reproduce the periodicity in time of the expectation value $\langle \hat{a}_j \rangle$ for a particular lattice site j.

In open quantum systems, where we have coupling to a thermal bath represented by a set of harmonic oscillators, one obtains a dissipative term (see example in sec. 3) which can be directly added to the DNSE. At large time scales, the effects of dissipation can wash out all the quantum scattering processes and also all purely quantum mechanical effects of the evolution of the system. This motivates us to believe that the TWA is a good approximation for such systems. A discussion about the role of dissipative terms and decoherence to provide the needed quantum-classical correspondence can be found in [47], [35].

2.2 Operator correspondences

The action of an operator $\hat{a}$ on a density operator $\hat{\rho}$ can be mapped onto the action of a differential operator on a P-, Q-, or Wigner function. The idea can be easily illustrated if we work in a basis of coherent states[14].

One has first to define the symmetrically ordered characteristic function:

$$\chi_{\mathcal{W}}(\lambda, \lambda^*) = \mathrm{tr}\left(\hat{\rho} e^{\lambda \hat{a}^\dagger - \lambda^* \hat{a}}\right) = \int d^2\alpha e^{\lambda \alpha^* - \lambda^* \alpha} \rho_{\mathcal{W}}(\alpha, \alpha^*), \tag{109}$$

where $\lambda, \lambda^* \in \mathbb{C}$ and $\hat{a}^\dagger, \hat{a}$ can be any pair of quantum conjugate operators and $d^2\lambda \equiv d\lambda d\lambda^*$. This name comes from the fact that:

$$\langle \{\hat{a}^s \hat{a}^{\dagger r}\}_{sym} \rangle = \frac{\partial^r}{\partial \lambda^r} (-1)^s \frac{\partial^{*s}}{\partial \lambda^{*s}} \chi_{\mathcal{W}}(\lambda, \lambda^*)|_{\lambda=0} = \int d^2\alpha \alpha^s \alpha^{*r} \rho_{\mathcal{W}}(\alpha, \alpha^*). \tag{110}$$

Here we show how $\hat{a}\hat{\rho}$ is mapped onto $\left(\alpha + \frac{1}{2}\partial_{\alpha^*}\right) \rho_{\mathcal{W}}(\alpha, \alpha^*)$. One first evaluates:

$$\begin{aligned}
\mathrm{tr}\left(\hat{a}\hat{\rho} e^{\lambda \hat{a}^\dagger - \lambda^* \hat{a}}\right) &= \mathrm{tr}\left(\hat{\rho} e^{\lambda \hat{a}^\dagger} e^{-\lambda^* \hat{a}} e^{-|\lambda|^2/2} \hat{a}\right) \\
&= \mathrm{tr}\left(\hat{\rho} e^{\lambda \hat{a}^\dagger} e^{-|\lambda|^2/2} e^{-\lambda^* \hat{a}} \hat{a}\right) \\
&= \mathrm{tr}\left(\hat{\rho} e^{\lambda \hat{a}^\dagger} e^{-|\lambda|^2/2} \left(-\partial_{\lambda^*} e^{-\lambda^* \hat{a}}\right)\right) \\
&= \mathrm{tr}\left(\hat{\rho} e^{\lambda \hat{a}^\dagger} \left(\left(\tfrac{1}{2}\lambda - \partial_{\lambda^*}\right) e^{-\lambda^* \hat{a}} e^{-|\lambda|^2/2}\right)\right) \\
&= \left(\tfrac{1}{2}\lambda - \partial_{\lambda^*}\right) \mathrm{tr}\left(\hat{\rho} e^{\lambda \hat{a}^\dagger} e^{-\lambda^* \hat{a}} e^{-|\lambda|^2/2}\right) \\
&= \left(\tfrac{1}{2}\lambda - \partial_{\lambda^*}\right) \chi_{\mathcal{W}}(\lambda, \lambda^*)
\end{aligned} \tag{111}$$

[13] One has to keep in mind that the map $\hat{\rho} \to \rho_{\mathcal{W}}$ does not carry over all the properties of $\hat{\rho}$ to $\rho_{\mathcal{W}}$. The Wigner function can take also negative values and special care is needed evaluating the average of Ω. In this work we always use coherent states as initial condition for $\hat{\rho}$ which are mapped to a non-negative Wigner function.

[14] A coherent state $|\psi\rangle$ is defined as an eigenstate of the annihilation operator $\hat{a}$: $|\psi\rangle_c = \exp(\sum_i \psi_i \hat{a}_i^\dagger)|vac\rangle$. The scalar product of two operators is: $\langle\psi|\phi\rangle = \exp(\sum_i \psi_i^* \phi_i)$. The identity operator is given as: $\int D[\phi] \exp(-\sum_i \phi_i^* \phi_i)\, |\phi\rangle\langle\phi| = 1$.

Taking $\lambda = 0$ on both sides confirms the consistence with eq (110). One takes the Fourier transform of the last expression and after partial integration obtains:

$$\tfrac{1}{\pi^2}\int d^2\lambda e^{\lambda^*\alpha-\lambda\alpha^*}\left(\tfrac{1}{2}\lambda-\partial_{\lambda^*}\right)\chi_W(\lambda,\lambda^*)=\left(\tfrac{1}{2}\partial_{\alpha^*}+\alpha\right)\rho_{\mathcal{W}}(\alpha,\alpha^*). \tag{112}$$

Similarly, the other correspondences are:

$$\begin{array}{rcl}\hat{a}^\dagger\hat{\rho} & \leftrightarrow & \left(\alpha^*-\frac{1}{2}\partial_\alpha\right)\rho_{\mathcal{W}}(\alpha,\alpha^*)\\ \hat{\rho}\hat{a} & \leftrightarrow & \left(\alpha-\frac{1}{2}\partial_{\alpha^*}\right)\rho_{\mathcal{W}}(\alpha,\alpha^*)\\ \hat{\rho}\hat{a}^\dagger & \leftrightarrow & \left(\alpha^*+\frac{1}{2}\partial_\alpha\right)\rho_{\mathcal{W}}(\alpha,\alpha^*).\end{array} \tag{113}$$

One has to keep in mind that these correspondences are not exact since we do not take $\lambda = 0$ in the middle step. In the end we also apply the following transformation:

$$\begin{array}{rclcrcl}\alpha & = & z_1+\imath z_2 & & \partial_\alpha & = & \frac{1}{2}\left(\partial_{z_1}-\imath\partial_{z_2}\right)\\ \alpha^* & = & z_1-\imath z_2 & & \partial_{\alpha^*} & = & \frac{1}{2}\left(\partial_{z_1}+\imath\partial_{z_2}\right).\end{array} \tag{114}$$

2.3 Mapping of a master equation in Lindblad form to a set of Langevin equations

In this thesis we will often work with the master equation in Lindblad form:

$$\tfrac{d}{dt}\hat{\sigma} \;=\; \tfrac{1}{i}[\hat{H},\hat{\sigma}]+\hat{\mathcal{L}}\hat{\sigma}. \tag{115}$$

The operators $\hat{\sigma}$, $\hat{H}$ are the density matrix and the Hamiltonian of the system we are interested in. The properties of the (in most cases much larger) enviroment are comprised in the superoperator $\hat{\mathcal{L}}$ that acts on $\hat{\sigma}$. In the particular case of a single quantum dot coupled to a Markovian reservoir we use the following ansatz:

$$\begin{array}{rcll}\hat{H} & = & \Delta\hat{a}^\dagger\hat{a}+\frac{U}{2}\hat{a}^\dagger\hat{a}^\dagger\hat{a}\hat{a} & \\ \hat{\mathcal{L}}(\hat{\sigma}) & = & -\Gamma(n+1)[\hat{a}^\dagger\hat{a}\hat{\sigma}+\hat{\sigma}\hat{a}^\dagger\hat{a}-2\hat{a}\hat{\sigma}\hat{a}^\dagger]-\Gamma n[\hat{a}\hat{a}^\dagger\hat{\sigma}+\hat{\sigma}\hat{a}\hat{a}^\dagger-2\hat{a}^\dagger\hat{\sigma}\hat{a}] & \qquad \Gamma,n\in\mathbb{R}_+.\end{array} \tag{116}$$

Γ is a measure for the refreshment rate of the particles in the dot. If it is the largest scale of the system then the mean occupation number of the particles in the dot is equal to n. The second term in the Hamiltonian represents an on-site particle-particle interaction. All varibles are discussed in detail in sec. 4.1. Here it is important only that this form of $\hat{\mathcal{L}}$ preserves all properties of the density matrix (positive definiteness, hermiticity, trace equal to one) as necessary for a consistent formalism [40]. By the use of the operator correspondences given in eq. (113) for every operator $\hat{a}_j$ $(j = 1,\ldots.\mathcal{N})$ of the problem and $\frac{d}{dt}\hat{\rho} \leftrightarrow \frac{d}{dt}\rho_{\mathcal{W}}$ one gets in general a differential equation of the form:

$$\tfrac{d}{dt}\rho_{\mathcal{W}}(\vec{z},t) \;=\; \left(-\nabla_{\vec{z}}\cdot\vec{f}(\vec{z},t)+\tfrac{1}{2}\partial_{z_i}\partial_{z_j}\mathcal{D}_{ij}+\mathcal{R}\right)\rho_{\mathcal{W}}(\vec{z},t) \qquad \vec{z}\in\mathbb{R}^{2\mathcal{N}}. \tag{117}$$

where $\mathcal{R}$ denotes all terms that contain at least three or more powers of a differential operator ∂_{z_j} $(j = 1,\ldots 2\mathcal{N})$. We can map this equation to an equation of motion for the conditional translation probability $\rho_{\mathcal{W}}(\vec{z},t|\vec{z}',t')$:

$$\begin{array}{rcl}\rho_{\mathcal{W}}(\vec{z}_1,t_1) & = & \int d\vec{z}_3\rho_{\mathcal{W}}(\vec{z}_1,t_1;\vec{z}_3,t_3)=\int d\vec{z}_3\rho_{\mathcal{W}}(\vec{z}_1,t_1|\vec{z}_3,t_3)\rho_{\mathcal{W}}(\vec{z}_3,t_3)\\ \frac{d}{dt_1}\rho_{\mathcal{W}}(\vec{z}_1,t_1) & = & \int d\vec{z}_3\frac{d}{dt_1}\left(\rho_{\mathcal{W}}(\vec{z}_1,t_1|\vec{z}_3,t_3)\right)\rho_{\mathcal{W}}(\vec{z}_3,t_3).\end{array} \tag{118}$$

Neglecting the $\mathcal{R}$-term we get in general a Fokker-Planck equation for $\rho_{\mathcal{W}}(\vec{z},t|\vec{z}',t')$. Assuming that $\rho_{\mathcal{W}}(\vec{z},t)$ is the pdf of a Markovian process with trajecories $\vec{z}(t)$, we can use the fact that the Fokker-Planck equation for the conditional translational probability function is equivalent to the equation of motion for the trajectories of the process $\vec{Z}_t$:

$$d\vec{Z}_t=\vec{f}(\vec{Z}_t,t)+\sigma(\vec{Z}_t,t).d\vec{W}_t, \qquad \vec{Z}_t\in\mathbb{R}^{2\mathcal{N}},\sigma(\vec{Z}_t,t)\in\mathbb{R}^{2\mathcal{N}\times m},W_t\in\mathbb{R}^m \tag{119}$$

where $\vec{W}_t$ is a Wiener process. The corresponding Langevin equation for the trajectory of the process $\vec{Z}_t$ is given by:

$$\tfrac{d}{dt}\vec{z}(t)=\vec{f}(\vec{z},t)+\sigma\cdot\vec{\xi}(t) \tag{120}$$

with $\vec{\xi}(t)$ - Gaussian white noise. For the particular problem given in eq. (116), we have $\mathcal{N} = 1$, $\mathcal{R} = -\frac{U}{8}(z_1\partial_{z_2} - z_2\partial_{z_1})(\partial_{z_1}^2 + \partial_{z_2}^2)$, $\sigma = \sqrt{\Gamma(n+1/2)}\mathbb{I}_{2\times 2}$ and the Langevin equation has the form:

$$\frac{d}{dt}\begin{bmatrix} z_1 \\ z_2 \end{bmatrix} = \begin{bmatrix} +\Delta z_2 - \Gamma z_1 \\ -\Delta z_1 - \Gamma z_2 \end{bmatrix} + U\begin{bmatrix} +z_2^3 + z_1^2 z_2 - z_2 \\ -z_1^3 - z_2^2 z_1 + z_1 \end{bmatrix} + \sqrt{\Gamma(n+1/2)}\begin{bmatrix} \xi_1(t) \\ \xi_2(t) \end{bmatrix}. \tag{121}$$

One can obtain the time evolution of the Wigner function $\rho_{\mathcal{W}}$ by calculating a finite number (N_T) of trajectories $\vec{z}^j(t)$, $j = 1 \dots N_T$, where the initial conditions $\vec{z}(t_0)$ at t_0 are sampled according to $\rho_{\mathcal{W}}(\vec{z}, t_0)$.

3 Connection between the Nonequilibrium Green's function method and the master equation in Lindblad form

In section 2, we have argued that the only quantum effects of the system dynamics that are taken into account in the calculation of an observable $\langle\hat{\mathcal{O}}\rangle$ in the TWA are captured at two points. The first one are the probabilistic initial conditions and the second one is the fact that we use a symmetrised operator $\hat{\mathcal{O}}_{sym}$ instead of $\hat{\mathcal{O}}$ that acts at the turning point of the time contour. The initial conditions do not play a role since the system we are interested in reaches a unique steady state. One can now try to change the contour in a way that its ends are at $t = -\infty$ and the turning point is at $t = \infty$. Since we are interested in the steady state properties of the system and not in the transient phenomena we can absorb the boundary terms of the path integral that describes the Keldysh partition function ($\hat{O} = \hat{\mathbb{I}}$) and get an expression like eq. (24):

$$\begin{aligned} \mathcal{Z} &= \int D[\vec{\varphi}, \vec{\varphi}^*] e^{i\mathcal{S}} \\ i\mathcal{S} &= i\int \tfrac{dw}{2\pi}\vec{\varphi}^\dagger \mathcal{G}^{-1}\vec{\varphi}, \end{aligned} \tag{122}$$

where $\mathcal{S}$, $\mathcal{G}$ are the action and nonequilibrium Green's function of the system. So both methods are equivalent as soon as one is interested only in steady state properties of the system and the Hamiltonian is quadratic in the fields.
In subsection 3.1, we show the action of a system described by the Langevin equation (96). This will allow us to apply the approximations used in the last chapter and compare the results with those from the TWA and Quantum jump approach 3.
In subsection 3.2, we discuss how the Langevin equation is modified if we consider a system with more general reservoirs.

3.1 Mapping of the Langevin equation to an action

The problem in performing this mapping lies in the fact that we do not have started with a particular Hamiltonian, but have used a Master equation in Lindblad form as an ansatz. The Langevin equations obtained after the Wigner mapping can be converted into a proper classical action. This procedure which is in essence an inversion of what was done in [32] and mentioned briefly in section 2 was formulated by Martin, Sigga and Rose (MSR)[15] [48]. In the following we start from the result obtained by the MSR-method and show that it reproduces the correct Langevin equations, i.e. we guess the form of the action and show that it is the right one. This is done for the simplest case of a quantum dot coupled to a bosonic reservoir. The generalisation to the case of larger systems is straightforward.
The current system of interest is described by the following action (w-dependence dropped):

$$\begin{aligned} i\mathcal{S} &= i\mathcal{S}_0 + i\mathcal{S}_{int} \\ i\mathcal{S}_0 &= i\int \tfrac{dw}{2\pi}\vec{\varphi}^\dagger\mathcal{G}^{-1}\vec{\varphi} \\ i\mathcal{S}_{int} &= i\int \tfrac{dw}{2\pi}\tfrac{U}{2}\left(\varphi_-^*\varphi_-^*\varphi_-\varphi_- - \varphi_+^*\varphi_+^*\varphi_+\varphi_+\right) \\ \mathcal{G}^{-1} &= \sigma_z(w-\Delta) - \textstyle\sum_k |\gamma_k|^2\sigma_z g_{kk}\sigma_z \\ \vec{\varphi} &= (\varphi_- \;\; \varphi_+)^T. \end{aligned} \tag{123}$$

The reservoir GF g_{kk} is given in eq. (20). We first set $U = 0$ and perform a Wigner transformation of the fields (the Jacobian of the transformation is equal to one):

$$\begin{bmatrix} \varphi_- \\ \varphi_+ \end{bmatrix} = A^{-1}\begin{bmatrix} \psi \\ \eta \end{bmatrix}; \qquad A^{-1} = \begin{bmatrix} 1 & 1/2 \\ 1 & -1/2 \end{bmatrix}. \tag{124}$$

[15] A good explanation of the method can be also found in [26]

The new fields ψ/η are called quantum/classical fields. In this basis the action is expressed in terms of retarded, advanced and Keldysh GF's:

$$\mathcal{S} = \int \tfrac{dw}{2\pi}[\psi^*,\eta^*]\begin{bmatrix} 0 & (w-\Delta)-i\Gamma \\ (w-\Delta)+i\Gamma & i2\Gamma(n+1/2)\end{bmatrix}\begin{bmatrix}\psi\\ \eta\end{bmatrix} \tag{125}$$

where $(\mathcal{G}^{-1})^{R(A)} = (\mathcal{G}^{R(A)})^{-1} = (w-\Delta)+(-)i\Gamma$, $\frac{1}{2}(\mathcal{G}^{-1})^K = i2\Gamma(n+1/2)$. We set the self-energy contributions coming from the reservoir to be energy independent, i.e. $n=\text{const}$, $\Gamma=\text{const}$ and express the action as a time integral over the Fourier transformed fields $\psi(w)=\int dt e^{-iwt}\psi(t)$. The fields ψ,η are rewritten as a sum of their real and imaginary parts and for the terms quadratic in $\Re\eta,\Im\eta$ one performs a Hubbard-Stratonovich transformation:

$$e^{-\frac{1}{2}\int d\tau(2\Re\eta)^2\Gamma(n+\frac{1}{2})} = \int D[\zeta]e^{-\frac{1}{2}\int d\tau\frac{\zeta^2}{\Gamma(n+1/2)}+i2\int d\tau(\Re\eta)\zeta}. \tag{126}$$

The Keldysh partition function then has the form:

$$\begin{aligned}\mathcal{Z} &= \int D[\zeta_1,\zeta_2]\exp\{-\tfrac{1}{2}\tfrac{\zeta_1^2+\zeta_2^2}{\Gamma(n+1/2)}\}\int D[\Re\psi,\Im\psi]\int D[\Re\eta,\Im\eta]\\ &\quad \exp\{i2\int d\tau(\Re\eta)[-\Delta(\Re\psi)-\Gamma(\Im\psi)-\tfrac{d}{d\tau}(\Im\psi)+\zeta_1]\}\\ &\quad \exp\{i2\int d\tau(\Im\eta)[-\Delta(\Im\psi)+\Gamma(\Re\psi)+\tfrac{d}{d\tau}(\Re\psi)+\zeta_2]\}\\ &= \int D[\zeta_1,\zeta_2]\exp\{-\tfrac{1}{2}\tfrac{\zeta_1^2+\zeta_2^2}{\Gamma(n+1/2)}\}\int D[\Re\psi,\Im\psi]\delta(\ldots)\delta(\ldots).\end{aligned} \tag{127}$$

The arguments of both δ-functions give the following equation of motion (EoM)[16]:

$$\frac{d}{dt}\begin{bmatrix}\Re\psi\\ \Im\psi\end{bmatrix} = \vec{f}(\Re\psi,\Im\psi)+\sigma\cdot\begin{bmatrix}\zeta_1(t)\\ \zeta_2(t)\end{bmatrix} \qquad \vec{f}(\Re\psi,\Im\psi)=\begin{bmatrix}+\Delta\Im\psi-\Gamma\Re\psi\\ -\Delta\Re\psi-\Gamma\Im\psi\end{bmatrix} \qquad \sigma=\mathbb{I}_{2\times2}. \tag{128}$$

The terms ζ_1,ζ_2 should be interpreted as stochastic processes which fulfill the condition $\langle\zeta_{i,t}\zeta_{j,t'}\rangle = \delta_{ij}\delta(t-t')\Gamma(n+1/2)$. In the equation above, one can also use a white noise process $\vec{\xi}_t$ with $\langle\xi_{i,t}\xi_{j,t'}\rangle = \delta_{ij}\delta(t-t')$ and $\sigma_{ij}=\sqrt{\Gamma(n+1/2)}\delta_{ij}$[17] . In order to calculate an observable that depends on classical fields one has to sample a finite number of $\vec{\psi}=(\Re\psi,\Im\psi)^T$ points, where $\Re\psi,\Im\psi$ are arbitrary since their initial distribution is not important for the steady state. One lets $\vec{\psi}$ evolve in time according to the equation of motion (EoM) given in the argument of the δ-function in eq. (127). At $t\to\infty$, a steady state must have been reached. Because of the probabilistic nature of ζ_1,ζ_2, one has to perform, again, many realisations of the trajectory $\vec{\psi}(t)$ (add an additional subscript j to count the different realisations). The expectation value of any arbitrary observable $\mathcal{O}$ at $t\to\infty$ that depends on classical fields after calculating N_T trajectories is given by:

$$\tfrac{1}{N_T}\textstyle\sum_{j=1}^{N_T}\mathcal{O}(\vec{\psi}_j(t)). \tag{129}$$

This is the same formula as the one used in the TWA (eq. (108)). The value of an observable $\mathcal{O}$ coincides with the corresponding value obtained in the TWA if the equation of motion in the arguments of the δ-function (eq. (127),(128)) coincides with the equation of motion of the trajectories in the TWA (eq. (121)). This is indeed the case if one identifies $\Re\psi\equiv z_1$, $\Im\psi\equiv z_2$. So we have shown that if we are only interested in the steady state properties of the system, the action (eq. (127)) is an equivalent description of the physics described by the Master equation in Lindblad form:

$$\begin{aligned}\tfrac{d}{dt}\hat{\rho} &= -i[\hat{H},\hat{\rho}]+\hat{\mathcal{L}}(\hat{\rho})\\ \hat{H} &= \Delta\hat{a}^\dagger\hat{a}\\ \hat{\mathcal{L}}(\hat{\rho}) &= -\Gamma(n+1)[\hat{a}^\dagger\hat{a}\rho+\hat{\rho}\hat{a}^\dagger\hat{a}-2\hat{a}\hat{\rho}\hat{a}^\dagger]-\Gamma[\hat{a}\hat{a}^\dagger\hat{\rho}+\hat{\rho}\hat{a}\hat{a}^\dagger-2\hat{a}^\dagger\hat{\rho}\hat{a}].\end{aligned} \tag{130}$$

[16] In order to have full equivalence one has to change $\zeta_1\to-\zeta_1$ in the δ-function in eq. (127). This does not change the stochastic equation since the probability density function (pdf) of the stochastic process is a Gaussian with zero mean and theere is no correlation between ζ_1 and ζ_2.

[17] One can check that:

$$\langle(\sigma_{ik}\xi_{k,t})(\sigma_{jl}\xi_{l,t'})\rangle = \sigma_{ik}\sigma_{jl}\langle\xi_{k,t}\xi_{l,t'}\rangle = \Gamma(n+1/2)\delta_{ij}\delta(t-t') = \langle\zeta_{i,t}\zeta_{j,t'}\rangle.$$

If we include the on-site interaction in the system and perform the same steps as we did for the noninteracting part of the action $\mathcal{S}_0$ we get:

$$\begin{aligned} i\mathcal{S}_{int} &= -i\int \tfrac{dw}{2\pi}\tfrac{U}{2}(\varphi_-^*\varphi_-^*\varphi_-\varphi_- - \varphi_+^*\varphi_+^*\varphi_+\varphi_+) \\ &= -i\tfrac{U}{2}\int d\tau\big[(\psi^{*2}\psi\eta + \eta^*\psi^*\psi^2) + (\eta^{*2}\eta\psi + \psi^*\eta^*\eta^2)\big] \\ &= -i2U\int d\tau \Re\eta\Re\psi(\Re\psi^2+\Im\psi^2) - i2U\int d\tau\Im\eta\Im\psi(\Re\psi^2+\Im\psi^2) + \text{terms cubic in } \eta. \end{aligned} \tag{131}$$

The terms cubic in the quantum fields are neglected. The other linear in η, η^* (called also classical part of the interaction) change the equation of motion (EoM) in the δ-functions such that the EoM for the classical fields for a system of a single quantum dot is given by:

$$\frac{d}{dt}\begin{bmatrix}\Re\psi\\ \Im\psi\end{bmatrix} = \vec{f}(\Re\psi,\Im\psi) + \sigma\cdot\begin{bmatrix}\zeta_1(t)\\ \zeta_2(t)\end{bmatrix} \qquad \vec{f}(\Re\psi,\Im\psi) = \begin{bmatrix}+\Delta\Im\psi - \Gamma\Re\psi\\ -\Delta\Re\psi - \Gamma\Im\psi\end{bmatrix} + U\begin{bmatrix}+\Im\psi^3 + \Re\psi^2\Im\psi\\ -\Re\psi^3 - \Im\psi^2\Re\psi\end{bmatrix} \qquad \sigma = \mathbb{I}_{2\times 2}, \tag{132}$$

where $\langle\zeta_{i,t}\zeta_{j,t'}\rangle = \delta_{ij}\delta(t-t')\Gamma(n+1/2)$. If one compares it with the corresponding eq. obtained through the TWA, we see that they are similar. The only difference lies in the fact that in the TWA we have interaction terms linear in the fields. They can be absorbed by the energy levels of the dots $\Delta \to \Delta - U$. In the case of large occupation numbers of the dots (1000 particles per site) a typical value of the interaction will be $U/J \sim 10^{-3}$, meaning that it will change the position of the energy level insignificantly.

3.2 Generalisation to arbitrary reservoirs

By now we have only dealt with stochastic processes driven by a white noise, which is not the common physical situation. A good understanding how the noise changes and how the memory is incorporated into the system can be gained if one considers an arbitrary but physically realistic density of states of the bosonic reservoir. The action can be obtained in the same way as we already did before but without performing a Fourier transformation of the bosonic and quantum dot Green's functions. After a Wigner transformation, one obtains the following action:

$$i\mathcal{S} = i\int d\tau_1 d\tau_2 \begin{bmatrix}\psi^*_{(\tau_1)} & \eta^*_{(\tau_2)}\end{bmatrix}\begin{bmatrix} 0 & \delta_{(\tau_1-\tau_2)}i\partial_{\tau_2} - 2i\tilde{\Gamma}_{(\tau_1-\tau_2)}\theta_{(\tau_2-\tau_1)} \\ \delta_{(\tau_1-\tau_2)}i\partial_{\tau_2} + 2i\tilde{\Gamma}_{(\tau_1-\tau_2)}\theta_{(\tau_1-\tau_2)} & 2i(\tilde{\Gamma}(n+1/2))_{(\tau_1-\tau_2)}\end{bmatrix}\begin{bmatrix}\psi_{(\tau_2)}\\ \eta_{(\tau_2)}\end{bmatrix}, \tag{133}$$

where $\tilde{\Gamma}_{(t)} = \int \frac{dw}{2\pi}\Gamma_{(w)}e^{iwt}$ and $(\tilde{\Gamma}(n+1/2))_{(t)} = \int \frac{dw}{2\pi}\Gamma_{(w)}(n_{(w)}+1/2)e^{iwt}$. If we assume that the density of states of the reservoir $D_{(w)}$ and the reservoir-dot coupling $\gamma_{(w)}$ are real functions, then $\Gamma_{(w)}$ is real and its Fourier transform fulfills the relation $\Gamma^*_{(t)} = \Gamma_{(-t)}$. With this relation, one can show that the Keldysh term quadratic in the quantum field η contains a real symmetric matrix $\Sigma_{(\tau_i,\tau_j)} = \Sigma_{(\tau_i-\tau_j)}$:

$$-\tfrac{1}{2}\int d\tau_1 d\tau_2 \begin{bmatrix}2\Re\eta_{(\tau_1)} & 2\Im\eta_{(\tau_1)}\end{bmatrix}\underbrace{\begin{bmatrix}\Re(\tilde{\Gamma}(n+1/2))_{(\tau_1-\tau_2)} & -\Im(\tilde{\Gamma}(n+1/2))_{(\tau_1-\tau_2)}\\ \Im(\tilde{\Gamma}(n+1/2))_{(\tau_1-\tau_2)} & \Re(\tilde{\Gamma}(n+1/2))_{(\tau_1-\tau_2)}\end{bmatrix}}_{\Sigma_{(\tau_1-\tau_2)}}\underbrace{\begin{bmatrix}2\Re\eta_{(\tau_2)}\\ 2\Im\eta_{(\tau_2)}\end{bmatrix}}_{2\vec{\eta}_{(\tau_2)}}, \tag{134}$$

where $[\Re(\Gamma(n+1/2))]_{ij} = \Re(\Gamma(n+1/2)_{(\tau_i-\tau_j)})$, $[\Im(\Gamma(n+1/2))]_{ij} = \Im(\Gamma(n+1/2)_{(\tau_i-\tau_j)})$. Discretising the time into $\mathcal{N}-1$ intervals one can again apply the Hubbard-Stratonovich transformation for the $2\mathcal{N}\times 2\mathcal{N}$ Σ-matrix (we also assume that it is positive definite):

$$e^{-\frac{1}{2}\int d\tau_1 d\tau_2 (2\vec{\eta}^T_{(\tau_1)})\Sigma_{(\tau_1-\tau_2)}(2\vec{\eta}_{(\tau_2)})} = e^{-\frac{1}{2}\int d\tau_1 d\tau_2 \vec{\zeta}_{(\tau_1)}\Sigma^{-1}_{(\tau_1-\tau_2)}\vec{\zeta}_{(\tau_2)}} e^{2i\int d\tau \vec{\eta}^T_{(\tau)}\vec{\zeta}_{(\tau)}} \tag{135}$$

with $(\Sigma^{-1})_{(\tau_1,\tau_2)} = (\Sigma^{-1})_{(\tau_1-\tau_2)}$ defined such that $\int d\tau_2 \Sigma_{(\tau_1-\tau_2)}\Sigma^{-1}_{(\tau_2-\tau_3)} = \delta_{(\tau_1-\tau_3)}$. The two noise processes $\zeta_{A,t}, \zeta_{B,t}$ are correlated if $\Im\tilde{\Gamma}_{(t)} \neq 0$ (i.e. if the function $\Gamma_{(w)}$ has nonzero odd contribution since this part survives an integration weighted with $i\sin(-wt) = \Im(e^{-iwt})$). Their autocorrelation is also in general nonzero for different times because of the nonzero off-diagonal terms of the four block-matrices contained in Σ.

After integrating out the quantum fields of the Keldysh partition function one gets two δ-functions whose arguments contain the following set of differential equations:

$$\tfrac{d}{dt}\begin{bmatrix}\Re\psi_{(t)}\\ \Im\psi_{(t)}\end{bmatrix} = \begin{bmatrix}\Delta\Im\psi_{(t)} & -\int_\infty^t d\tau(2\Re\tilde{\Gamma}_{(t-\tau)}\Re\psi_{(\tau)} - 2\Im\tilde{\Gamma}_{(t-\tau)}\Im\psi_{(\tau)})\\ -\Delta\Re\psi_{(t)} & -\int_\infty^t d\tau(2\Im\tilde{\Gamma}_{(t-\tau)}\Re\psi_{(\tau)} + 2\Re\tilde{\Gamma}_{(t-\tau)}\Im\psi_{(\tau)})\end{bmatrix} + \begin{bmatrix}-\zeta_{B(t)}\\ \zeta_{A(t)}\end{bmatrix}. \tag{136}$$

Besides the form of the noise process which we have already mentioned, the inclusion of a more complex bath leads to the appearance of memory integrals. The current value of the field $\psi_{(t)}$ depends not only on its latest value (which is characteristic for a Markov process), but also depends on its previous values since both integrals in eq. (136) are only over times smaller than t. The importance of the past values of ψ for its future evolution depends on $\tilde{\Gamma}$. With an increase of the number of bath modes and the frequency range they are distributed in, the function $\tilde{\Gamma}_{(t)}$ decays faster for $|t| > 0$. In the limit where the bath contains modes, equally distributed in the whole range $w \in (-\infty, \infty)$, the function $\tilde{\Gamma}_{(t)}$ equals zero for $t \neq 0$ and one reaches the white noise (Markovian) limit. The memory integrals now only contain the latest value of ψ and the autocorrelation function of the noise process $\vec{\zeta}_t$ becomes a δ-function. In the opposite limit, when the frequency range of bath modes decrease, the correlation function $\tilde{\Gamma}_{(t)}$ decays slowly. If, at some point, one considers that the number of modes is finite, the motion of the system becomes completely deterministic and the evolution of the trajectory $\psi_{(t)}$ depends only on the initial conditions of the system[18].
In principle, it makes no sense to solve this equation numerically if we deal with an action that is quadratic in its fields, since the exact solution can be obtained much easier with the formalism of the previous chapter. But if the classical part of the on-site interaction $\frac{U}{2}\hat{a}^\dagger\hat{a}^\dagger\hat{a}\hat{a}$ is added, the nonequilibrium GF formalism is not capable of solving this problem exactly. The set of Langevin equations similar to those in eq. (136) is still exact, so one can try to solve them numerically. The realisation of this task is not trivial. The discretisation of the time evolution and the calculation of the time integrals of an equation like eq. (136) should not be a serious problem, since the integration is only over past states of the trajectory and one can use an explicit numerical method to do this. The simulation of a stochastic process with arbitrary autocorrelation function is in principle possible for a partition of the time intervall into $\mathcal{N}$ parts if $\mathcal{N}$ is small. In this case one can generate a collection of random variables Y_{t_j} $(j = 0, \ldots, \mathcal{N}; \quad t_i < t_j \text{ for } i < j)$ with the desired autocorrelation sequence $\{\tilde{\Gamma}_{(t_0)}, \ldots, \tilde{\Gamma}_{(t_\mathcal{N})}\}$. The random variable Y_{t_j} is generated iteratively from the previous random variables of the sequence and with the help of an additional set of $\mathcal{N}+1$ independent normally distributed random variables ζ_{t_j} [44]. However, the generation of the coefficients of the iterative formula and the memory needed to save them are operations of complexity $\mathcal{O}(\mathcal{N}^3)$ and $\mathcal{O}(\mathcal{N}^2)$ respectively. This limits the range of applicability of the numerical method. One can find faster methods for generation of a collection of random variables but they work only for specific collections of autocorrelation functions.

4 Quantum dot coupled to a Markovian reservoir

In the first subsection, we start from a problem described by the full density matrix of the system plus enviroment and reduce it to a problem for the smaller system density matrix. Doing this, we motivate the form of the Lindblad operator given in sec. 2.3 and explain its physical meaning. In the second subsection, we apply all methods discussed in this chapter to solve this problem in order to have a better understanding of how the methods work and what are their drawbacks and advantages.

4.1 Motivation of the Master equation in Lindblad form

Given the Hamiltonian $\hat{H} = \hat{H}_D + \hat{H}_R + \hat{H}^i$ where $\hat{H}_D = \Delta\hat{a}^\dagger\hat{a}$ describes the only energy level of the first system, $\hat{H}_R = \sum_k \varepsilon_k \hat{R}_k^\dagger \hat{R}_k$ - the bosonic bath and $\hat{H}^i = \sum_k \left(\gamma_k \hat{R}_k \hat{a}^\dagger + \gamma_k^* \hat{R}_k^\dagger \hat{a}\right)$ - the coupling between the two systems. Our aim is to find the time dependence of the reduced density operator $\hat{\sigma}$. In order to do this, we have to reduce the von Neumann equation, which describes the time dependence of the density operator of the whole system, to an equation of motion of the reduced density matrix $\hat{\sigma}$. It is appropriate to use the Interaction picture representation for the following calculations. The von

[18] On can, of course, make the motion indeterministic again by assuming that the bath is represented by a finite set of oscillators whose initial conditions are unknown and obey some distribution. In most problems, one often chooses that they obey the Boltzmann statistics, which is parametrised by the temperature T. In this case, the memory of the system (i.e. the decay of $\tilde{\Gamma}_{(t)}$) depends on T. For small T the Boltzmann distribution $p_{(w)}$ is more condensed in the sense that almost the whole part of the area under the graph of $p_{(w)}$ comes from a small frequency intervall. This means that $\tilde{\Gamma}$ decays slower. In the high temperature limit however, the spread of the distribution function becomes so large that $\tilde{\Gamma}_{(t)}$ practically decays instantaneously and one again reaches the situation where $\psi_{(t)}$ is driven by a white noise. So one can say that the white noise limit is reached in the regime of high temperatures.

Neumann equation in this representation is given by ($\hat{H}_0 = \hat{H}_D + \hat{H}_R$):

$$\begin{aligned} i\hbar\tfrac{d}{dt}\hat{\rho}_{H_0}(t) &= \left[\hat{H}^i_{H_0}(t), \hat{\rho}_{H_0}(t)\right] \\ \hat{H}^i_{H_0}(t) &= e^{\frac{i}{\hbar}\hat{H}_0(t-t_r)}\hat{H}^i e^{-\frac{i}{\hbar}\hat{H}_0(t-t_r)} \\ \hat{\rho}_{H_0}(t) &= e^{\frac{i}{\hbar}\hat{H}_0(t-t_r)}\hat{\rho} e^{-\frac{i}{\hbar}\hat{H}_0(t-t_r)}, \end{aligned} \tag{137}$$

where the subscript H_0 indicates that we define the operators in the interaction picture, $\hat{\rho}(t)$ is the density operator in the Schrödinger picture and t_r is the time where both pictures coincide. We integrate the last line of eq. (137):

$$\hat{\rho}_{H_0}(t) = \hat{\rho}_{H_0}(-\infty) + \tfrac{1}{\imath\hbar}\int_{-\infty}^{t} dt' \left[\hat{H}^i_{H_0}(t'), \hat{\rho}_{H_0}(t')\right]. \tag{138}$$

Then we use this ansatz for $\rho_{H_0}(t)$ and replace $\rho_{H_0}(t')$ with it:

$$\hat{\rho}_{H_0}(t) = \hat{\rho}_{H_0}(-\infty) + \frac{1}{\imath\hbar}\int_{-\infty}^{t} dt' \left[\hat{H}^i_{H_0}(t'), \hat{\rho}_{H_0}(-\infty)\right] + \left(\frac{1}{\imath\hbar}\right)^2 \int_{-\infty}^{t} dt' \int_{-\infty}^{t'} dt'' \left[\hat{H}^i_{H_0}(t'), \left[\hat{H}^i_{H_0}(t''), \hat{\rho}_{H_0}(t'')\right]\right]. \tag{139}$$

Now we use the fact that we can prepare the system at $t \to -\infty$ such that the density matrix is not entangled ($\rho_{H_0}(-\infty) = \sigma_{H_0}(-\infty) \otimes \rho^R_{H_0}(-\infty)$) and take a derivative with respect to t on both sides of eq. (139):

$$\tfrac{d}{dt}\hat{\rho}_{H_0}(t) = \tfrac{1}{\imath\hbar}\left[\hat{H}^i_{H_0}(t), \hat{\rho}_{H_0}(-\infty)\right] + \left(\tfrac{1}{\imath\hbar}\right)^2 \int_{-\infty}^{t} dt' \left[\hat{H}^i_{H_0}(t), \left[\hat{H}^i_{H_0}(t'), \hat{\rho}_{H_0}(t')\right]\right]. \tag{140}$$

To obtain the equation of motion of $\hat{\sigma}_{H_0}(t)$, we have to take the partial trace over the reservoir degrees of freedom on both sides of the last equation:

$$\begin{aligned} \tfrac{d}{dt}\hat{\sigma}_{H_0}(t) &= \tfrac{d}{dt}\mathrm{tr}_{\mathrm{R}}[\hat{\rho}_{H_0}(t)] \\ &= \mathrm{tr}_{\mathrm{R}}\left[\tfrac{d}{dt}\hat{\rho}_{H_0}(t)\right] \\ &= \mathrm{tr}_{\mathrm{R}}\left[\tfrac{1}{\imath\hbar}\left[\hat{H}^i_{H_0}(t), \hat{\rho}_{H_0}(-\infty)\right]\right] + \mathrm{tr}_{\mathrm{R}}\left[\left(\tfrac{1}{\imath\hbar}\right)^2 \int_{-\infty}^{t} dt' \left[\hat{H}^i_{H_0}(t), \left[\hat{H}^i_{H_0}(t'), \hat{\rho}_{H_0}(t')\right]\right]\right] \\ &= \left(\tfrac{1}{\imath\hbar}\right)^2 \int_{-\infty}^{t} dt' \mathrm{tr}_{\mathrm{R}}\left[\left[\hat{H}^i_{H_0}(t), \left[\hat{H}^i_{H_0}(t'), \hat{\rho}_{H_0}(t')\right]\right]\right]. \end{aligned} \tag{141}$$

We have to justify why the first trace in the next-to-last line vanishes. First, we assume that at time $t \to -\infty$ the reservoir is in thermal equilibrium. This means that we can write explicitly:

$$\hat{\rho}^R(-\infty) = \hat{\rho}^R = \frac{e^{-\beta\hat{H}_R}}{\mathrm{tr}_{\mathrm{R}}\left[e^{-\beta\hat{H}_R}\right]} = \hat{\rho}^R_{H_0}(-\infty). \tag{142}$$

In the last step we used the relation $\left[\hat{H}_R, \hat{H}_D\right] = 0$.
Next, with the help of the relations $[\hat{H}_D, \hat{a}^\dagger] = \Delta\hat{a}^\dagger$, $[\hat{H}_D, \hat{a}] = -\Delta\hat{a}$ and $[\hat{H}_R, \hat{R}^\dagger_k] = \varepsilon_k\hat{R}^\dagger_k$, $[\hat{H}_R, \hat{R}_k] = -\varepsilon_k\hat{R}_k$, one can show that:

$$\hat{H}^i_{H_0}(t) = \textstyle\sum_k \left(\gamma_k\hat{R}_k\hat{a}^\dagger e^{-\imath(\varepsilon_k-\Delta)t} + \gamma^*_k\hat{R}^\dagger_k\hat{a}e^{\imath(\varepsilon_k-\Delta)t}\right). \tag{143}$$

This operator contains only terms which have different powers of $\hat{R}^\dagger$ and $\hat{R}$, but $\hat{\rho}_{H_0}(t=-\infty)$ has only terms with equal powers of $\hat{R}^\dagger$ and $\hat{R}$, so their product contains only terms which have different powers of both operators. Thus the partial trace over the reservoir degrees of freedom is zero.

4.1.1 Born and Markov approximations

To continue the calculation, we have to do some approximations.

- **Born approximation**
  The density matrix can always be written in the form:

$$\hat{\rho}_{H_0}(t) = \hat{\sigma}_{H_0}(t) \otimes \hat{\rho}^R_{H_0}(t) + \hat{\rho}_{corel}(t) \tag{144}$$

If $\hat{\rho}_{corel} = 0$ we can interprete the total state as a probability distribution of two uncorrelated product states. What we want to do is to justify the following approximation:

$$\hat{\rho}_{H_0}(t) \approx \hat{\sigma}_{H_0}(t) \otimes \hat{\rho}^R_{H_0}. \tag{145}$$

First, we define the two time scales τ_R and T_D. The first one is a measure for the time scale over which the reservoir R reaches its stationary state (and information from previous interactions is lost). The second one defines a characteristic time scale at which significant changes in $\hat{\sigma}_{H_0}$ may occur. If $\tau_R \ll T_D$, the reservoir is, in a good approximation, in its stationary state all the time. In addition, we assume that the statistical properties of the reservoir are unaffected by the weak coupling to the system D and the stationary state is purely defined by $\hat{H}_R$ ($\hat{\rho}^R(t) = \hat{\rho}^R_{H_0}(t) = \hat{\rho}^R$). In the nonequilibrium Green's function approach, we have always used $\tau_R = 0$, i.e. the reservoir is always in equilibrium.

- **Markov approximation**
  After the approximations we have done, the equation of motion for $\hat{\sigma}_{H_0}(t)$ is:

$$\tfrac{d}{dt}\hat{\sigma}_{H_0}(t) = \left(\tfrac{1}{\imath\hbar}\right)^2 \int_{-\infty}^{t} dt' \mathrm{tr}_R\big[\big[\hat{H}^i_{H_0}(t), \big[\hat{H}^i_{H_0}(t'), \hat{\sigma}_{H_0}(t') \otimes \hat{\rho}^R\big]\big]\big]. \tag{146}$$

  The term on the right hand side depends on the state of the density matrix at times earlier than t. One can imagine that in this case the system memorises the events that have happened at $t' < t$ and takes them into account for the current evolution. We assume that the two-point correlation function of the reservoir decays very fast (in a time scale much smaller than the typical evolution time of $\hat{\sigma}_{H_0}(t)$). So we can replace $\hat{\sigma}_{H_0}(t')$ by $\hat{\sigma}_{H_0}(t)$. In other words we assume that the density of states of the reservoir is constant from which follows that the two-point correlation function $\langle \hat{R}_k(t)\hat{R}_k(t')\rangle \sim \delta(t-t')$.

4.1.2 Further calculations

For the evaluation of the second trace we take into account that only terms proportional to $(\hat{R}^\dagger \hat{R})^n$, $n \in \mathbb{N}_0$ survive and use $\mathrm{tr}_R[\hat{R}^\dagger_k \hat{R}_k \rho^R] = [\exp(\beta\varepsilon_k) - 1]^{-1} = n_k$. So from eq. (146) we get (we drop some of the indices):

$$\begin{aligned}\tfrac{d}{dt}\hat{\sigma}_{H_0}(t) \;=\; & \tfrac{1}{(\imath\hbar)^2}\textstyle\sum_q |\gamma_q|^2 \int_{-\infty}^{t} dt' \big[\hat{a}\hat{a}^\dagger\hat{\sigma}n_q - \hat{a}\hat{\sigma}\hat{a}^\dagger(n_q+1) - \hat{a}^\dagger\hat{\sigma}\hat{a}n_q + \hat{\sigma}\hat{a}^\dagger\hat{a}(n_q+1)\big] e^{+\imath(\varepsilon_q-\Delta)(t-t')} + \\ & \tfrac{1}{(\imath\hbar)^2}\textstyle\sum_q |\gamma_q|^2 \int_{-\infty}^{t} dt' \big[\hat{a}^\dagger\hat{a}\hat{\sigma}(n_q+1) - \hat{a}^\dagger\hat{\sigma}\hat{a}n_q - \hat{a}\hat{\sigma}\hat{a}^\dagger(n_q+1) + \hat{\sigma}\hat{a}\hat{a}^\dagger n_q\big] e^{-\imath(\varepsilon_q-\Delta)(t-t')}\end{aligned} \tag{147}$$

To calculate the time integral, we use eq. (192). After regrouping the terms and transforming back into the Schrödinger picture, we get:

$$\begin{aligned}\tfrac{d}{dt}\hat{\sigma}(t) \;=\; & \tfrac{d}{dt}\big[e^{-\frac{\imath}{\hbar}\hat{H}_0(t-t_r)}\hat{\sigma}_{H_0}(t)e^{\frac{\imath}{\hbar}\hat{H}_0(t-t_r)}\big] \\ =\; & e^{-\frac{\imath}{\hbar}\hat{H}_0(t-t_r)}\big[\tfrac{d}{dt}\hat{\sigma}_{H_0}(t) - \tfrac{\imath}{\hbar}\big[\hat{H}_0, \hat{\sigma}_{H_0}(t)\big]\big]e^{\frac{\imath}{\hbar}\hat{H}_0(t-t_r)} \\ =\; & -\imath\big[\tfrac{1}{\hbar}\Delta - \tfrac{1}{\hbar^2}\mathcal{P}\big(\textstyle\int d\varepsilon D(\varepsilon)|\gamma(\varepsilon)|^2 \tfrac{1}{\varepsilon - E_d}\big)\big]\big[\hat{a}^\dagger\hat{a}, \hat{\sigma}(t)\big] \\ & -\Gamma\,(n_\Delta + 1)\,\big[\hat{a}^\dagger\hat{a}\hat{\sigma}(t) + \hat{\sigma}(t)\hat{a}^\dagger\hat{a} - 2\hat{a}\hat{\sigma}(t)\hat{a}^\dagger\big] \\ & -\Gamma n_\Delta\big[\hat{a}\hat{a}^\dagger\hat{\sigma}(t) + \hat{\sigma}(t)\hat{a}\hat{a}^\dagger - 2\hat{a}^\dagger\hat{\sigma}(t)\hat{a}\big],\end{aligned} \tag{148}$$

where $D(\varepsilon)$ is the density of states of the reservoir and $\Gamma = \pi g(\Delta)|\gamma(\Delta)|^2$. The next-to-last line describes the particle loss of the quantum dot with rate $\sim \Gamma$ and the last line describes the particle gain of the QD. This equation looks exactly like a Master equation in Lindblad form for a single quantum dot:

$$\partial_t\hat{\sigma} = \tfrac{1}{\imath}\big[\hat{H}, \hat{\sigma}\big] + \hat{\mathcal{L}}\hat{\sigma}. \tag{149}$$

The energy of the dot in this case is not Δ but is shifted by a finite amount because of the principal-value term in the third line of eq. (148). The division of the $\hat{\mathcal{L}}$ into particle gain and loss terms can be traced back in the definition of the quantum jump method (see sec. 3 of the appendix). There, the first two terms of the last two lines of eq. (148) were responsible for the nonunitary evolution of a given state of the system. The third term in the last two lines of eq. (148) caused quantum jumps into states with lower/higher particle number.

4.2 Calculation of the mean occupation number of the quantum dot. Comparison between the methods.

4.2.1 Exact calculation

The calculation of the time dependence of the expectation value of $\hat{a}^\dagger\hat{a}$ is straight forward ($\mathrm{tr_D}$ - trace over the dot degrees of freedom):

$$\partial_t\langle\hat{a}^\dagger\hat{a}\rangle = \mathrm{tr_D}\left[\hat{a}^\dagger\hat{a}\partial_t\hat{\sigma}(t)\right] = 2\Gamma\left(n_\Delta - \langle\hat{a}^\dagger\hat{a}\rangle\right).$$

The solution for the population of the single well is:

$$\langle\hat{a}^\dagger\hat{a}\rangle(t) = \left(\langle\hat{a}^\dagger\hat{a}\rangle_0 - n_\Delta\right)e^{-2\Gamma t} + n_\Delta \longrightarrow n_\Delta. \tag{150}$$

So the system reaches a steady state.

4.2.2 Wigner method

In sec. 3, we have already written the Fokker-Planck equation for the conditional probability function $\rho_{\mathcal{W}}(\vec{z},t|\vec{z}',t')$ and the Langevin equation for the corresponding Ito process. The only thing we have to do is to impose an initial condition of $\rho_{\mathcal{W}}(\vec{z},t_0)$. We take the initial probability density function (pdf) to be generated from a coherent state with mean particle number equal to N. It can be represented by a product of two Gaussian pdf's with mean values $\langle z_1\rangle = \sqrt{N}$ and $\langle z_2\rangle = 0$ and standard deviation $1/2$ although any combination, for which $\langle z_1\rangle^2 + \langle z_2\rangle^2 = N$, is allowed:

$$\rho_{\mathcal{W}}(\vec{z}_0,t_0) = \frac{2}{\pi}e^{-\frac{1}{2}\frac{(z_1-\sqrt{N})^2}{(1/2)^2}}e^{-\frac{1}{2}\frac{z_2^2}{(1/2)^2}}. \tag{151}$$

If we sample N_T points $\vec{z}_j = (z_{1,j}, z_{2,j})$, $j = 1,\ldots,N_T$ from $\rho_{\mathcal{W}}(\vec{z},t_0)$, the evolution of the population number of the quantum dot is given by:

$$\begin{aligned}\langle\hat{a}^\dagger\hat{a}\rangle(t) &= \langle\hat{a}^\dagger\hat{a}\rangle_{sym}(t) - \tfrac{1}{2}\\ &= \int d\alpha^2\rho_{\mathcal{W}}(\alpha,\alpha^*,t)\alpha\alpha^* - \tfrac{1}{2}\\ &= \tfrac{1}{N_T}\textstyle\sum_{j=1}^{N_T}|\alpha_j(t)|^2 - \tfrac{1}{2}\\ &= \tfrac{1}{N_T}\textstyle\sum_{j=1}^{N_T}\left(z_{1,j}^2(t) + z_{2,j}^2(t)\right) - \tfrac{1}{2}\end{aligned} \tag{152}$$

In the last step we used the variable resubstitution given in eq. (114). The time evolution of the observable is plotted for different number of trajectories together with the exact result (eq. (150)) in figure 11.

From the example, one can conclude that the exact method is by far faster than the stochastic one since in the first case one has to solve only one equation and in the second case one needs to calculate thousands of trajectories to get a good approximation. The situation changes drastically if we are interested in observables like $\langle\hat{a}_i^\dagger\hat{a}_j^\dagger\hat{a}_i\hat{a}_j\rangle$ and go to larger systems like a chain of $\mathcal{N}$ quantum dots coupled to two bosonic reservoirs (the indices i,j refer to the position on the lattice). In the TWA one has to calculate m trajectories for the vector $\vec{z}$ with $2\mathcal{N}$ components, i.e. one has to solve $2m\mathcal{N}$ equations to get the desired result. On the other side, to get the exact solution one has to calculate all two-point correlation functions whose number is proportional to $\mathcal{N}^2$ despite some of the possible symmetries of the system. So, for large $\mathcal{N}$ the Wigner method becomes numerically faster. The complexity of the method also does not change if one includes nonquadratic terms in the Hamiltonian. By changing m dependent on the computational resources available, one can get results with high enough accuracy (but never exact) and acceptable computation time.

4.2.3 Quantum jump method

The method is described briefly in sec. 3 of the appendix. Starting from eq. (115), (116) the non-hermitian Hamiltonian is given by:

$$\hat{H} = \Delta\hat{a}^\dagger\hat{a} - i\hbar\Gamma(n_\Delta+1)\hat{a}^\dagger\hat{a} - i\hbar\Gamma n_\Delta\hat{a}\hat{a}^\dagger. \tag{153}$$

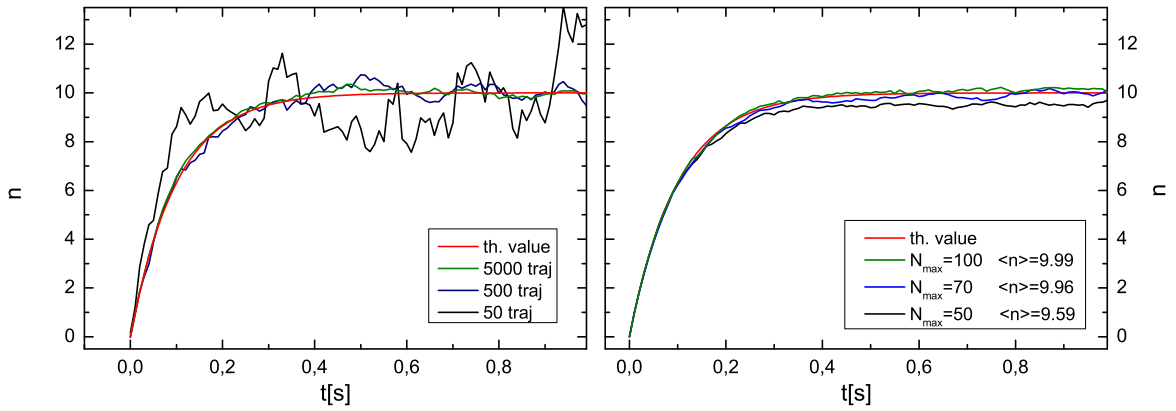

Figure 11: Left panel: Evolution of $\langle \hat{a}^\dagger a \rangle$ obtained after averaging over different number of trajectories; $\Gamma = 5s^{-1}$, mean particle number in the reservoir in the mode with energy Δ is $n_\Delta = 10$, initial mean particle number in the well $n(t_0) = 0$, time step $dt = 10^{-5}s$.
Right panel: Evolution of the mean occupation number of a quantum dot coupled to a Markovian reservoir. Its expectation value $\langle n \rangle$ is given in the legend. N_{max} denotes the cut-off of the Fock-space. $\Gamma = 5s^{-1}$, $n_\Delta = 10$.

As a basis of the infinite dimensional Hilbert space of the system (dot) we use the Fock-basis $\{|n\rangle\}_{n\in\mathbb{N}_0}$ with $|n\rangle = \frac{\hat{a}^{\dagger\, n}}{\sqrt{n!}}|0\rangle$. We cut it by using $\{|n\rangle\}_{n\in I}$, $I = \{0, 1, \dots N_{max}\}$ and define $\hat{a}^\dagger|N_{max}\rangle = 0$. The time step dt is chosen such that the conditon $\delta p \ll 1$ (see eq. (185)) is fulfilled. We take the initial state of the system to be $|\phi(0)\rangle = |0\rangle$.
The results of the expectation value of the occupation number $\hat{a}^\dagger\hat{a}$ are plotted in fig. 11. One sees that the dynamics of the system can be significantly influenced by the choise of the cut-off N_{max}. If N_{max} is not large enough the contribution of the states $|n\rangle$, $n > N_{max}$ to the evolution of the system is not negligible and excluding their weight from the calculation of the expectation value of the mean particle number results in underestimation of the result.

4.2.4 Nonequilibrium GF method

As already mentioned one can not compute the time evolution of an observable but only its steady state. From the GF given in eq. (33) for a dot coupled to two reservoirs we set the coupling to the right reservoir to be equal to zero $\Gamma_R = 0$, set $\Gamma_L = \Gamma = \text{const}$ and $n_L = n_\Delta = \text{const}$ as already discussed. The mean occupation number of the dot is then:

$$\langle \hat{a}^\dagger \hat{a} \rangle = \int \tfrac{dw}{2\pi} i\mathcal{G}^{-+}_{(w)} = \int \tfrac{dw}{2\pi} \tfrac{2\Gamma}{(w-\Delta)^2+\Gamma^2} n_\Delta = n_\Delta \tag{154}$$

The result is independent of Γ and Δ since they change only the width and the center of the Loretzian curve that has to be integrated but not the area under the graph. Even in the limit $\Gamma \to 0$ the Loretzian transforms into a δ-function and the result is unchanged. As expected it coincides with the result from eq. (150) in the limit $t \to \infty$.

5 Linear chain of $\mathcal{N}$ lattice sites coupled to two Markovian reservoirs.

We investigate the system of a linear chain of three/four quantum dots, both ends of which are coupled to two different Markovian reservoirs. The effect of the coupling is described by the superoperator $\mathcal{L}$, which adds and removes particles at the zeroth and last lattice sites and assures that the particle number at both ends of the chain remains constant. The time evolution of the system is described by the Master equation in Lindblad form:

$$\frac{d}{dt}\hat{\rho} = \frac{1}{i}\left[\hat{H}, \hat{\rho}\right] + \hat{\mathcal{L}}\hat{\rho} \tag{155}$$

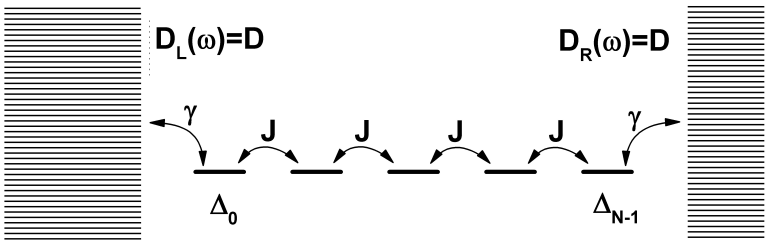

Figure 12: Linear chain of $\mathcal{N}$ lattice sites coupled to two Markovian reservoirs. If one maps the Master equation in Lindblad form to a Langevin equation, then the stochastic differential equation describes the dynamics of a chain of quantum dots coupled to two reservoirs with constant density of states $D(w) = D$ and constant occupation of these states $n_L(w) = n_L = \text{const}$, $n_R(w) = n_R = \text{const}$.

The Bose-Hubbard Hamiltonian is given by:

$$\hat{H} = \sum_{j=0}^{\mathcal{N}-1} \Delta_j \hat{a}_j^\dagger \hat{a}_j - \sum_{j=0}^{\mathcal{N}-2} J_j \left(\hat{a}_{j+1}^\dagger \hat{a}_j + \hat{a}_j^\dagger \hat{a}_{j+1} \right) + \tfrac{1}{2} \sum_{j=0}^{\mathcal{N}-1} U_j \hat{a}_j^\dagger \hat{a}_j^\dagger \hat{a}_j \hat{a}_j, \tag{156}$$

where only the hopping between two neighbouring sites J and the interaction between particles in the same lattice site U is taken into account. The effect of a coupling to a bosonic reservoir is descibed by $\hat{\mathcal{L}}$:

$$\hat{\mathcal{L}}\hat{\rho} = - \sum_{j \in \{0, \mathcal{N}-1\}} \Gamma_j (N_{res,j} + 1) \left(\hat{a}_j^\dagger \hat{a}_j \hat{\rho} + \hat{\rho} \hat{a}_j^\dagger \hat{a}_j - 2 \hat{a}_j \hat{\rho} \hat{a}_j^\dagger \right) - \sum_{j \in \{0, \mathcal{N}-1\}} \Gamma_j N_{res,j} \left(\hat{a}_j \hat{a}_j^\dagger \hat{\rho} + \hat{\rho} \hat{a}_j \hat{a}_j^\dagger - 2 \hat{a}_j^\dagger \hat{\rho} \hat{a}_j \right) \tag{157}$$

It captures the process of particle transfer between the quantum dot and the reservoir. If Γ_j is the largest scale in the system the mean particle number of the j-th dot is approximately equal to $N_{res,j}$. So the $\mathcal{L}$ operator just keeps this number constant and also gives an easy way to adjust it. Γ can be interpreted as a measure how fast a deviation from the steady-state particle number in the dot $N_{res,j}$ is damped. In the following we will denote $N_{res,0} \equiv n_L, N_{res,\mathcal{N}-1} \equiv n_R$.
In order to solve eq. (157) we map it to a differential equation for the Wigner function $\rho_{\mathcal{W}}$ using the correspondence rules given in eq. (113), (114) for every operator $\hat{a}_j$ of the theory ($j = 0, \ldots, \mathcal{N}-1$):

$$\begin{aligned}
\tfrac{d}{dt}\rho_{\mathcal{W}} \;=\; & - \sum_{j=0}^{\mathcal{N}-1} \Delta_j \left(x_j \partial_{y_j} - y_j \partial_{x_j} \right) \rho_{\mathcal{W}} \\
& - \sum_{j=0}^{\mathcal{N}-2} J_j \left(x_j \partial_{y_{j+1}} + x_{j+1} \partial_{y_j} - y_j \partial_{x_{j+1}} - y_{j+1} \partial_{x_j} \right) \rho_{\mathcal{W}} \\
& + \sum_{j=0}^{\mathcal{N}-1} U_j \left(x_j^3 \partial_{y_j} - y_j^3 \partial_{x_j} + x_j y_j^2 \partial_{y_j} - x_j^2 y_j \partial_{x_j} - x_j \partial_{y_j} + y_j \partial_{x_j} \right) \rho_{\mathcal{W}} \\
& + \sum_{j=0}^{\mathcal{N}-1} U_j \tfrac{1}{4} \left(x_j \partial_{y,j} - y_j \partial_{x,j} \right) \left(\partial_{x,j}^2 + \partial_{y,j}^2 \right) \rho_{\mathcal{W}} \\
& + \sum_{j \in \{0, \mathcal{N}-1\}} \tfrac{1}{2} \Gamma_j (N_{res,j} + 1/2) \left(\partial_{x,j}^2 + \partial_{y,j}^2 \right) \rho_{\mathcal{W}} + \Gamma_j \left(\partial_{x,j} x_j + \partial_{y,j} y_j \right) \rho_{\mathcal{W}}
\end{aligned} \tag{158}$$

In order to map this equation to a solvable type of stochastic differential equation we neglect all therms where a third or a higher order derivatives occur (fourth line). This is exactly the truncated Wigner approximation.
In the end, we map $x_j \mapsto z_{2j}$, $y_j \mapsto z_{2j+1}$ to get an equation of the form:

$$\partial_t \rho_{\mathcal{W}}(\vec{z}, t) = -\vec{\bigtriangledown}_z . \vec{f}(\vec{z}, t) \rho_{\mathcal{W}}(\vec{z}, t) + \frac{1}{2} \frac{\partial^2}{\partial_{z,i} \partial_{z,j}} \mathcal{D}_{i,j}(t) \rho_{\mathcal{W}}(\vec{z}, t) \tag{159}$$

with $\mathcal{D}_{i,j} = \Gamma_j (N_{res,j} + \frac{1}{2}) \delta_{ij}$. As already mentioned in this work, we use the Euler-Maryama method and the Taylor method of strong order 1.5 to obtain the needed trajectories. Since the noise is additive the first method coincides with the Milstein one that has a strong order of convergence equal to one.

Next, we discuss in detail the accuracy of the numerical solution of the equation above (sec. 5.1.1) and formulate the same problem in the language of nonequilibrium Green's functions (sec. 5.2). In both cases we work with a lattice chain of three wells since the generalisation to larger lattices is analogous. The explicit form of the Langevin equation corresponding to the truncated version of eq. (158) will also be needed in the following subsections:

$$d\vec{Z}_t = \vec{f}(\vec{Z}_t, t)dt + \sigma(\vec{Z}_t, t)d\vec{W}_t \tag{160}$$

with:

$$\vec{Z} = \begin{bmatrix} Z^0 \\ Z^1 \\ Z^2 \\ Z^3 \\ Z^4 \\ Z^5 \end{bmatrix} \qquad \vec{f}(\vec{Z}, t) = \begin{bmatrix} & J[-Z^3] & -\Gamma_0 Z^0 \\ & J[+Z^2] & -\Gamma_0 Z^1 \\ \Delta_1 Z^3 + & J[-Z^5 - Z^1] & +U_1[+(Z^3)^3 + (Z^2)^2 Z^3 - Z^3] \\ -\Delta_1 Z^2 + & J[+Z^4 + Z^0] & +U_1[-(Z^2)^3 - (Z^3)^2 Z^2 + Z^2] \\ & J[-Z^3] & -\Gamma_2 Z^4 \\ & J[+Z^2] & -\Gamma_2 Z^5 \end{bmatrix} \tag{161}$$

and $\sigma = \mathrm{diag}(\sqrt{\Gamma(\mathrm{N}_{\mathrm{res},0} + 1/2)}, \sqrt{\Gamma(\mathrm{N}_{\mathrm{res},0} + 1/2)}, 0, 0, \sqrt{\Gamma(\mathrm{N}_{\mathrm{res},2} + 1/2)}, \sqrt{\Gamma(\mathrm{N}_{\mathrm{res},2} + 1/2)})$.

5.1 TWA. Details on the numerical evaluation

5.1.1 Numerical computation. Noninteracting case

Since the Lipschitz and growth conditions are fulfilled (see sec. 2 of the appendix) we know that an unique solution of the stochastic equation exist.

Comparison with the numerical results

We calculate a finite number of trajectories N_T that evolve within the time interval $[0, T]$ and average an observable over them. After some time $t' < T$ we assume that the system is in a steady state, and take an additional time average of the observable, e.g. for the mean occupation number n_i of the i-th quantum dot this means ($\langle n_i(t) \rangle$ calculated in eq. (152)):

$$n_i = \frac{1}{T - t'} \int_{t'}^{T} d\tau \langle n_i(\tau) \rangle \tag{162}$$

The time integration is needed since there are fluctuations of the observable due to the finite number of trajectories, so assuming that the fluctuations are around the true mean value we should get a better result.

In order to get a feeling for the number of trajectories and the time step needed to obtain good results, we plot the relative errors of the expectation value of the current between the last two lattice sites of the chain in dependence of the chosen time step dt and number of trajectories N_T (tab. 1). The strength of the fluctuations in dependence of N_T can be seen in figure (13). The results from those observations do not change if the system one investigates is a chain of four or five quantum dots.

dt	10^{-1}	10^{-2}	10^{-3}	10^{-4}
Δ Euler-Maruyama	0.694	0.049	0.004	0.004
Δ Taylor 1.5	0.509	0.054	0.003	0.004

Table 1: Relative error of the steady-state current between the zeroth and first element of a chain of three quantum dots in dependence of the chosen method and time step. System parameters: $\Gamma_0/J = \Gamma_2/J = 5$, $J = 1s^{-1}$, $\Delta_1/J = 0$, $N_{res,1} = 4000$, $N_{res,2} = 100$, $U/J = 0.001$. The number of trajectories used to calculate the observable is $N_T = 10^4$.

5.1.2 Numerical computation: Interacting case

The drift vector $\vec{f}(\vec{z}, t)$ from eq. (160) now contains terms that are cubic in z and thus the Lipshitz condition is not fulfilled. Therefore we do not know apriori if a solution of the stochastic differential equation exists. But if we construct the action $\mathcal{S}$ that corresponds to eq. (160), we see that no terms proportional to the interaction are included in the Keldysh part of the full Green's function. Since this part of the action is responsible for the convergence of the path integral, and is unchanged by

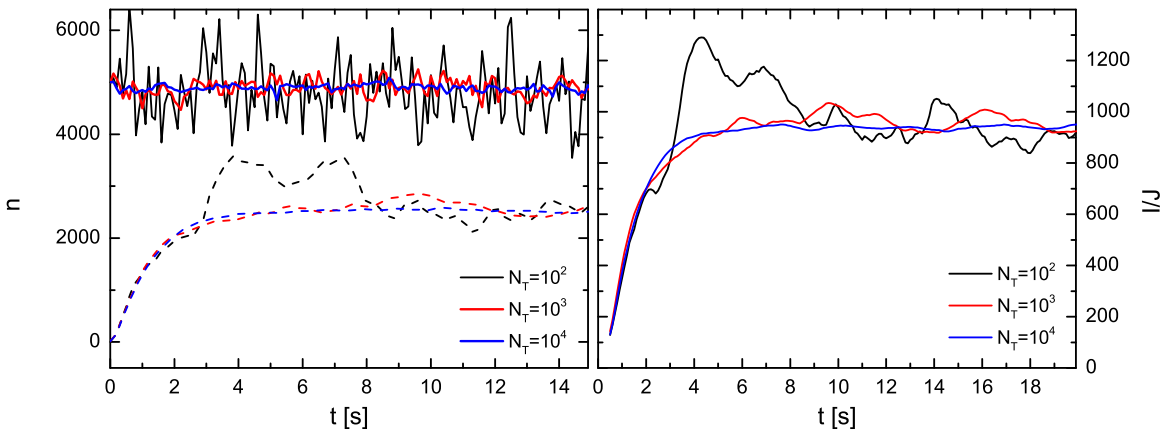

Figure 13: Left panel: Time evolution of the occupation number of the zeroth (solid line) and first (dashed line) quantum dot (the same observable for the third dot is not plotted because of the different scales of the results). Used parameters are $\Gamma_0/J = \Gamma_1/J = 5$, $\Delta_1/J = 0$, $J = 1s^{-1}$. Right panel: Time evolution of the current between the first and second well of the lattice for N_T trajectories. The parameters used are the same as in the left figure.

introducing $U \neq 0$, it follows that the Keldysh partition function is still well defined. All terms of $i\mathcal{S}$ proportional to U are purely imaginary. Their influence on the dynamics can be seen by the following example. Consider an arbitrary path $\vec{z}^T(t) = (z_0(t), \ldots, z_5(t))$ that is nonzero and slowly varying in its second and third components (those that are coupled to U in the Langevin equation). The role of the interaction is to give a rapidly oscillating weight to this path such that it has no contribution to the Keldysh partition function.
One can also look at the solutions of eq. (160) by setting the stochastic force equal to zero. For $U = 0$ the terms proportional to Γ are responsible for the convergence of the solutions to the zero-vector. An increase of U leads to oscillations of the components of $\vec{z}$. The stronger U, the larger is the frequency and the initial amplitude of the oscillations. But even in this case, the amplitude of the oscillations is damped in time.
From the above discussion, one can assume that the failure of some of the numerical methods to converge for large U is due to the finite time step one uses, but not because of the divergent behaviour of the equation.

5.2 Formulation of the problem with nonequilibrium Green's functions

The main idea of the method is already discussed in the previous chapter, so we only write down the explicit form of the needed Green's functions. The noninteracting GF of the chain of three quantum dots is given by:

$$\mathcal{G}^{-1}_{(w)} = \begin{bmatrix} -\Sigma_L & J\sigma_z & 0_{2\times 2} \\ J\sigma_z & (w-\Delta)\sigma_z & J\sigma_z \\ 0_{2\times 2} & J\sigma_z & -\Sigma_R \end{bmatrix} \qquad \Sigma_{L/R} = \begin{bmatrix} -i\Gamma_{L/R}(2n_{L/R}+1) & i\Gamma_{L/R}2n_{L/R} \\ i\Gamma_{L/R}(2n_{L/R}+2) & -i\Gamma_{L/R}(2n_{L/R}+1) \end{bmatrix} \tag{163}$$

and the self-energy is:

$$\Sigma_{int(w)} = \begin{bmatrix} 0_{2\times 2} & 0_{2\times 2} & 0_{2\times 2} \\ 0_{2\times 2} & \Sigma_{(w)} & 0_{2\times 2} \\ 0_{2\times 2} & 0_{2\times 2} & 0_{2\times 2} \end{bmatrix}, \tag{164}$$

where $\Sigma_{int(w)} = \Sigma_{tad} + \Sigma_{sun(w)}$ is the sum of the Sunset and Tadpole contributions to the self-energy. The subscript ij $(i,j = 0,1,2)$ denotes the block matrix position and the superscript η, η' $(\eta, \eta' = \pm)$ denotes the element of the block matrix. In the following, we will not calculate $\Sigma_{sun(w)}$ since the Tadpole approximations gives results that coincide qualitatively with those from the TWA. The Tadpole self-energy is given by:

$$\Sigma_{tad} \quad = \quad 4\tfrac{iU}{2} \int \tfrac{dw}{2\pi} \mathcal{G}_{11(w)} = U(1 + n_L + n_R). \tag{165}$$

If we use the fact that for every Δ the mean particle occupation in the middle well is $n_1 = 0.5(n_L + n_R)$, one can rewrite the correction to the energy level of the middle dot in the following form:

$$\Delta_1 \to \Delta_1 + U(1 + 2n_1).$$

6 Results

We present a systematical discussion of how the different parts of the Hamiltonian (see eq. (156)) influence the system behaviour.

6.1 First and second order coherence function

As already mentioned in section 2 the only quantum effects of the system that are captioned in the truncated Wigner approximation come from the initial conditions (the probability density function at t_0) and from the fact that we have mapped the observable operator $\hat{\Omega}$ to its Weyl symbol. We have also argued that the coupling to a bosonic reservoir (or some dissipative term) should lead to decoherence. So we expect to have a dependence between the reservoir constant $\Gamma = \Gamma_0 = \Gamma_2$ and the first and second order coherence functions $g^{(1)}(i,j)$, $g^{(2)}(i,j)$. Both functions are defined as:

$$\begin{aligned} g^{(1)}(i,j) &= \frac{\langle \hat{a}_i^\dagger \hat{a}_j \rangle}{\sqrt{\langle \hat{a}_i^\dagger \hat{a}_i \rangle \langle \hat{a}_j^\dagger \hat{a}_j \rangle}} \\ g^{(2)}(i,j) &= \frac{\langle \hat{a}_i^\dagger \hat{a}_j^\dagger \hat{a}_j \hat{a}_i \rangle}{\langle \hat{a}_i^\dagger \hat{a}_i \rangle \langle \hat{a}_j^\dagger \hat{a}_j \rangle}. \end{aligned} \tag{166}$$

The observables are plotted in fig. 15 for the noninteracting case $U/J = 0$ and $\Gamma/J = 5, 50$. First we discuss the behaviour of $g^{(2)}(i,i)$. It is equal to two which is a direct consequence of the fact that the Hamiltonian of the system is quadratic in the fields[19]. In the limit of large occupation numbers this value can be measured via the variance of the mean occupation number:

$$\begin{aligned} & g^{(2)}(i,i) = \frac{\langle \hat{a}_i^\dagger \hat{a}_i^\dagger \hat{a}_i \hat{a}_i \rangle}{\langle \hat{a}_i^\dagger \hat{a}_i \rangle^2} = \frac{\langle \hat{a}_i^\dagger \hat{a}_i \hat{a}_i^\dagger \hat{a}_i \rangle - \langle \hat{a}_i^\dagger \hat{a}_i \rangle}{\langle \hat{a}_i^\dagger \hat{a}_i \rangle^2} \approx \frac{\langle \hat{n}_i^2 \rangle}{\langle \hat{n}_i \rangle^2} = 2 \Leftrightarrow \langle n_i^2 \rangle = 2 \langle n_i \rangle^2 \\ \Rightarrow \quad & \mathrm{Var}(\hat{n}_i) = \langle \hat{n}_i^2 \rangle - \langle \hat{n}_j \rangle^2 = \langle \hat{n}_j \rangle^2 \end{aligned} \tag{167}$$

If we recall the theory of photon detector counting statistics, the result in the equation above can be intepreted as having atoms that arrive at the dot in bunches. The statistics is analogous to that of an incoming thermal light as soon as one compares the first two moments of the corresponding distribution functions. In fig. 15 one observes that a decrease of Γ increase the coherence as expected.

The same conclusions can also be made from the second order coherence functions plotted in fig. 15 . For $i \neq j$ the value $g^{(2)}(i,j) = 1$ means that there is no correlation between the particle number operators in the different wells, since

$$g^{(2)}(i,j) = 1 \Leftrightarrow \langle \hat{n}_i \hat{n}_j \rangle = \langle \hat{n}_i \rangle \langle \hat{n}_j \rangle \ . \tag{168}$$

[19] If one draws an arbitrary Feynmann diagram contributing to the expectation value of $g^{(2)}(i,i)$ one will first realise that the symmetry factor is equal to two. Since there is no nonquadratic term in the Hamiltonian, the paths of two particles to their final destination do not depend on each other (i.e. there is no graph that connects both paths). One has first to count the different outcomes of the journey of the particle pair. There are two and they are plotted in fig. 14. Because of the independence of both paths on each other and because the symmetry factor of every Feynmann diagramm is the same, the sum of the paths of both particles factorises into a product of the sum of the paths of every one of the particles. This product is cancelled by the denominator in the definition of $g^{(2)}(i,i)$, so only the combinatorial factor of two remains.
In the same way one can show that

$$g^{(2)}(i,j) = 1 + g^{(1)}(i,j) g^{(1)}(j,i).$$

Figure 14

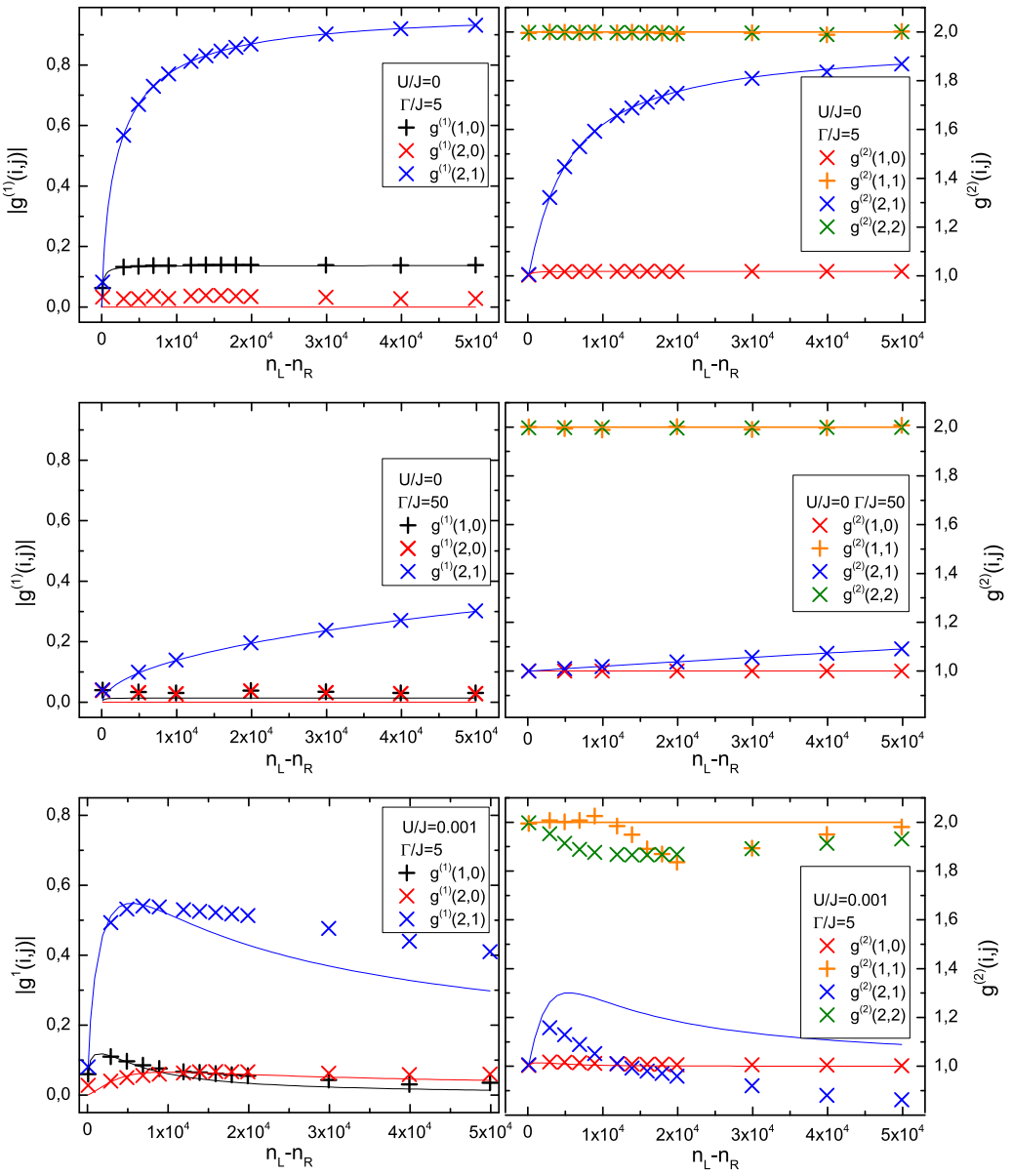

Figure 15: First (left panel) and second (right panel) order coherence function for a lattice chain of three quantum dots. The crosses (solid lines) denote the result obtained from the TWA (Tadpole approximation). Used parameters are $\Delta_j/J = 0$ $(j = 0, 1, 2)$, $n_L = 100$, $\Gamma/J = \Gamma_0/J = \Gamma_2/J = 5$ (upper panel), $\Gamma/J = \Gamma_0/J = \Gamma_2/J = 50$ (middle panel) and $U/J = 0.001$, $\Gamma/J = \Gamma_0/J = \Gamma_2/J = 5$ (lower panel).

The result from fig. 15 can also be obtained exactly in the noninteracting case with the nonequilibrium GF method. Assuming that $\Gamma^2 > 8J^2$, the values of the first order coherence functions are[20]

[20]Imposing $\Gamma^2 > 8J^2$, the determinant of $\mathcal{G}^{-1}$ has six roots that lie on the imaginary axis ($x = J/\Gamma$):

$$w_{1,2} = \pm i\Gamma \qquad w_{3,4} = \pm i\alpha \qquad w_{5,6} = \pm\beta \qquad \alpha = \Gamma\sqrt{\frac{1}{2} - 2x^2 - \sqrt{\frac{1}{4} - 2x^2}} \qquad \beta = \Gamma\sqrt{\frac{1}{2} - 2x^2 + \sqrt{\frac{1}{4} - 2x^2}}$$

It follows that all components of the Green's function have six poles on the imaginary axis (which can be also removable). With the use of the relations $\alpha + \beta = \Gamma$, $\alpha\beta = 2\eta^2$ and the Residue theorem all quantities of interest in this subsection can be calculated since they are integrals over some linear combination of Green's functions.

$(x = J/\Gamma, \zeta = n_L/n_R)$:

$$\begin{aligned} |g^{(1)}(1,0)| &= \frac{|\mathcal{G}^{-+}_{01}(0)|}{\sqrt{\mathcal{G}^{-+}_{11}(0)\mathcal{G}^{-+}_{00}(0)}} = \frac{x}{\sqrt{1+x^2}}\frac{\zeta-1}{\zeta+1}\frac{1}{\sqrt{x^2+\frac{2\zeta}{\zeta+1}}} \\ |g^{(1)}(2,0)| &= 0 \\ |g^{(1)}(2,1)| &= \frac{|\mathcal{G}^{-+}_{12}(0)|}{\sqrt{\mathcal{G}^{-+}_{22}(0)\mathcal{G}^{-+}_{11}(0)}} = \frac{x}{\sqrt{1+x^2}}\frac{\zeta-1}{\zeta+1}\frac{1}{\sqrt{x^2+\frac{2}{\zeta+1}}}. \end{aligned} \tag{169}$$

Comparing the results of both approaches (that should be equal), we see that $|g^{(1)}(2,0)|$ deviates from zero in the TWA. This is due to the finite number of trajectories. Even though $g^{(1)}(2,0)$ oscillates around zero its absolute value is always greater than zero.

Additional effects that appear in the system by switching on the on-site interaction in the middle well can be seen in the first and second order coherence functions plotted in fig. 15. From the upper and lower panel of the figure, one sees that the first order coherence between the left/right and the middle well decreases (black and blue crosses) and the first order coherence between the left-right wells increases (red crosses). If we think in classical terms, this can be connected with the fact that a particle transfer from the middle site to the left/right reservoir changes the energy of the system, and this process should be correlated with other additional processes in order to fulfill the energy constraint. Tunneling from the left to the right reservoir does not change the energy of the system so it becomes more favourable.

The physics behind the deviations of the first and second order coherence functions can be better unserstood in the case of a chain of four quantum dots, the middle two of them having a non-zero on-site interaction. The result that $g^{(2)}(2,1) < 1$, in fig 16, is equivalent to having a negative correlation between an arrival of particles at the site one and two[21]. At the classical level, for large "voltages" $(n_L \gg n_R)$ we assume that the particles arriving at site j come mostly from its left neighbour, site $j-1$. If both $j-1$ and j have nonzero on-site particle-particle interaction, a simultaneous arrival of a particle at sites $j-1$ and j should in most cases increase the total number of atoms in both wells by one. But this is connected with an increase of the total energy of the system and makes such a simultaneous arrival unlikely to happen.
The increase of $g^{(2)}(2,2)$ and $g^{(2)}(1,1)$ means that particles arrive in large bunches, which leads to strong oscillations of the current between the first and second lattice site around its steady state. Indeed, if one compares the time evolution of the current between the neighbouring sites $j-1$ and j $I_{j-1\to j}(t)$, one will see that the oscillations around the steady state for $I_{1\to 2}$ are larger than $I_{2\to 3}$.

We end the discussion about the coherence functions with a final remark about the Tadpole approximation which can also be seen in fig. 15 and 16. We see that it qualitatively reproduces the same behaviour of the first order coherence as the TWA. The Tadpole approximation fails completely in describing bunching and antibunching effects that are visible in the TWA. This is because the effect of interactions does not change the quadratic structure of the Hamiltonian but only modifies some of the prefactors of the qudratic terms, e.g. in the case of a lattice chain of three wells with on-site interaction in the middle one we have only modified the energy level of the middle well from Δ to $\Delta+U(1+n_L+n_R)$.

6.2 Mean occupation number and current.

6.2.1 Chain of three lattice sites

The linear dependence of the mean occupation number in the middle well and the steady state current can be confirmed by the nonequilibrium GF method. The exact expectation value of the observables

[21] One can check that the autocorrelation between n_i, n_j is given by:

$$\frac{\left\langle \big(n_i - \langle n_i\rangle\big)\big(n_j - \langle n_j\rangle\big)\right\rangle}{\sqrt{\big(\langle n_i^2\rangle - \langle n_i\rangle^2\big)\big(\langle n_j^2\rangle - \langle n_j\rangle^2\big)}} = \frac{g^{(2)}(i,j)-1}{\sqrt{\big(g^{(2)}(i,i)-1\big)\big(g^{(2)}(j,j)-1\big)}}$$

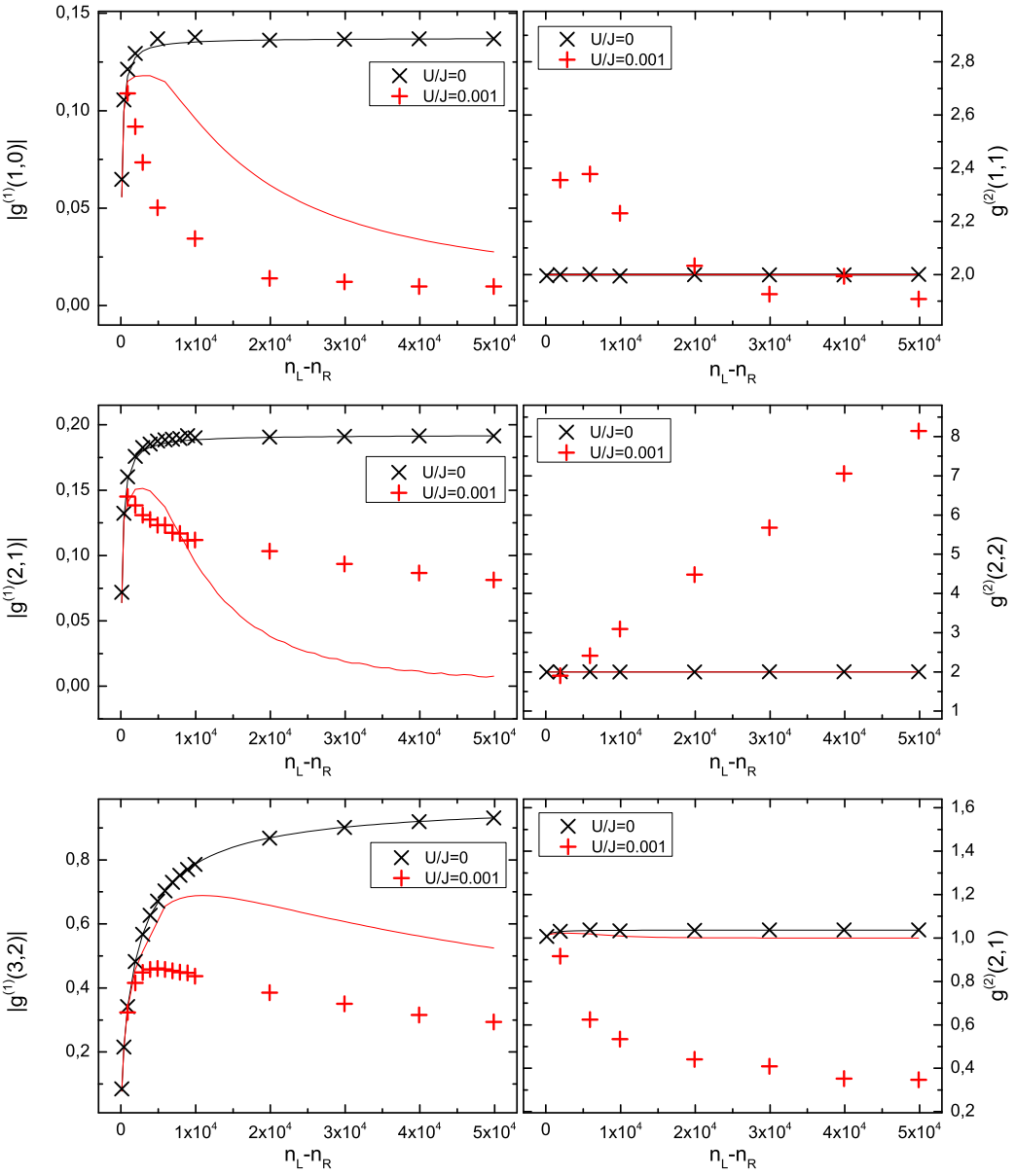

Figure 16: First and second order coherence functions for a lattice chain of four quantum dots. The crosses and solid lines denote the results obtained from the TWA and Tadpole approximations respectively. Used parameters are $\Delta_j/J = 0$ $(j = 0, 1, 2, 3)$, $J = 1s^{-1}$, $n_R = 100$, $\Gamma/J = \Gamma_0/J = \Gamma_3/J = 5$.

we are interested in is in the case $\Gamma^2 > 8J^2$ given by $(x = J/\Gamma)$:

$$\begin{aligned} \langle \hat{I} \rangle &= J\tfrac{x}{1+x^2}(n_L - n_R) \\ n_0 &= \int \tfrac{dw}{2\pi} i\mathcal{G}^{-+}_{00}(w) = n_L - \tfrac{n_L - n_R}{2}\tfrac{x^2}{1+x^2} \\ n_1 &= \int \tfrac{dw}{2\pi} i\mathcal{G}^{-+}_{11}(w) = \tfrac{n_L + n_R}{2} \\ n_2 &= \int \tfrac{dw}{2\pi} i\mathcal{G}^{-+}_{22}(w) = n_R - \tfrac{n_R - n_L}{2}\tfrac{x^2}{1+x^2}. \end{aligned} \tag{170}$$

They are confirmed quantitatively by the results from the numerical solution of the Langevin equation (eq. (160)) shown in fig. 17. They also prove the statement made in the beginning of section 5 that, if Γ is the largest scale of the system $(x \to 0)$, the particle number in the wells connected with the reservoirs is approximately equal to n_L, n_R.

In the interacting case, one observes that there is no change in the mean occupation number in the

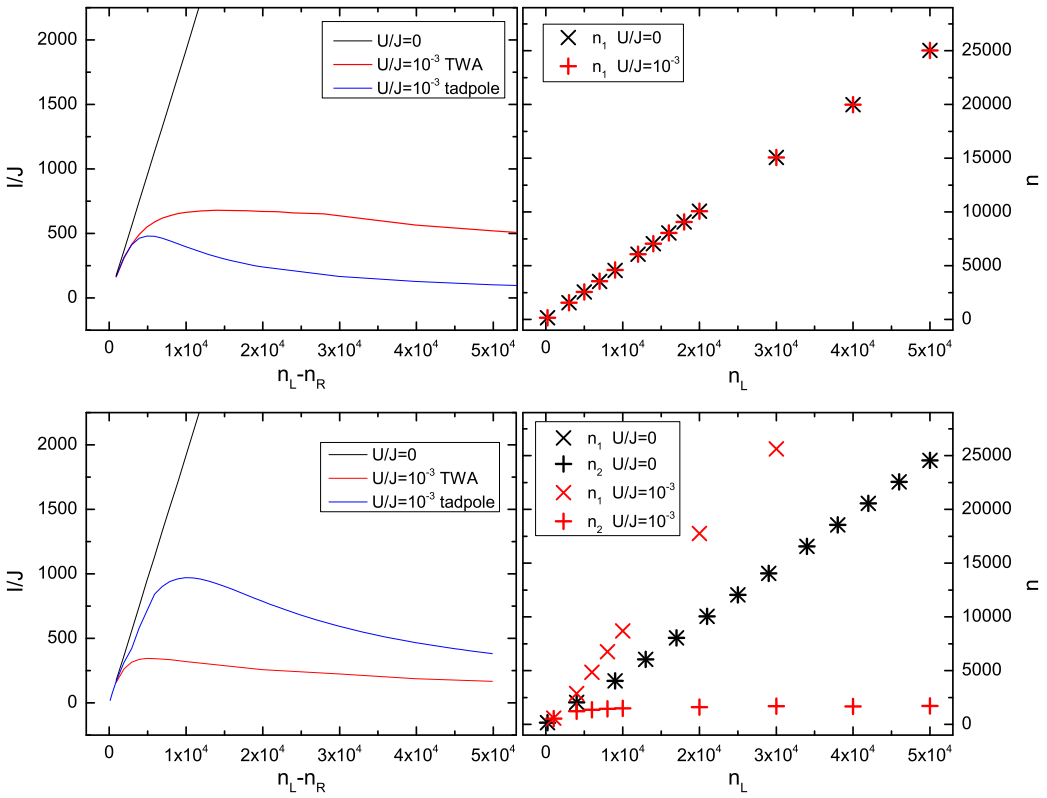

Figure 17: Steady state current I and mean occupation number n of the middle lattice site for a chain of three (upper panel) and four (lower panel) quantum dots. The results in the noninteracting case are plotted with black lines or black crosses, the results from the TWA - with red lines and crosses, the results from the Tadpole approximation - with blue lines. In the right panel there are no results from the Tadpole approximation since they are the same as in the noninteracting case. Used parameters are $\Delta_j/J = 0$ $(j = 0, 1, 2)$, $J = 1s^{-1}$, $n_R = 100$, $\Gamma/J = \Gamma_0/J = \Gamma_2/J = 5$.

middle well, but the current does not have a linear dependence on the applied "voltage" any more. By comparison of the current-voltage curves for different interaction strengths one can see that the deviation from linear behaviour occurs at $Un_1/J \sim 1$. In order to show this, we denote the mean occupation number in the middle well with n_1 and the current through the well with I. For different interaction strengths we take points n_1 where the relative current difference in the noninteracting and interacting case is 0.3. The plot U vs. Un_1 is shown in fig. 18. It follows that the above defined condition for the breakdown of the linear behaviour of the current is fulfilled for $Un_1/J \approx 1.8$. One obtains analogous results for lattice chains of four sites, the middle two of them having nonzero on-site particle-particle interaction.

6.2.2 Chain of four and five lattice sites

We observe additional effects since there are two (three) sites with labels $1, 2$ (and 3) whose mean particle occupation is not fixed by the largest energy scale of the system. In the TWA, the linear dependence of the mean occupation number in the middle sites $1, 2, (3)$ on the applied voltage is interrupted if the interactions $U_1, U_2, (U_3)$ are switched on. From fig. 17 one sees that this difference increases with increasing interaction strength and "voltage" $(n_L - n_R)$.
The nonlinear behaviour of the current can again be explained with the arguments used in the previous subsection. The middle states of a classical particle transport from the zeroth to the third (fourth) via the first, second (and third) lattice sites are energetically higher than the initial/final states. Since the number of energetically unfavourable states in a larger lattice is higher, we expect that the current in this system is smaller than the current through a system of three quantum dots. One can suggest that a kind of a primitive Ohmic law exists, where the role of resistance is substituted by the interaction

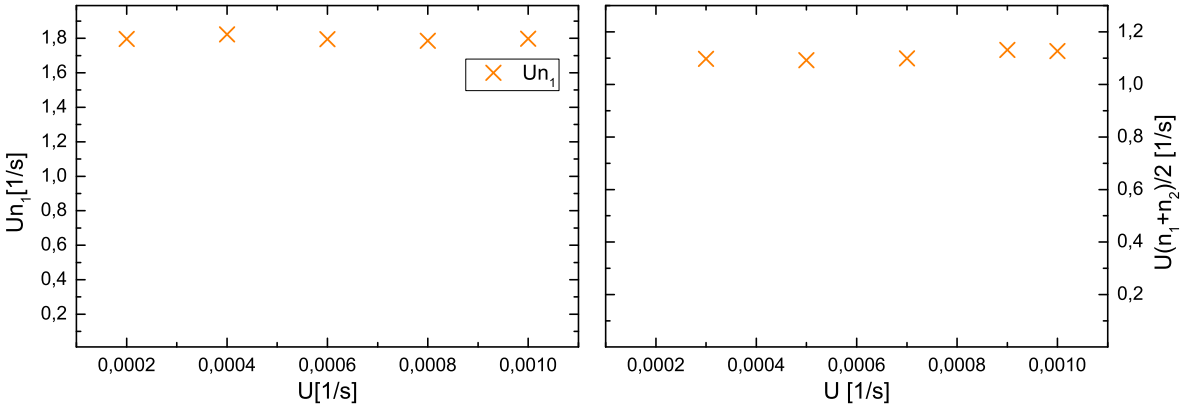

Figure 18: Left panel: Interaction energy per particle at the middle well of a lattice of three sites; U is the on-site interaction at the middle well; The points in the graph are taken when the relative difference between the current in the noninteracting system and the interacting system is equal to 0.3. Parameters: $\Gamma_0 = \Gamma_2 = 5s^{-1}$, $\Delta_j = 0$ $(j = 0, 1, 2)$, $n_R = 100$, $\eta = 1s^{-1}$, $dt = 10^{-6}s$.
Right panel: Averaged interaction energy per particle at the middle two wells of a lattice of four sites; U is the on-site interaction at the middle two wells; The points in the graph are taken when the relative difference between the current in the noninteracting system and the interacting system is equal to 0.3. The parameters are the same as in the left panel.

energy $UN = \sum_{j=1}^{\mathcal{N}-2} U_j n_j$ ($\mathcal{N}$ - total number of lattice sites). This statement is examined for lattice chains of length 3,4,5. The results are plotted in fig. (19) and do not reject our primitive statement.

In fig. 17 one can compare the TWA and the Tadpole approximation. The behaviour of the current is qualitatively the same in both cases. In the TWA the current is a result of the competition between two effects: an increase $\sim (n_L - n_R)$ that can be seen directly in the formula of the current of a noninteracting system; a decrease because of the shift of the energy level of the middle dot $\Delta \to \Delta + U(1 + n_L + n_R)$. On the other hand the Tadpole approximation fails to reproduce the difference in the mean particle occupation number of the middle sites of the chain.

6.3 Energy level of the middle well.

The decrease of the current because of an increase of the on-site interactions in the middle lattice site(s) can be interpreted on the mean field level with the fact that an energy barrier for the particles tunneling through the middle well arise. As explained in subsection 6.2, this originates from the fact that the

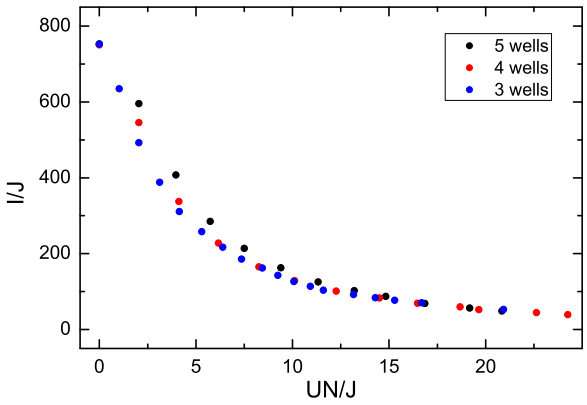

Figure 19: Current vs. interaction energy for the case of a lattice chain of length $\mathcal{N} = 3, 4, 5$; $UN = \sum_{j=1}^{\mathcal{N}-2} U_j n_j$, U_j - particle-particle interaction strength at the j-th quantum dot, n_j-mean particle occupation of the j-th quantum dot.

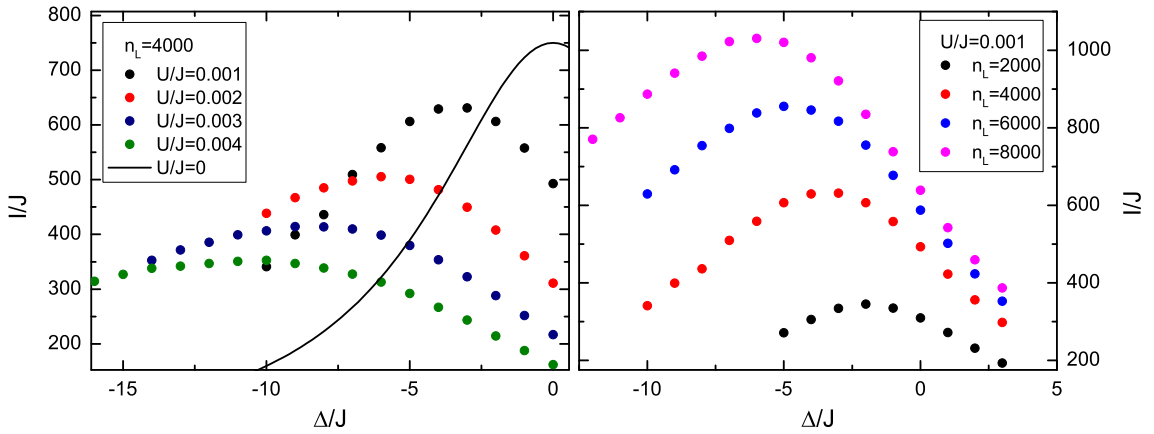

Figure 20: Steady state current (I) for a chain of three quantum dots in dependence of the energy level Δ and the on-site interaction U of the middle dot. Used parameters are $J = 1s^{-1}$, $n_R = 100$, $\Gamma/J = \Gamma_0/J = \Gamma_2/J = 5$.

energy of the sytem changes by an order of Un_1 if a particle moves from one of the boundary wells to the middle one. The situation changes if one varies the energy level Δ of the middle dot. If we are completely in the mean-field regime, then we can tune Δ such that the maximal current value is reached, as in the noninteracting case. This possibility is checked in fig. 20. In the left subfigure the maximum of I for different nonzero U shifts linearly with Δ, but the absolute maximal value decreases. The shape of the graph $I(\Delta)$ becomes wider for increasing U (left subfigure) but is unchanged for increasing "voltage" in the system (right subfigure). So the mean-field theory is not enough to explain the qualitative changes in the left subfigure.

6.4 Coupling strength to the reservoir

We consider again the case of a lattice chain of three quantum dots and non-zero on-site interaction in the middle well. In order to understand the behaviour of the current in the TWA and the Tadpole approximation in fig. 21, we will need more information about the spectral functions of the quantum dots.
We recall the fact, that the spectral function of an isolated QD has a δ-peak, that in general turns into a wider curve after a coupling with some reservoir. This means that a quantum dot at energy ε_0 is not only accessible for particles with energy ε_0 but also for particles with different energies. The time, that a particle spends at this level becomes also finite.
For the case of a chain of three lattice sites coupled to two Markovian reservoirs, the spectral function at the zeroth and last quantum dots ($\mathcal{S}_0(w), \mathcal{S}_2(w)$) is the same. For increasing Γ one sees, as expected, that the spectral function becomes wider. The result does not change, if we vary the position of the energy level Δ of the middle QD, except the appearance of a tight peak at $w = \Delta$. In the following discussion this effect is not important and we will not mention it any more.
The spectral function of the middle quantum dot ($\mathcal{S}_1(w)$) has different behaviour. For larger values of Γ the peak at $w = \Delta$ is almost unchanged. A shift of the position of Δ results in a shift of $\mathcal{S}_1(w)$ leaving also an additional small peak at $w = 0$ (see fig. 22).

Now, we look at the overlap of the spectral functions of the left and the middle quantum dots. ($\mathcal{S}_0(w), \mathcal{S}_1(w)$) (the results for the overlap between $\mathcal{S}_1(w)$ and $\mathcal{S}_2(w)$ are the same). For $\Delta = 0$ and increasing Γ the overlap is in the same energy range since the width of $\mathcal{S}_1(w)$ is almost unchanged in comparison to the width of $\mathcal{S}_0(w)$. Only particles in the left dot with energies, that are also accessible in $\mathcal{S}_1(w)$, can tunnel to the middle dot. But this number is smaller since $\mathcal{S}_0(w)$ spreads over a larger range of energies and the particles at the left dot are distributed over this range. It follows that the current should also decrease. This should explain the difference in the slope of the curves plotted in fig. 21 for small voltages $n_L - n_R$. The same behaviour can be seen also in the first line of eq. (170).

With this simple picture we will also explain the position of the peaks of the curves plotted in fig.

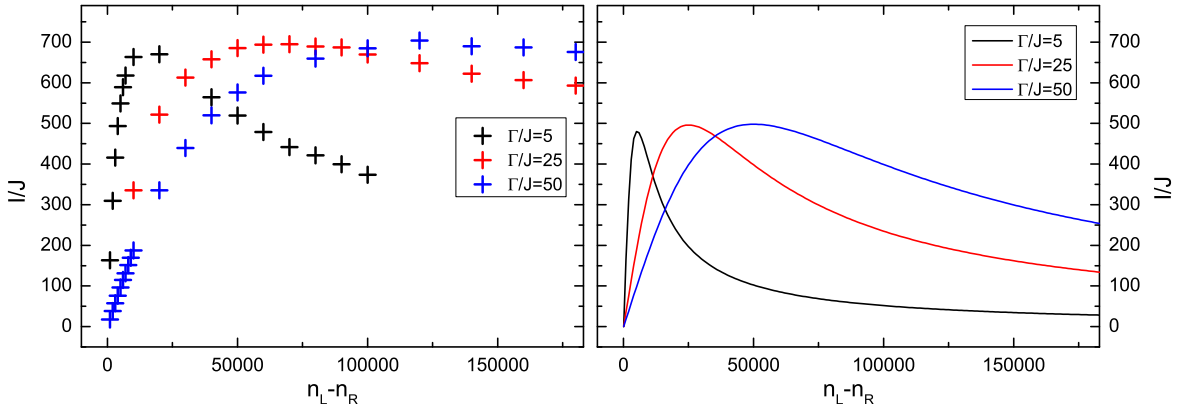

Figure 21: Steady state current for a lattice chain of three quantum dots coupled to two Markovian reservoirs in dependence of $\Gamma = \pi D(w)\gamma^2$ ($D(w) = \text{const}$ - density of states of the reservoir, $\gamma = \text{const}$ - coupling between the chain and the reservoir). TWA (left panel) and Tadpole approximation (right panel). Used parameters are: $U/J = 0.001$, $\Delta/J = 0$, $n_R = 100$.

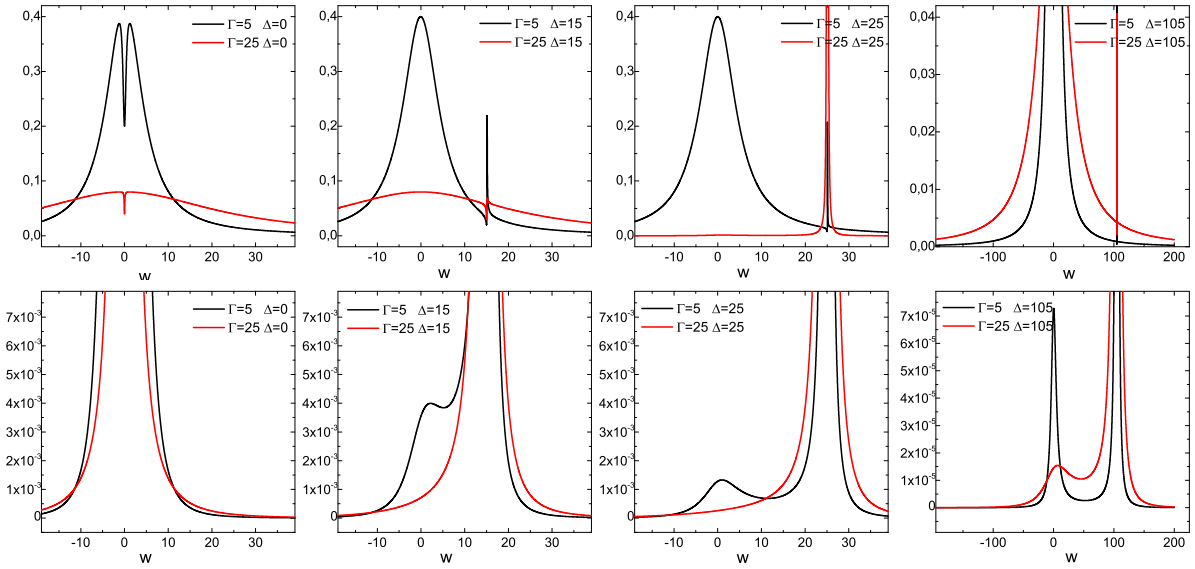

Figure 22: Spectral function of the left,right quantum dot (upper panel) and of the middle quantum dot (lower panel) of a lattice chain of three quantum dots coupled to a Markovian reservoir. $\Gamma = \pi D(w)\gamma^2$, $D(w)$ - density of states of the reservoir, γ - coupling between the reservoir and the lattice, Δ-energy level of the middle quantum dot; w, Γ, Δ in the figure are given in units of J. An increase of Γ leads to a broadening of the spectral function of the left,right quantum dot $\mathcal{S}_0(w), \mathcal{S}_2(w)$. The spectral function of the middle quantum dot is almost unchanged in comparison to the change of $\mathcal{S}_0(w)$.

21. In the Tadpole approximation we know that an increase of the interaction strength leads to a change of the energy level of the quantum dot ($\Delta \to \Delta + U(1 + n_L + n_R)$) We have to take into account the following facts:

- For higher values of Γ $\mathcal{S}_0(w)$ is non-zero in a larger range around $w = 0$. So there is an overlap between $\mathcal{S}_0(w)$ and the peak of $\mathcal{S}_1(w)$ at $w = \Delta$ for a larger range of values of Δ. Since Δ is proportional to $U(1 + n_L + n_R) \approx Un_L$ this means that if we keep U and Δ constant, then the overlap between $\mathcal{S}_0(w)$ and the peak of $\mathcal{S}_1(w)$ around $w = \Delta$ is non-zero for a larger range of values of n_L.
  $\Longrightarrow$ Particles in the middle dot with energy $\varepsilon = \Delta$ can tunnel to the left quanum dot, because the left QD can be excited at this energy level, and vice versa.

- If Δ is above some value, the overlap between $\mathcal{S}_0(w)$ and the peak of $\mathcal{S}_1(w)$ at $w = \Delta$ drops

significantly.
$\Longrightarrow$ The number of possibilities for particle exchange between the dots decrease.
$\Longrightarrow$ The current decrease.

So this should explain the fact that the peak in the curves plotted in fig. 21 shifts to the right for higher Γ.

6.5 Limit of low occupation numbers. Comparisson with the Quantum jump method.

We close the section with a short comparisson between the TWA and the quantum jump method in the limit of low occupation numbers and high interaction strengths. The only approximation that is applied in the Quanum jump methid is the use of a cut-off for the maximal occupation of a quanum dot. In our case the maximal occupation number $N_{max} = 40$. The behaviour of the steady state current in dependence of the interaction strength U is given in fig. 23. Both approaches give in this range quantitatively close results. Although the Quantum jump method can be applied for higher interaction strengths, it requires larger evolution times and a smaller evolution step in time, which makes the use of the method for this problem not appropriate.

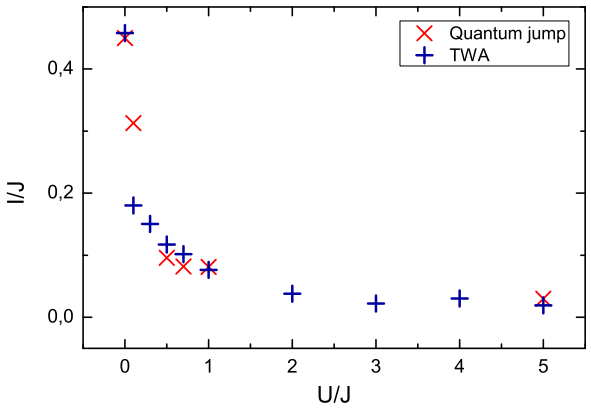

Figure 23: Steady state current (I) for a chain of three quantum dots in dependence of the on-site interaction U. TWA (blue crosses), Quantum jump (red crosses). Used parameters are $J = 1s^{-1}$, $n_L = 5$, $n_R = 4$, $\Delta/J = 0$, $\Gamma/J = \Gamma_0/J = \Gamma_2/J = 5$.

Part IV
Conclusions

In this thesis we have investigated the quantum transport through a quantum dot coupled to two bosonic reservoirs.
In part two we have discussed how to describe the effect of a noninteracting bosonic gas condensed in energy, that is coupled to the system. Next, we have added an on-site particle-particle interaction to the system and we have assumed that the particles in the bosonic reservoirs are confined by a harmonic potential. Using a simple self-energy approximation that conserves the causality condition, we have extracted the change of the spectral function of the quantum dot. From another current conserving approximation we have calculated the dependence of the steady state current on the interaction strength. We have made the following observations:

- The inclusion of a noninteracting bosonic gas, condensed in energy (ε_0), does not modify the steady state of the system. The system is modified only by the existence of the energy level ε_0.
- For an increasing interaction strength the peak of the spectral funciton shifts to higher energies and gets wider, as expected. Although we have taken corrections to the self-energy that go beyond the Tadpole approximation, it turns out that these corrections are not significant.
- There is a resonance condition for the strength of the current, that depends on the position of the energy level of the dot. Because the interaction U effectively shifts the energy level of the dot, we observe an increase/decrease of the current in dependence of U and the initial position Δ of the energy level.

We have to note that in calculating the Sunset approximation of the Self-energy we have chosen the system parameters such that no poles in the noninteracting Green's function occur. This makes the multidimensional integrals over a product of Green's funcitons well defined. If there are poles, then one has probably to sum over an additional set of Green's functions such that these poles are removed.

In part three we have studied a chain of quantum dots with on-site particle-particle interaction, that is coupled to two Markovian reservoirs. First, we have motivated the use of a Master equation in Lindblad form and then we have mapped the problem to a set of Langevin equations. We have shown how to derive the same set of equations from an action. This has allowed us to apply two approaches to solve the problem: the Truncated Wigner approximation (TWA) and the approximations applied in part two.

The behaviour of the system in the noninteracting case is solved exactly via the nonequilibrium Green's funciton method and we have written down the results for the current, mean occupation number, first and second order coherence. There are two interesting aspects to point out:

- The connection between the degree of coherence and the coupling to a Markovian reservoir is shown explicitly in eq. (169). The expectation that a stronger coupling to the enviroment should decrease the coherence is fulfilled.
- In eq. (170) we see a linear dependence of the current on the applied voltage.

In the interacting case we have rewritten the action in terms of classical and quantum fields and pointed out, that the classical part of the interaction is completely taken into account in the TWA. From the numerical simulations we have observed that in the TWA the following changes of the observables occur:

(i) The current vs. voltage curve does not have a linear dependence any more but has a clear maximum at finite voltage. The position of the maximum is approximately at the point where the interaction energy is equal to tunneling energy. The behaviour of the current in dependence of the applied voltage, the interaction strength and the coupling to the reservoir can be described qualitatively with the Tadpole approximation. We have found also a simple explanation for these effects, that is based on the form of the spectral functions of the quantum dots.

(ii) The mean occupation number of the lattice sites that are not connected directly to a reservoir is not the same any more but one observes self-trapping effects. This effect is not captured by the Tadpole approximation.

(iii) For the case of a chain of four lattice sites there is a negative correlation between an arrival of particles in the middle two quantum dots. The second order coherence $g^{(2)}(i,i)$ also increases for very high voltages, i.e. the particles arrive at the dots in bunches. For the first effect we have found a qualitative explanation with the use of arguments based on the change of the total energy of the system.

The problem of an increasing lattice chain coupled to two Markovian reservoirs is also solved approximately with the use of nonequilibrium Green's functions. We have applied only the Tadpole approximation since it conserves the causality condition and the steady state current. So we also know apriori that the points (ii), (iii) can not be fulfilled. If one compares the behaviour of the steady state current in dependence of the voltage $n_L - n_R$ and the interaction strength U, there is a qualitative agreement with the TWA. But the position and height of the peaks is different in both approximations. In the end, we have assumed that there is an universal behaviour of the current, which depends on the interaction energy of the system ($UN = \sum_{j=1}^{\mathcal{N}-2} U_j n_j$), n_j - mean particle occupation at site j. We have done simulations for a lattice chain of 3,4,5 wells with on-site interaction in the middle one,two,three wells. The reults plotted in fig. 19 do not reject our assumption.

In this work we have managed to obtain and explain the behaviour of a system coupled to two Markovian reservoirs by the use of two methods. But considering a more realistic reservoir we faced with a large amount of difficulties and we were not able to capture the influence of the particle-particle interaction that go beyond the mean-field effects. A possible way to do this is to describe the problem in the form of a set of stochastic intgro-differential equations like those given in eq. (136) and solve them numerically. We have already mentioned that the main drawback of this method is the memory and computation time needed to simulate a stochastic process with the desired autocorrelation function. But if we consider a reservoir whith density of states $D(w)$ such that the Fourier transform $\tilde{\Gamma}(t)$ of $\pi D(w)\gamma^2(w)$ is a function decaying sufficiently fast in time, then the autocorrelation matrix given in eq. (134) can be approximated with a band-matrix. The faster the function $\tilde{\Gamma}(t)$ decays, the smaller is the width of the band of the autocorrelation matrix. The decomposition of such a matrix and the memory needed to save the coefficients, which we need in order to generete the desired collection of random variables, are problems which complexity dependes linearly on the width m of the band of the matrix. So if m is sufficiently small, the problem can be solved numerically.

Part V
Appendix

1 Higher order approximation of a stochastic integral. Ito formula.

In part 3 we have argued that the increments of a Wiener process $dW_t = W_{t+dt} - W_t$ can be approximated by $\zeta_t\sqrt{dt}$, i.e. dW_t is an infinitesimal of order 1/2. In order to derive a better approximation of the stochastic differential equation one has to know how to approximate products of infinitesimals like $(dW_t)^2$, $dW_t dt$, etc. One can show [34] that $(dW_t)^2 = dt$ in the sense that for any nonanticipating function $G(t)$ the following relation holds in the mean-square limit:

$$\int_{t_0}^{t}(dW_{t'})^2 G(t') = \int_{t_0}^{t} dt' G(t') \tag{171}$$

One can also show that $(dW_t)^N = 0$ for $N > 2$ and $dW_t^i dW_t^j = \delta_{ij} dt$ for two different Wiener processes labeled with i, j. With these basics the formula for an infinitesimal change of a function f that depends on some stochastic process $\vec{X}_t$ can be derived[22] ($\vec{X} \in \mathbb{R}^d$, $\vec{A} \in \mathbb{R}^d$, $B \in \mathbb{R}^{d\times m}$, $\vec{W} \in \mathbb{R}^m$):

$$\begin{aligned} dX_t^i &= A^i(\vec{X}_t)dt + B^{ij}dW_t^j \\ df(\vec{X}_t) &= \left(\tfrac{dX_t^k}{dt}\right)\tfrac{\partial f(\vec{X})}{\partial X^k}\Big|_{\vec{X}=\vec{X}_t} dt + \left(\tfrac{dX_t^k}{dW_t^j}\right)\tfrac{\partial f(\vec{X})}{\partial X^k}\Big|_{\vec{X}=\vec{X}_t} dW_t^j + \tfrac{1}{2}\left(\tfrac{dX_t^k}{dW_t^j}\right)\left(\tfrac{dX_t^{\tilde{k}}}{dW_t^{\tilde{j}}}\right)\tfrac{\partial^2 f(\vec{X})}{\partial X^k \partial X^{\tilde{k}}}\Big|_{\vec{X}=\vec{X}_t} dW_t^j dW_t^{\tilde{j}} \end{aligned} \tag{172}$$

If one replaces the derivatives of $\vec{X}_t$ with respect to dt and dW_t with the expressions in the first line of the last equation one arrives at the Ito formula. It allows the calcualtion of the trajectories of a function of a knwon porcess:

$$f(\vec{X}_t) = f(\vec{X}_{t_0}) + \int_{t_0}^{t} ds\Big[A^k(\vec{X}_s)\tfrac{\partial f(\vec{X})}{\partial X^k}\Big|_{\vec{X}=\vec{X}_s} + \tfrac{1}{2}B^{kj}B^{\tilde{k}j}\tfrac{\partial^2 f(\vec{X})}{\partial X^k \partial X^{\tilde{k}}}\Big|_{\vec{X}=\vec{X}_s}\Big] + \int_{t_0}^{t} dW_s^j B^{kj}\tfrac{\partial f(\vec{X})}{\partial X^k}\Big|_{\vec{X}=\vec{X}_s} \tag{173}$$

One can apply the same formula for the drift and diffusion coefficients of the last equation and so obtain an approximation of higher order. In this thesis we deal with stochastic equations where the matrix B is constant (In this case the Euler algorithm coincides with the Milstein algorithm which has a strong order of convergence equal to 1). This makes the expansion of a stochastic process up to second order in dt a relatively simple task ($\vec{X} \in \mathbb{R}^d$, $\vec{A} \in \mathbb{R}^d$, $B \in \mathbb{R}^{d\times m}$, $\vec{W} \in \mathbb{R}^m$):

$$\begin{aligned} X_t^i = {} & X_{t_0}^i + A^i(\vec{X}_{t_0})\int_{t_0}^{t} ds + B^{ij}\int_{t_0}^{t} dW_s^j + \\ & \Big[A^k(\vec{X}_{t_0})\tfrac{\partial A^i(\vec{X})}{\partial X^k} + \tfrac{1}{2}B^{kj}B^{\tilde{k}j}\tfrac{\partial^2 A^i(\vec{X})}{\partial X^k \partial X^{\tilde{k}}}\Big]\Big|_{\vec{X}=\vec{X}_{t_0}}\int_{t_0}^{t} ds\int_{t_0}^{s} ds' + \\ & B^{kj}\tfrac{\partial A^i(\vec{X})}{\partial X^k}\Big|_{\vec{X}=\vec{X}_{t_0}}\int_{t_0}^{t} ds\int_{t_0}^{s} dW_{s'}^j + B^{kj}B^{\tilde{k}\tilde{j}}\tfrac{\partial^2 A^i(\vec{X})}{\partial X^{\tilde{k}}\partial X^k}\Big|_{\vec{X}=\vec{X}_{t_0}}\int_{t_0}^{t} ds\int_{t_0}^{s} dW_{s'}^j\int_{t_0}^{s'} dW_{s''}^j \end{aligned} \tag{174}$$

For $t = t_0 + \Delta t$ the integrals in the first two lines are known. The first integral in the last line is a process which increments can be approximated by a normal distributed random variable ΔZ with zero mean, variance equal to $\frac{1}{3}\Delta t^3$ and covariance $\langle \Delta Z \Delta W^j\rangle = \frac{1}{2}\Delta t^2$ (ΔW^j is the incrment of the Wiener process W^j). Both, the increments if the Wiener process and of the new process, can be generated with the use of two independent random variables $\zeta^1, \zeta^2 \sim \mathcal{N}(0,1)$:

$$\begin{bmatrix} \Delta W^j \\ \Delta Z \end{bmatrix} = \underbrace{\begin{bmatrix} (\Delta t)^{1/2} & 0 \\ \frac{1}{2}(\Delta t)^{3/2} & \frac{1}{2\sqrt{3}}(\Delta t)^{3/2} \end{bmatrix}}_{U} \underbrace{\begin{bmatrix} \zeta_1 \\ \zeta_2 \end{bmatrix}}_{\vec{\zeta}} \tag{175}$$

One can proove that this gives the right covariance matrix:

$$\langle (U\vec{\zeta})(U\vec{\zeta})^T\rangle = U\langle \vec{\zeta}\vec{\zeta}^T\rangle U^T = UU^T = \begin{bmatrix} \Delta t & \frac{1}{2}(\Delta t)^2 \\ \frac{1}{2}(\Delta t)^2 & \frac{1}{3}(\Delta t)^3 \end{bmatrix} = \begin{bmatrix} \langle \Delta W^j \Delta W^j\rangle & \langle \Delta W^j \Delta Z\rangle \\ \langle \Delta Z \Delta W^j\rangle & \langle \Delta Z \Delta Z\rangle \end{bmatrix} \tag{176}$$

[22] In this section the superscript denotes an element of a vector and the subscript refers to the time.

For the special problem we are interested in, all coefficients that are multiplied to the last integral are equal to zero, so there is no need to evaluate the last integral.
The use of this second order Taylor method allows us to work with larger time step dt, but one needs to perform more trajectories of the process $\vec{X}_t$ than in the Euler method in order to capture the additional correlations between the processes ΔW^j and ΔZ.

2 Strong order of convergence of a process

The Strong order of convergence of some method for an Ito process can be defined only if the process obeys the existence and uniqueness condition. It is given below.
Existence and uniqueness condition.
It is given the Ito process

$$dX_t = f(t, X_t)dt + g(t, X_t)dW_t \tag{177}$$

with the following properties:

- $f, g : [t_0, T] \times \mathbb{R} \to \mathbb{R}$ are continuous in both variables.
- f, g fulfill the Lipshitz condition, i.e:

$$\begin{array}{rcll} |f(t,x) - f(t,y)| & \leq & L|x-y| & L \geq 0 \\ |g(t,x) - g(t,y)| & \leq & L|x-y| & L \geq 0 \end{array} \tag{178}$$

  for all $x, y \in \mathbb{R}$, uniformly in $t \in [t_0, T]$.

- f, g fulfill the Growth condition, i.e:

$$\begin{array}{rcll} |f(t,x)| & \leq & K(1+|x|) & K \geq 0 \\ |g(t,x)| & \leq & K(1+|x|) & K \geq 0 \end{array} \tag{179}$$

  for all $x, y \in \mathbb{R}$.

- The initial variable X_{t_0} is non-anticipative transformation of a Wiener process, i.e. it does not dependes on W_t for $t > t_0$.
- The initial random variable X_{t_0} fulfills the condition:

$$\langle X_{t_0} \rangle < \infty \tag{180}$$

Under these conditions the Ito process has an unique solution with initial value X_{t_0}.
Now, for an Ito process that obeys the above condition, we denote the exact solution with $\tilde{X}_t$, $t \in [t_0, T]$. The solution obtained by some numerical algorithm with time step Δ is denoted by X_t, $t \in \{t_0, t_1, \ldots t_{\mathcal{N}}\}$, $t_j = t_0 + j\Delta$, $t_{\mathcal{N}} = t_0 + \mathcal{N}\Delta \equiv T$. The numerical algorithm has a strong convergence of order $\gamma > 0$ if:

$$\max_n \langle |X_{t_n} - \tilde{X}_{t_n}| \rangle \leq K_T \Delta^\gamma \tag{181}$$

where K_T is some positive T-dependent constant.

3 Quantum Jump method

This method is an alternative of the TWA in the limit of very low occupation numbers. We start again with a Master equation in Lindblad form but instead of using the correspondence principle we truncate the Hilbert space. If its dimension is $\mathcal{N}$ then the master equation in Lindblad form for the density matrix is equivalent to a set of $\mathcal{N}^2$ coupled differential equations. The complexity of the method we present is of order $\mathcal{N}$.

For the Master equation in Lindblad form given in eq. (115) we rewrite the definition of $\mathcal{L}$ in the following form:

$$\begin{aligned}
\mathcal{L}(\hat{\sigma}) &= -\tfrac{1}{2}\sum_m \left(\hat{c}_m^\dagger \hat{c}_m \hat{\sigma} + \hat{\sigma}\hat{c}_m^\dagger \hat{c}_m - 2\hat{c}_m \hat{\sigma} \hat{c}_m^\dagger\right) - \tfrac{1}{2}\sum_m \left(\hat{\tilde{c}}_m \hat{\tilde{c}}_m^\dagger \hat{\sigma} + \hat{\sigma}\hat{\tilde{c}}\hat{\tilde{c}}_m^\dagger - 2\hat{\tilde{c}}_m^\dagger \hat{\sigma}\hat{\tilde{c}}_m\right) \\
\hat{c}_m &= \sqrt{2\Gamma_m(N_m+1)}\hat{a}_m \\
\hat{c}_m^\dagger &= \sqrt{2\Gamma_m(N_m+1)}\hat{a}_m^\dagger \\
\hat{\tilde{c}}_m &= \sqrt{2\Gamma_m N_m}\hat{a}_m \\
\hat{\tilde{c}}_m^\dagger &= \sqrt{2\Gamma_m N_m}\hat{a}_m^\dagger.
\end{aligned} \tag{182}$$

Since we work with a chain of quantum dots m is an index that denotes the different dots of the system. We assume first that at the beginning of the time evolution the system is in a pure state, i.e. $\sigma(0) = |\phi(0)\rangle\langle\phi(0)|$ but the approach can be generalised to arbitrary states. The wave function $|\phi(t)\rangle$ is evolved in small steps. For every step it has in general two possibilities for evolution: it can evolve via a non-hermitian Hamiltonian or it can perform a quantum jump to another state.

1. In the first case the non-Hermitian Hamiltonian is given in the form:

$$\hat{\mathcal{H}} = \hat{H} - \tfrac{i\hbar}{2}\textstyle\sum_m \hat{c}_m^\dagger \hat{c}_m - \tfrac{i\hbar}{2}\sum_m \hat{\tilde{c}}_m \hat{\tilde{c}}_m^\dagger \tag{183}$$

   One applies an infinitesimal evolution of the state $|\phi(t)\rangle$ with $\hat{\mathcal{H}}$ followed by an additional renormalisation:

$$|\phi(t+\delta t)\rangle = \frac{\left(1 - \frac{i}{\hbar}\hat{\mathcal{H}}\delta t\right)|\phi(t)\rangle}{\left(\langle\phi(t)|\left(1+\frac{i}{\hbar}\hat{\mathcal{H}}^\dagger\delta t\right)\left(1-\frac{i}{\hbar}\hat{\mathcal{H}}\delta t\right)|\phi(t)\rangle\right)^{1/2}} \tag{184}$$

   From the denominator of the last expression one takes only the terms in zeroth and first order in δt:

$$\langle\phi(t)|\left(1+\tfrac{i}{\hbar}\hat{\mathcal{H}}^\dagger\delta t\right)\left(1-\tfrac{i}{\hbar}\hat{\mathcal{H}}\delta t\right)|\phi(t)\rangle = 1 - \sum_m \underbrace{\delta t\langle\phi(t)|\hat{c}_m^\dagger\hat{c}_m|\phi(t)\rangle}_{\delta p_m} - \sum_m \underbrace{\langle\phi(t)|\hat{\tilde{c}}_m\hat{\tilde{c}}_m^\dagger|\phi(t)\rangle}_{\delta\tilde{p}_m}. \tag{185}$$

   The probability that this evolution is applied is defined as $(1-\delta p)$ with $\delta p = \sum_m \delta p_m + \sum_m \delta\tilde{p}_m$. The quantities δp_m, $\delta\tilde{p}_m$ define the probability of the system to perform a quantum jump into a state with lower, higher particle number at the m-th site respectively.

2. The second possibility for the evolution of the function - the quantum jump, is given by:

$$\begin{aligned}
|\phi(t+\delta t)\rangle &= \frac{\hat{c}_m|\phi(t)\rangle}{\sqrt{\delta p_m/\delta t}} \qquad \text{with probability } \delta p_m, \\
|\phi(t+\delta t)\rangle &= \frac{\hat{\tilde{c}}_m^\dagger|\phi(t)\rangle}{\sqrt{\delta\tilde{p}_m/\delta t}} \qquad \text{with probability } \delta\tilde{p}_m.
\end{aligned} \tag{186}$$

   The denominator renormalises the new wave-function.

The sum of all evolution possibilities is equal to one by construction. One has only to choose a time step that is so small that $\delta p < 1$ since we want to have a positive probability for nonunitary time evolution. In order to evolve the state from t_0 to t we generate at every step a random number ε uniformly distributed in the intervall $[0,1]$. We divide the intervall into subintervalls with lengths $1-\delta p, \delta p_1, \ldots, \delta p_{\mathcal{N}}, \delta\tilde{p}_1, \ldots, \delta\tilde{p}_{\mathcal{N}}$. Dependent on the case in which domain ε lies we perform one of the evaluation steps given in eq. (184),(186) The density matrix for one particular realisation from t_0 to t is then:

$$\sigma_i(t) = |\phi_i(t)\rangle\langle\phi_i(t)| \tag{187}$$

The average density matrix of the system after performing N_T evolutions of the state $|\phi(t)\rangle$ is:

$$\bar{\sigma}(t) = \tfrac{1}{N_T}\textstyle\sum_{i=1}^{N_T} |\phi_i(t)\rangle\langle\phi_i(t)|. \tag{188}$$

If the initial state of the system is not a pure state we can always represent it as a sum of pure states weighted with some probability:

$$\sigma(t_0) = \textstyle\sum_j p_j |\phi^j(t)\rangle\langle\phi^j(t)| \tag{189}$$

and we have to perform an additional sampling of the initial states such that the probability to pick $|\phi^j(t_0)\rangle$ is equal to p_j for all j.
The calculation of the expectation value of some observable $\hat{\mathcal{O}}$ is straight forward:

$$\langle\hat{\mathcal{O}}\rangle = \tfrac{1}{N_T}\sum_{i=1}^{N_T}\langle\phi_i(t)|\hat{\mathcal{O}}|\phi_i(t)\rangle. \tag{190}$$

One can prove that $\bar{\sigma}(t)$ coincides with $\sigma(t)$ by showing that they obey the same equation of motion. A simple proof can be found in [43].

4 Sokhotsky-Plemelj-theorem

Given $f(z)$ - complex valued function which is well defined on the real line; for $a, b \in \mathbb{R}$ with $a < 0 < b$, it follows:

$$\lim_{\varepsilon\to 0^+}\int_a^b \frac{f(x)}{x \pm i\varepsilon}dx = \mp i\pi f(0) + \mathcal{P}\int_a^b \frac{f(x)}{x}dx \tag{191}$$

where $\mathcal{P}$ is the Couchy principal value. For $f(x) = \delta(x - x')$ one gets the following relation:

$$\lim_{\varepsilon\to 0^+}\tfrac{1}{x'\pm i\varepsilon} \quad = \quad \mp i\pi\delta(x') + \mathcal{P}\tfrac{1}{x'} \tag{192}$$

5 Short notation for the arguments of a Green's function

In a steady state the propagator depends only on the time difference of its arguments. So one often uses the following short notation:

$$G_{(w,w')} \quad = \quad 2\pi\delta_{(w-w')}G_{(w)} \tag{193}$$

The short notation in the time domain is:

$$\begin{array}{rcl} G_{(t,t')} & = & \int \frac{dwdw'}{(2\pi)^2}e^{-iwt}e^{+iw't'}G_{(w,w')} \\ & = & \int \frac{dwdw'}{(2\pi)^2}e^{-iwt}e^{+iw't'}2\pi\delta_{(w-w')}G_{(w)} \\ & = & \int \frac{dw}{2\pi}e^{-iw(t-t')}G_{(w)} \\ & = & G_{(t-t')} \end{array} \tag{194}$$

The inverse of the steady-state Green's function is given by $G^{-1}_{(w,w')} = \frac{1}{2\pi}\delta_{(w-w')}G^{-1}_{(w)}$. One can verify that:

$$\int dw' G_{(w,w')}G^{-1}_{(w',w'')} \quad = \quad \int dw' 2\pi\delta_{(w-w')}G_{(w)}\tfrac{1}{2\pi}\delta_{(w'-w'')}G^{-1}_{(w')} = \delta_{(w-w'')}. \tag{195}$$

The short notation for the self-energy Σ is extracted from the following equation:

$$\begin{array}{rcrcl} & & G^{-1}_{(w',w'')} & = & g^{-1}_{(w',w'')} - \Sigma_{(w',w'')} \\ \iff & & \frac{1}{2\pi}\delta_{(w'-w'')}G^{-1}_{(w')} & = & \frac{1}{2\pi}\delta_{(w'-w'')}g^{-1}_{(w')} - \Sigma_{(w',w'')} \\ \implies & & \Sigma_{(w',w'')} & \equiv & \frac{1}{2\pi}\delta_{(w'-w'')}\Sigma_{(w')} \end{array} \tag{196}$$

6 Derivation of eq. (49)

In the following we consider the Hamiltonian $\hat{H}' = \hat{H}_0 + \sum_k \left(\gamma_{kL}\hat{L}^\dagger_k\hat{a} + \gamma^*_{kL}\hat{a}^\dagger\hat{L}_k\right)$, $\hat{H}_0 = \sum_k \varepsilon_k\hat{L}^\dagger_k\hat{L}_k$ but the result can be generalised to a wider class of systems.
One writes down $G_{k1}(t)$ in the Interaction picture representation and then expands the exponential function in the expression below, namely the time evolution operator $\hat{\mathcal{U}}_{H_0}$[23]

$$\begin{array}{rcl} G_{k1}(t) & = & -i\langle\hat{T}_c\hat{L}_{H_0,k(t)}\hat{a}^\dagger_{H_0(0)}e^{-i\int_c d\tau\left(\gamma_{\tilde{k}}\hat{L}^\dagger_{H_0,\tilde{k}(\tau)}\hat{a}_{H_0(\tau)}+\gamma^*_{\tilde{k}}\hat{a}^\dagger_{H_0(\tau)}\hat{L}_{H_0,\tilde{k}(\tau)}\right)}\rangle_0 \\ & = & -i\sum_{n=0}^{\infty}\frac{(-i)^n}{n!}\int_c d_{\tau_{1\ldots n}}\langle\hat{T}_c\hat{L}_{k(t)}\hat{a}^\dagger_{(0)}\prod_{j=1}^{n}\left(\gamma_{k_j}\hat{L}^\dagger_{k_j(\tau_j)}\hat{a}_{(\tau_j)} + \gamma^*_{k_j}\hat{a}^\dagger_{(\tau_j)}\hat{L}_{k_j(\tau_j)}\right)\rangle_0 \\ & = & -i\sum_{n=0}^{\infty}\frac{(-i)^{2n+1}}{(2n+1)!}\int_c d_{\tau_{1\ldots 2n+1}}\langle\hat{T}_c\hat{L}_{k(t)}\hat{a}^\dagger_{(0)}\prod_{j=1}^{2n+1}\left(\gamma_{k_j}\hat{L}^\dagger_{k_j(\tau_j)}\hat{a}_{(\tau_j)} + \gamma^*_{k_j}\hat{a}^\dagger_{(\tau_j)}\hat{L}_{k_j(\tau_j)}\right)\rangle_0 \end{array} \tag{197}$$

[23] We have dropped the subscript $_{H_0}$ in the second and third line of the equation.

In the last line we used the fact that the even powers of the exponential have zero contribution to the Green's function since the total number of $\hat{L}, \hat{L}^\dagger$ fields is odd. We select only terms of the exponential that contain (n+1) times $\hat{L}^\dagger$ and n times $\hat{L}$. The combinatorial factor we get from this selection of terms is $\frac{(2n+1)!}{(n+1)!n!}$ since $(\alpha+\beta)^{2n+1} \ni \alpha^{n+1}\beta^n \frac{(2n+1)!}{(n+1)!n!} = \alpha^{n+1}\beta^n \binom{2n+1}{n+1}$. Then we contract $\hat{L}_{k(t)}$ with one of the $\hat{L}^\dagger_{k_j(\tau_j)}$-terms. Since there are $n+1$ possibilities to do this we get the factor $(n+1)$. So the overall combinatorial factor in every term with $(2n+1)$ integrals over time is $\frac{1}{n!n!}$. We also use the Green's function of a noninteracting bosonic reservoir:

$$g_{kk';L(t,t')} = \delta_{kk'} g_{kk;L(t,t')} = -i\,\mathrm{tr}\big[\hat{\rho}_0 \hat{T}_c \hat{L}_{H_0,k(t)} \hat{L}^\dagger_{H_0,k'(t')}\big] = \delta_{kk'}(-i)\langle \hat{T}_c \hat{L}_{H_0,k(t)} \hat{L}^\dagger_{H_0,k'(t')}\rangle_0 \tag{198}$$

So we get[24]:

$$G_{k1}(t) = -i \sum_{n=0}^{\infty} \tfrac{(-i)^{2n}}{n!n!} \int_c d_{\tau_{1\ldots 2n+1}} \gamma_k g_{kk;L(t-\tau_1)} \Big\langle \hat{T}_c \hat{a}_{(\tau_1)} \hat{a}^\dagger_{(0)} \prod_{j=1}^{n+1} \big(\gamma_{k_j} \hat{L}^\dagger_{k_j(\tau_j)} \hat{a}_{(\tau_j)}\big) \prod_{j=n+2}^{2n+1} \big(\gamma^*_{k_j} \hat{a}^\dagger_{(\tau_j)} \hat{L}_{k_j(\tau_j)}\big)\Big\rangle_0 \tag{199}$$

One can compare for every $n \in \mathbb{N}_0$ the terms from the sum in the last equation with the terms from $G_{11}(\tau_1, 0)$[25]

$$\begin{aligned} G_{11}(\tau_1,0) &\equiv -i\big\langle \hat{T}_c \hat{a}_{H_0(\tau_1)} \hat{a}^\dagger_{H_0(0)} e^{-i\int_c d\tau \left(\gamma_{\tilde{k}} \hat{L}^\dagger_{\tilde{k}(\tau)} \hat{a}_{(\tau)} + \gamma^*_{\tilde{k}} \hat{a}^\dagger_{(\tau)} \hat{L}_{\tilde{k}(\tau)}\right)}\big\rangle_0 \\ &= -i \textstyle\sum_{n=0}^{\infty} \frac{(-i)^{2n}}{(2n)!} \int_c d_{\tau_{2\ldots 2n+1}} \big\langle \hat{T}_c \hat{a}_{(\tau_1)} \hat{a}^\dagger_{(0)} \prod_{j=2}^{2n+1} \big(\gamma_{k_j} \hat{L}^\dagger_{k_j(\tau_j)} \hat{a}_{(\tau_j)} + \gamma^*_{k_j} \hat{a}^\dagger_{(\tau_j)} \hat{L}_{k_j(\tau_j)}\big)\big\rangle_0 \\ &= -i \textstyle\sum_{n=0}^{\infty} \frac{(-i)^{2n}}{n!n!} \int_c d_{\tau_{2\ldots 2n+1}} \langle \hat{T}_c \hat{a}_{(\tau_1)} \hat{a}^\dagger_{(0)} \prod_{j=2}^{n+1} \big(\gamma_{k_j} \hat{L}^\dagger_{k_j(\tau_j)} \hat{a}_{(\tau_j)}\big) \prod_{j=n+2}^{2n+1} \big(\gamma^*_{k_j} \hat{a}^\dagger_{(\tau_j)} \hat{L}_{k_j(\tau_j)}\big)\rangle_0 \end{aligned} \tag{200}$$

We have used again the fact that terms with odd number of $\hat{L}^\dagger + \hat{L}$ operators are equal to zero (second line) and that the number of $\hat{L}^\dagger$ and $\hat{L}$ operators should be equal (third line) and $(\alpha+\beta)^{2n} \ni \alpha^n\beta^n\binom{2n}{n} = \alpha^n\beta^n \frac{2n!}{n!n!}$. Comparing eq. (199) and eq. (200) one gets the relation:

$$G_{k1(t,0)} = \gamma_k \textstyle\int_c d\tau\, g_{kk;L(t,\tau)} G_{11(\tau,0)} \tag{201}$$

The same proof can be made also for the Hamiltonian in eq. (45).

7 Detailed calculation of the Green's function of a chain of two quantum dots

The Hamiltonian of the system is[26]:

$$\hat{H} = \Delta_1 \hat{a}^{1\dagger}\hat{a}^1 + \Delta_2 \hat{a}^{2\dagger}\hat{a}^2 - \eta \hat{a}^{1\dagger}\hat{a}^2 - \eta^* \hat{a}^{2\dagger}\hat{a}^1 \tag{202}$$

We use the coherent states basis $\{|\vec{a}_j\rangle\}$ with $|\vec{a}_j\rangle \equiv |a^1_j \;\; a^2_j\rangle$ (the index j refers to the time) which have the properties:

$$\begin{aligned} \langle \vec{b}_{j'}|\vec{a}_j\rangle &= e^{\vec{b}^*_{j'}\cdot\vec{a}_j} = e^{b^{1*}_{j'} a^1_j + b^{2*}_{j'} a^2_j} && \diamondsuit \\ \hat{a}^m|\vec{a}_j\rangle &= a^m_j|\vec{a}_j\rangle && \diamondsuit\diamondsuit \\ \hat{1} &= \textstyle\int \prod_{m=1}^2 \big(\frac{da^{m*}_j da^m_j}{\pi}\big) e^{-\vec{a}^*\cdot\vec{a}_j} && \diamondsuit\diamondsuit\diamondsuit \end{aligned}$$

We define the contour in the Keldysh partition function such that the beginning and the return points are at the finite times t_0 and t_f:

$$\begin{aligned} \mathcal{Z} &= \frac{\mathrm{tr}\big[\hat{\rho}_0 \hat{T}_C \big(e^{-\frac{i}{\hbar}\int_c d\tau \hat{H}(\tau)}\big)\big]}{\mathrm{tr}[\hat{\rho}_0]} \\ &= \textstyle\int \prod_{m=1}^2 \frac{da^{m*}_0 da^m_0}{\pi} \langle \vec{a}_0|\hat{\rho}_0|\vec{a}_0\rangle e^{-\vec{a}^*_0\cdot\vec{a}_0} \\ &= \textstyle\int \prod_{m=1}^2 \frac{da^{m*}_{-0} da^m_{-0}}{\pi} \prod_{n=1}^2 \frac{da^{n*}_{+0} da^n_{+0}}{\pi} \langle \vec{a}_{-0}|\hat{\rho}_0|\vec{a}_{+0}\rangle \langle \vec{a}_{+0}|\vec{a}_{-0}\rangle e^{-\vec{a}^*_{-0}\cdot\vec{a}_{-0} - \vec{a}^*_{+0}\cdot\vec{a}_{+0}} \end{aligned} \tag{203}$$

[24] $\langle \ldots\rangle_0 \equiv tr[\rho \ldots]$.

[25] all operators are again in the Interaction picture representation and we drop H_0 after the first line of eq. (200).

[26] In this section the superscript of an operator denotes the postion in the lattice and the subscript denotes the position at the time contour.

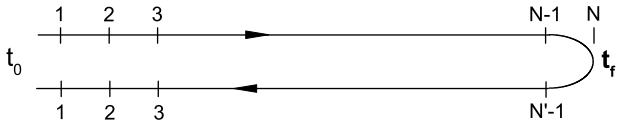

Figure 24: Contour branch on which the operator $\hat{T}_c$ acts. The forward (from t_r to t) and the backward (from t_r to t) branches denoted with $(-)$ and $(+)$ are divided into N and N' peices.

In the second and in the third lines we have inserted the completeness relation ($\diamondsuit\diamondsuit\diamondsuit$). Since both fields are at the initial time t_0 (the subscript $_0$ of a refers to the time t_0) we have added an additional subscript $l = \pm$ to distinguish them. The minus will refer later to the forward and the plus to the backward contour. Now divide the forward and backward contours into N, N' parts as shown in fig. 24 and then let $N \to \infty$, $N' \to \infty$, $t_f \to \infty$ and $t_i \to -\infty$. Insert at the division points the completeness relation ($\diamondsuit\diamondsuit\diamondsuit$). The propagation from t_0 at the forward branch to t_0 at the backward branch can be expressed in the form ($\hbar = 1$):

$$\begin{aligned}\langle\vec{a}_{+,0}|\vec{a}_{-,0}\rangle \;=\; & \prod_{j=1}^{N}\Big[\int\Pi_{m=1}^{2}\Big(\tfrac{da^{*m}_{-,j}da^{m}_{-,j}}{\pi}\Big)e^{-\vec{a}^{*}_{-,j}.\vec{a}_{-,j}}\Big]\prod_{l=1}^{N'-1}\Big[\int\Pi_{m=1}^{2}\Big(\tfrac{da^{*m}_{+,l}da^{m}_{+,l}}{\pi}\Big)e^{-\vec{a}^{*}_{+,l}.\vec{a}_{+,l}}\Big]\\ & \langle\vec{a}_{+,0}|e^{i\hat{H}\Delta t}|\vec{a}_{+,1}\rangle\langle\vec{a}_{+,1}|e^{i\hat{H}\Delta t}\ldots e^{i\hat{H}\Delta t}|\vec{a}_{+,N'-1}\rangle\langle\vec{a}_{+,N'-1}|e^{i\hat{H}\Delta t}|\vec{a}_{-,N}\rangle\\ & \langle\vec{a}_{-,N}|e^{-i\hat{H}\Delta t}|\vec{a}_{-,N-1}\rangle\langle\vec{a}_{-,N-1}|e^{-i\hat{H}\Delta t}\ldots e^{-i\hat{H}\Delta t}|\vec{a}_{-,1}\rangle\langle\vec{a}_{-,1}|e^{-i\hat{H}\Delta t}|\vec{a}_{-,0}\rangle\end{aligned} \tag{204}$$

For very small Δt one can approximate $e^{-i\Delta t\hat{H}}$ with the corresponding normal ordered expression and replace $\hat{a}, \hat{a}^\dagger$ with a, a^*. The final result is:

$$\begin{aligned}&\langle\vec{a}_{+,0}|\vec{a}_{-,0}\rangle e^{-(\vec{a}^{*}_{-,0}.\vec{a}_{-,0})-(\vec{a}^{*}_{+,0}.\vec{a}_{+,0})} =\\ &D[\vec{a}^*,\vec{a}]\exp\Big[\sum_{m=1}^{N}-\vec{a}^{*}_{-,m}.\vec{a}_{-,m}+\sum_{m=1}^{N}\vec{a}^{*}_{-,m}.\vec{a}_{-,m-1}-i\Delta t\sum_{m=1\ldots N}^{n\in\{1,2\}}\Delta_n a^{*n}_{-,m}a^{n}_{-,m-1}\\ &\qquad+i\Delta t\sum_{m=1\ldots N}\big(\eta a^{*1}_{-,m}a^{2}_{-,m-1}+\eta^* a^{*2}_{-,m}a^{1}_{-,m-1}\big)\Big] &&\spadesuit\ 1\\ &\times\exp\Big[\sum_{m'=1}^{N'-1}-\vec{a}^{*}_{+,m'}.\vec{a}_{+,m'}+\sum_{m'=1}^{N'-1}\vec{a}^{*}_{+,m'-1}.\vec{a}_{+,m'}+i\Delta t\sum_{m'=1\ldots N'-1}^{n\in\{1,2\}}\Delta_n a^{*n}_{-,m'-1}a^{n}_{-,m'}\\ &\qquad-i\Delta t\sum_{m'=1\ldots N'-1}\big(\eta a^{*1}_{-,m'-1}a^{2}_{-,m'}+\eta^* a^{*2}_{-,m'-1}a^{1}_{-,m'}\big)\Big] &&\spadesuit\ 2\\ &\times\exp\big[-\vec{a}^{*}_{-,0}.\vec{a}_{-,0}-\vec{a}^{*}_{+,0}.\vec{a}_{+,0}\big] &&\spadesuit\ 3\\ &\times\exp\big[\vec{a}^{*}_{+,N'-1}.\vec{a}_{-,N}+i\Delta t\big(\Delta_1 a^{*1}_{+,N'-1}a^{1}_{-,N}+\Delta_2 a^{*2}_{+,N'-1}a^{2}_{-,N}-\eta a^{*1}_{+,N'-1}a^{2}_{-,N}-\eta^* a^{*2}_{+,N'-1}a^{1}_{-,N}\big)\big] &&\spadesuit\ 4\end{aligned} \tag{205}$$

We have used the shorthand notation for the integration measure:

$$D[\vec{a}^*,\vec{a}]=\prod_j\Big(\prod_{m=1}^{2}\tfrac{da^{*m}_{-,j}da^{m}_{-,j}}{\pi}\Big)\prod_{j'}\Big(\prod_{m'=1}^{2}\tfrac{da^{*m'}_{+,j'}da^{m'}_{+,j'}}{\pi}\Big). \tag{206}$$

The terms ($\spadesuit$ 1) come from the division of the upper part of the contour $(-\infty,\infty)$ into N parts, the terms ($\spadesuit$ 2) come from the division of the lower part of the contour $(\infty,-\infty)$ into $N'-1$ parts (Δt-terms have plus-sign), ($\spadesuit$ 3) is the exponential from the very first line of the last equation and ($\spadesuit$ 4) comes from $\langle\vec{a}_{+,N'-1}|e^{i\Delta tH}|\vec{a}_{-,N}\rangle$.
Look at the terms from ($\spadesuit$ 1) line. For $\Delta t\to 0$ they can be represented in the form:

$$\begin{aligned}&-\Delta t\sum_{m=1\ldots N}^{j=1,2}\Big[a^{*j}_{-,m}\tfrac{[a^{j}_{-,m}-a^{j}_{-,m-1}]}{\Delta t}+i\Delta_j a^{*j}_{-,m}a^{j}_{-,m-1}\Big]+i\Delta t\sum_{m=1\ldots N}\big[\eta a^{*2}_{-,m}a^{1}_{-,m-1}+\eta^* a^{*1}_{-,m}a^{2}_{-,m-1}\big]=\\ &\quad-\int_{-\infty}^{\infty}d\tau\,\big[a^{*1}_{-(\tau)}\big(\partial_\tau+i\Delta_1\big)a^{1}_{-(\tau)}+a^{*2}_{-(\tau)}\big(\partial_\tau+i\Delta_2\big)a^{2}_{-(\tau)}-i\eta a^{*1}_{-(\tau)}a^{2}_{-(\tau)}-i\eta^* a^{*2}_{-(\tau)}a^{1}_{-(\tau)}\big]\end{aligned} \tag{207}$$

In the same limit the terms from (♠ 2), (♠ 3), (♠ 4) are equal to:

$$\int_{-\infty}^{\infty} d\tau \left[a^{*1}_{+\,(\tau)}\big(\partial_\tau + i\Delta_1\big)a^1_{+(\tau)} + a^{*2}_{+\,(\tau)}\big(\partial_\tau + i\Delta_2\big)a^2_{+(\tau)} - i\eta a^{*1}_{+\,(\tau)}a^2_{+(\tau)} - i\eta^* a^{*2}_{+\,(\tau)}a^1_{+(\tau)}\right] + a^*_{+(\infty)}a_{-(\infty)} - a^*_{+(\infty)}a_{+(\infty)} - a^*_{-(-\infty)}a_{-(-\infty)} \tag{208}$$

One has to use now the definition of a Fourier transformation of a field to obtain:

$$\begin{aligned} \int_{-\infty}^{\infty} d\tau a^{*j}_{l\,(\tau)}\big(\partial_\tau + i\Delta_j\big)a^j_{l\,(\tau)} &= -i\int_{-\infty}^{\infty}\tfrac{dw}{2\pi}a^{*j}_{l\,(w)}\big(w-\Delta_j\big)a^j_{l\,(w)} \\ \int_{-\infty}^{\infty} d\tau a^{*j}_{l\,(\tau)}a^{\bar{j}}_{l\,(\tau)} &= \int_{-\infty}^{\infty}\tfrac{dw}{2\pi}a^{*j}_{l\,(w)}a^{\bar{j}}_{l\,(w)} \end{aligned} \tag{209}$$

$l \in \{+,-\}$, $j \in \{1,2\}$; in the second line $\bar{j}$ is the complement of j. Going from the discrete to the continuous notation one can drop for a moment the boundary terms of the second line in eq. (208) in the definition of the partition function $\mathcal{Z}$. One also drops the term $\langle \vec{a}_{-,0}|\hat{\rho}_0|\vec{a}_{+,0}\rangle$. So one can formally write the partition function in the continuous notation as:

$$\mathcal{Z} = \int D_{[\vec{\alpha}^*_{(w)},\vec{\alpha}_{(w)}]} e^{i\mathcal{S}_{[\vec{\alpha},\vec{\alpha}^*]}} \tag{210}$$

The action $\mathcal{S}$ is defined as:

$$\begin{aligned} \mathcal{S}_{[\vec{\alpha}^*,\vec{\alpha}]} &= \int \tfrac{dw}{2\pi}\vec{\alpha}^\dagger{}_{(w)}\mathcal{G}^{-1}_{(w)}\vec{\alpha}_{(w)} \\ \vec{\alpha}^T_{(w)} &= \begin{pmatrix} a^1_{-\,(w)} & a^1_{+(w)} & a^2_{-\,(w)} & a^2_{+(w)}\end{pmatrix} \end{aligned} \tag{211}$$

The Green's function is given by the 4x4 matrix (σ_z - Pauli z-matrix):

$$\mathcal{G}^{-1}{}_{(w)} = \begin{bmatrix} g^{-1}_{11\,(w)} & \eta\sigma_z \\ \eta^*\sigma_z & g^{-1}_{22\,(w)} \end{bmatrix} \tag{212}$$

and the GF for an isolated singe quantum dot is $g^{-1}_{jj\,(w)} = (w-\Delta_j)\sigma_z$ ($jj \in \{11,22\}$). One should note that the $+,-$ fields are correlated because of $\langle \vec{a}_{-0}|\hat{\rho}_0|\vec{a}_{+0}\rangle$ and the terms in the second line of eq. (208). One can show [26] that going from the discrete to the continuous notation the Green's functions takes automatically these correlations into account.

8 Quantum dot coupled to two bosonic reservoirs. Self-energy approximation

In the following example the self-energy of a chain of sunset diagrams will be derived. The same idea can be applied also to a chain of tadpole diagrams and generalised to the case where both diagrams are included simultaneously.
The Hamiltonian of the system is given by[27]:

$$\begin{aligned} \hat{H} &= \Delta\hat{a}^\dagger\hat{a} + \textstyle\sum_k \varepsilon_k \hat{L}^\dagger_k\hat{L}_k + \sum_{k'}\varepsilon_{k'}\hat{R}^\dagger_{k'}\hat{R}_{k'} \\ &\quad + \textstyle\sum_k\left(\gamma_{kL}\hat{L}^\dagger_k\hat{a} + \gamma^*_{kL}\hat{a}^\dagger\hat{L}_k\right) + \sum_{k'}\left(\tilde{\gamma}_{k'R}\hat{a}^\dagger\hat{R}_{k'} + \tilde{\gamma}^*_{k'R}\hat{R}^\dagger_{k'}\hat{a}\right) + \tfrac{U}{2}\hat{a}^\dagger\hat{a}^\dagger\hat{a}\hat{a} \end{aligned} \tag{213}$$

We will use the following notation:

[27] In this section we have changed the sign of the tunneling terms . So we do not have to count the additional minus signs arising from these terms in the following approximations.

$$
\begin{aligned}
\langle \dots \rangle &\equiv \tfrac{1}{\mathcal{N}} \mathrm{tr}\big[\hat{\rho}_0 \dots e^{-\imath \int d_\tau \hat{H}^{\imath}_{H_0(\tau)}}\big] \\
\langle \dots \rangle_{\tilde{0}} &\equiv \tfrac{1}{\mathcal{N}} \mathrm{tr}\big[\hat{\rho}_0 \dots e^{-\imath \int d_\tau \hat{H}^{\imath}_{H_0(\tau)|_{U=0}}}\big] \\
\langle \dots \rangle_{0} &\equiv \tfrac{1}{\mathcal{N}} \mathrm{tr}\big[\hat{\rho}_0 \dots e^{-\imath \int d_\tau \hat{H}^{\imath}_{H_0(\tau)|_{U,\gamma,\tilde{\gamma}=0}}}\big]
\end{aligned}
$$

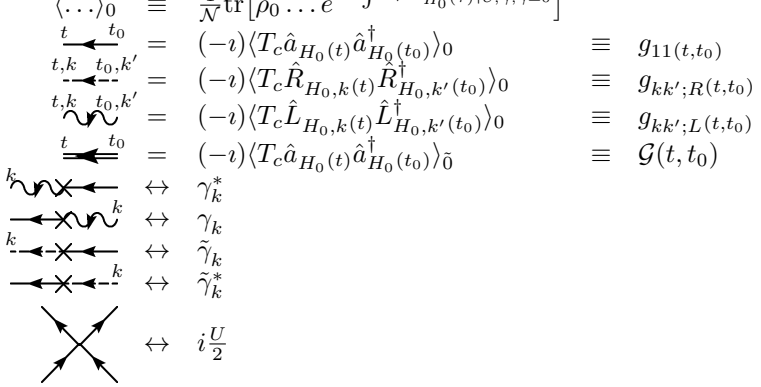

$$
\begin{aligned}
&= (-\imath)\langle T_c \hat{a}_{H_0(t)} \hat{a}^\dagger_{H_0(t_0)} \rangle_0 && \equiv g_{11(t,t_0)} \\
&= (-\imath)\langle T_c \hat{R}_{H_0,k(t)} \hat{R}^\dagger_{H_0,k'(t_0)} \rangle_0 && \equiv g_{kk';R(t,t_0)} \\
&= (-\imath)\langle T_c \hat{L}_{H_0,k(t)} \hat{L}^\dagger_{H_0,k'(t_0)} \rangle_0 && \equiv g_{kk';L(t,t_0)} \\
&= (-\imath)\langle T_c \hat{a}_{H_0(t)} \hat{a}^\dagger_{H_0(t_0)} \rangle_{\tilde{0}} && \equiv \mathcal{G}(t,t_0) \\
&\leftrightarrow \gamma^*_k \\
&\leftrightarrow \gamma_k \\
&\leftrightarrow \tilde{\gamma}_k \\
&\leftrightarrow \tilde{\gamma}^*_k \\
&\leftrightarrow i\tfrac{U}{2}
\end{aligned}
$$

8.1 Symmetry factor of diagram contributing to the full propagator in the U=0 case

We use a shorter notation for the operators in the Interaction picture $\hat{a}_1 \equiv \hat{a}_{H_0(\tau_1)}$ and the contour integration $\int_c d_{\tau_{1\dots n}} \equiv \int_c d_{\tau_1} \int_c d_{\tau_2} \dots d_{\tau_n}$. For simplicity we assume that the reservoir consists of only one mode ($\gamma_k = \gamma$, $\tilde{\gamma}_k = \tilde{\gamma}$, $\hat{R}_k = \hat{R}$, etc...) but the results can be generalised for many modes. Now we expand $\mathcal{G}_{(t,t_0)}$ (t ⟸ t_0) in powers of the exponential weighting factor:

$$
\begin{aligned}
(-\imath)\langle T_c \hat{a}_t \hat{a}^\dagger_{t_0} \rangle &= (-\imath)\langle T_c \hat{a}_t \hat{a}^\dagger_{t_0} e^{-\imath \int d\tau \left(\gamma \hat{L}^\dagger \hat{a} + \gamma^* \hat{a}^\dagger \hat{L} + \tilde{\gamma} \hat{a}^\dagger \hat{R} + \tilde{\gamma}^* \hat{R}^\dagger \hat{a}\right)} \rangle_0 \\
&= (-\imath)\langle T_c \hat{a}_t \hat{a}^\dagger_{t_0} \rangle_0 + (-\imath)^3 \tfrac{|\gamma|^2}{2!} \int_{1,2} \langle T_c \hat{a}_t \hat{a}^\dagger_{t_0} \hat{L}^\dagger_1 \hat{a}_1 \hat{a}^\dagger_2 \hat{L}_2 \rangle_0 + \dots \\
&= \quad t \longleftarrow t_0 \quad + \quad t \longleftarrow\!\sim\!\sim\!\longleftarrow t_0 \quad + \quad \dots
\end{aligned}
\tag{214}
$$

One can show that the symmetry factor for every diagram is the same. Take one diagram that consist of n_1 ⟵×∼∼, n_2 ∼∼×⟵, n_3 ⟵×⟵--, n_4 --⟵×⟵ parts. The relative order of the different parts is also known. To obtain the symmetry factor we look onto the expansion of t ⟸ t_0 and extract from it the diagram we need:

$$
\begin{aligned}
\mathcal{G}(t,t_0) \quad \ni \quad & \tfrac{(-\imath)^{\mathrm{n}_1+\mathrm{n}_2+\mathrm{n}_3+\mathrm{n}_4+1}}{(\mathrm{n}_1+\mathrm{n}_2+\mathrm{n}_3+\mathrm{n}_4)!} \langle T_c \hat{a}_t \hat{a}^\dagger_{t_0} \left(\int d_\tau \gamma \hat{L}^\dagger_\tau \hat{a}_\tau + \gamma^* \hat{a}^\dagger_\tau \hat{L}_\tau + \tilde{\gamma} \hat{a}^\dagger_\tau \hat{R}_\tau + \tilde{\gamma}^* \hat{R}^\dagger_\tau \hat{a}_\tau \right)^{\mathrm{n}_1+\mathrm{n}_2+\mathrm{n}_3+\mathrm{n}_4} \rangle_0 \\
\ni \quad & \tfrac{(-\imath)^{\mathrm{n}_1+\mathrm{n}_2+\mathrm{n}_3+\mathrm{n}_4+1}}{(\mathrm{n}_1+\mathrm{n}_2+\mathrm{n}_3+\mathrm{n}_4)!} \gamma^{\mathrm{n}_1} \gamma^{*\mathrm{n}_2} \tilde{\gamma}^{*\mathrm{n}_3} \tilde{\gamma}^{\mathrm{n}_4} \tfrac{(\mathrm{n}_1+\mathrm{n}_2+\mathrm{n}_3+\mathrm{n}_4)!}{(\mathrm{n}_1!)(\mathrm{n}_2!)(\mathrm{n}_3!)(\mathrm{n}_4!)} \int d\tau_{1\dots,\mathrm{n}_1+\mathrm{n}_2+\mathrm{n}_3+\mathrm{n}_4} \langle T_c \hat{a}_t \hat{a}^\dagger_{t_0} \times \\
& \times \prod_{j=1}^{\mathrm{n}_1} \left(\hat{L}^\dagger_{t_j} \hat{a}_{t_j} \right) \prod_{j=\mathrm{n}_1+1}^{\mathrm{n}_1+\mathrm{n}_2} \left(\hat{a}^\dagger_{t_j} \hat{L}_{t_j} \right) \prod_{j=\mathrm{n}_1+\mathrm{n}_2+1}^{\mathrm{n}_1+\mathrm{n}_2+\mathrm{n}_3} \left(\hat{R}^\dagger_{t_j} \hat{a}_{t_j} \right) \prod_{j=\mathrm{n}_1+\mathrm{n}_2+\mathrm{n}_3+1}^{\mathrm{n}_1+\mathrm{n}_2+\mathrm{n}_3+\mathrm{n}_4} \left(\hat{a}^\dagger_{t_j} \hat{R}_{t_j} \right) \rangle_0 \\
= \quad & \gamma^{\mathrm{n}_1} \gamma^{*\mathrm{n}_2} \tilde{\gamma}^{*\mathrm{n}_3} \tilde{\gamma}^{\mathrm{n}_4} \tfrac{1}{\mathrm{n}_1! \mathrm{n}_2! \mathrm{n}_3! \mathrm{n}_4!} \int_{1,\dots} \underbrace{(-\imath)^{\sum_i \mathrm{n}_i + 1} \langle \dots \rangle_0}_{\star}
\end{aligned}
\tag{215}
$$

In the second line we used that $(a_1 + \dots + a_m)^{n_1+\dots n_m} \ni \frac{(n_1+\dots+n_m)!}{n_1!\dots n_m!} a_1^{n_1} \dots a_m^{n_m}$. The graph we are interested in is contained in the $\star$ expression. One applies the Wick's theorem (i.e sum overall possible factorisations into pairs). A part of this sum gives the expression for our graph which consists of a product of GF's and a symmetry factor S'. One can easily realize that $S' = n_1! n_2! n_3! n_4!$. One can imagine that the graph has n_1 ⟵×∼∼, n_2 ∼∼×⟵, n_3 ⟵×⟵--, n_4 --⟵×⟵ empty places and exactly the same number of blocks for disposal. For every i then the number of possibilities to distribute the n_i blocks at the n_i free places is $n_i!$ and one gets the above result. S' cancels the denominator from the last equation and one gets that the graph we are interested in can be expressed as a product of the propagators given in the beginning of the subsection and $\gamma^{n_1} \gamma^{*n_2} \tilde{\gamma}^{*n_3} \tilde{\gamma}^{n_4}$. There is no additional symmetry factor.

Allowing to have more modes in the reservoir does not change the result. One just has to add an additional index j to $n_{1j}, n_{2j}, n_{3j}, n_{4j}$ where the second index refers to the mode of the reservoir, e.g. $n_{1,j}$ is the number of 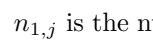 and the proove can be done in the same way as for one-mode reservoirs.

8.2 Expansion of the full propagator ($U \neq 0$) in diagrams

Expand the full propagator in diagrams in the same way as given in eq. (214). First select the diagrams proportional to U^0. They sum up to 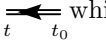 which is already known.

Derivation of the symmetry factor of a Sunset diagram.
Select one Sunset diagram $\sim U^2$ (see fig. (8.2))[28]. On every one of the five legs there is a finite number of $n_{l,1}$  , $n_{l,2}$ 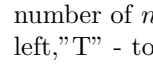 , $n_{l,3}$ 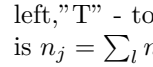 , $n_{l,4}$ blocks ($l = L, T, M, B, R$), ("L" - left,"T" - top, "M"-middle, "B"-bottom, "R" - right). The total number of the of blocks of every type is $n_j = \sum_l n_{l,j}$ $(j = 1, \ldots, 4)$. There are also two vertices with four legs. In order to find the symmetry factor of the diagram we look at the expansion of the full propagator $G(t, t_0)$ and extract from it the diagram we need:

$$
\begin{aligned}
G(t,t_0) \quad &\ni \quad \tfrac{(-\imath)^{n_1+n_2+n_3+n_4+3}}{(n_1+n_2+n_3+n_4+2)!}\langle T_c \hat{a}_t \hat{a}^\dagger_{t_0} \Big(\int d\tau \gamma \hat{L}^\dagger_\tau \hat{a}_\tau + \gamma^* \hat{a}^\dagger_\tau \hat{L}_\tau + \tilde{\gamma} \hat{a}^\dagger_\tau \hat{R}_\tau + \tilde{\gamma}^* \hat{R}^\dagger_\tau \hat{a}_\tau + U \hat{a}^\dagger_\tau \hat{a}^\dagger_\tau \hat{a}_\tau \hat{a}_\tau \Big)^{n_1+n_2+n_3+n_4+2} \rangle_0 \\
&\ni \quad \tfrac{1}{(n_1+n_2+n_3+n_4+2)!} \gamma^{n_1} \gamma^{*n_2} \tilde{\gamma}^{*n_3} \tilde{\gamma}^{n_4} (i\tfrac{U}{2})^2 \tfrac{(n_1+n_2+n_3+n_4+2)!}{2!(n_1!)(n_2!)(n_3!)(n_4!)} \int d_{\tau_{1,2\cdots}} \underbrace{(-\imath)^{n_1+n_2+n_3+n_4+5} \langle \ldots \rangle_0}_{\star\star}
\end{aligned}
\tag{216}
$$

The U-term carries four operators unlike the other terms in the Hamiltonian that have only two. In

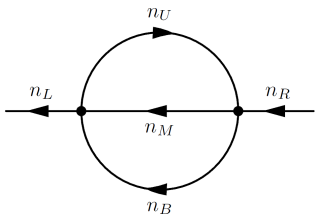

Figure 25: Sunset diagram. Every line of the diagram can contain an arbitrary number of $n_{l,1}, n_{l,2}, n_{l,3}, n_{l,4}$ blocks.

the $\langle\rangle_0$ brackets there are $n_1 + n_2 + n_3 + n_4 + 5$ pairs of operators and we extract an $(-i)$ factor from U in order to have an equal number of $(-i)$ and operator pairs in $(\star\star)$. This is the reason why the interaction vertex is equal to iU and not just to U. In the second line of the last equation we took the symmetry factor from $(a + b + c + d + e)^{n_1+n_2+n_3+n_4+2} \ni \frac{(n_1+n_2+n_3+n_4+2)!}{2!(n_1!)(n_2!)(n_3!)(n_4!)} a^{n_1} b^{n_2} c^{n_3} d^{n_4} e^2$. The $(\star\star)$ term can be expressed as before as a sum over all possible factorisations into propagators. A part of this sum gives the expression for our graph which consist of a product of GF's and a symmetry factor S'. S' is equal to 8 if both the middle and lower internal lines propagating in the left direction (labeled with M,B) are bare propagators and it is equal to 16 in all other cases. This factor does not depend on the configuration of the two external legs and one can "tear" them off from the diagram if this is needed. If one adds all Sunset diagrams from the expansion of $G(t, t_0)$ one gets:

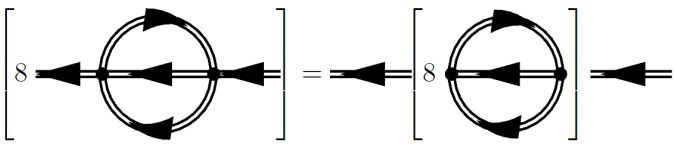

Boring and lengthy derivation

1. Connect $\hat{a}_{(t)}$ with some 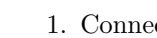 or 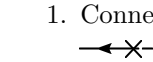 or equivalently choose some of the or blocks that are not connected. Do this until the left external leg (labelled with L) is

[28] here every line of the graph could be any contribution form the propagator $\mathcal{G}(t, t_0)$

complete. The number of possibilities to do this step is:

$$\begin{array}{l} n_1 \cdot (n_1-1)\cdots(n_1-n_{L,1}+1)\times \\ n_2 \cdot (n_2-1)\cdots(n_2-n_{L,2}+1)\times \\ n_3 \cdot (n_3-1)\cdots(n_3-n_{L,3}+1)\times \\ n_4 \cdot (n_4-1)\cdots(n_4-n_{L,4}+1) \end{array} \tag{217}$$

2. Pick one of the two vertices. The number of possibilities to do this step is 2.

3. Pick one of the two outgoing legs and connect it with the L-leg $\Rightarrow$ two possibilities to do this step.

4. From the already picked vertex take the other outgoing leg and build the propagator labelled with index U (the only one that moves in the right direction)The number of possibilities to do this step is:

$$\begin{array}{l} (n_1-n_{L,1})\cdots(n_1-n_{L,1}-n_{U,1}+1)\times \\ (n_2-n_{L,2})\cdots(n_2-n_{L,2}-n_{U,2}+1)\times \\ (n_3-n_{L,3})\cdots(n_3-n_{L,3}-n_{U,3}+1)\times \\ (n_4-n_{L,4})\cdots(n_4-n_{L,4}-n_{U,4}+1) \end{array} \tag{218}$$

5. Pick one of the remaining unselected vertices. The number of possibilities to do this step is 1.

6. Pick one of the two incoming legs from this vertex and connect it with the propagator labelled with index U. The number of possibilities to do this step is 2.

7. From the already picked vertex take the other incoming leg and build the propagator labelled with index R in the same way as done in step 1. The M,B-legs can be constructed in the same way but in the end one side of both legs is not connected. The number of possibilities to do this step is:

$$(n_1-n_{L,1}-n_{U,1})!(n_2-n_{L,2}-n_{U,2})!(n_3-n_{L,3}-n_{U,3})!(n_4-n_{L,4}-n_{U,4})! \tag{219}$$

8. In the end one has to connect the M,B-legs to the rest of the graph. The symmetry factor for this step is 2.

The number of possibilities to do the contraction of $\langle\ldots\rangle_0$ is $8\cdot 2!n_1!n_2!n_3!n_4!$. The 2! comes from steps 2 and 5. After multiplying with the factor of the last line of eq (216) one gets the symmetry factor 8. One can extend this result for reservoirs with more modes. In this case one has to add an additional index to $n_{l,j}$, e.g. $n_{L,1,j}$ will denote the number of 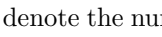

graphs in the left leg of the Sunset diagram. The proof is the same with the difference that the number of columns in eq. (217),(218) will not be four but $2\times$ (number of modes in the left reservoir + number of modes in the right reservoir).

Calculation of the symmetry factor of a diagram of the form of a chain of $\mathcal{N}$ Sunset diagrams.
Now take one diagram of the expansion which has the form of a chain of $\mathcal{N}$ Sunset diagrams (see fig. (**??**)). The sum of the 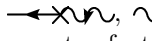 , 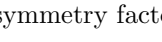 , 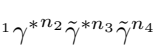 , elements is n_1, n_2, n_3 and n_4 respectively. Calculate the symmetry factor as before:

$$G(t,t_0) \quad \ni \quad (iU)^{2\mathcal{N}}\gamma^{n_1}\gamma^{*n_2}\tilde{\gamma}^{*n_3}\tilde{\gamma}^{n_4}\tfrac{1}{(2\mathcal{N})!n_1!n_2!n_3!n_4!}\int_{1,2\ldots}\underbrace{(-i)^{4\mathcal{N}+n_1+n_2+n_3+n_4+1}\langle\ldots\rangle_0}_{\star\star\star} \tag{220}$$

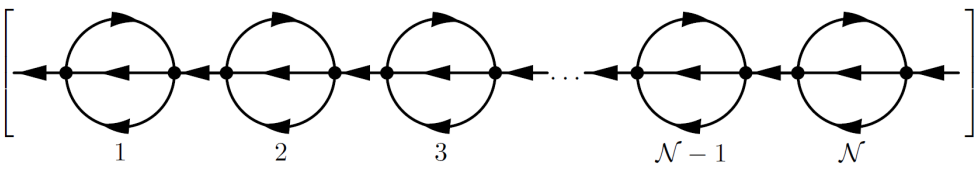

Figure 26: Chain of Sunset diagrams. Every line of the diagram can be an arbitrary contribution from the $\mathcal{G}_{(\tau,\tau')}$ propagator and should not be interpreted as $g_{(\tau,\tau')}$.

The only difference from the procedure described in the last two subsections is that the steps 2,5 where one has to choose a vertex from the still unselected vertices one gets for the first Sunset diagram not a symmetry factor of $2 \cdot 1$ but $2\mathcal{N}(2\mathcal{N}-1)$. For the second Sunset diagram the symmetry factor is $(2\mathcal{N}-2)(2\mathcal{N}-3)$ etc ... This symmetry factor cancels the $1/(2\mathcal{N}!)$ from eq. (220). The total symmetry factor is then $\Pi_{j=1}^{\mathcal{N}}(8)$.
If one adds all diagrams wich have the form of a chain of $\mathcal{N}$ Sunset rings then one gets:

$$\int d_{\tau_{1,2,\ldots}\in T_c} \mathcal{G}_{(t,\tau_1)} M_{(\tau_1,\tau_2)} \mathcal{G}_{(\tau_2,\tau_3)} \ldots M_{(\tau_{2\mathcal{N}-1},\tau_{2\mathcal{N}})} \mathcal{G}_{(\tau_{2\mathcal{N}},t_0)} \tag{221}$$

$M_{(t_2,t_2)}$ is defined as:

$$M_{(t_1,t_2)} = (i\tfrac{U}{2})^2 8 \mathcal{G}_{(t_1,t_2)} \mathcal{G}_{(t_1,t_2)} \mathcal{G}_{(t_2,t_1)} \tag{222}$$

Now suppose we do the same summation for every $\mathcal{N} \in \mathbb{N}_0$. For $\mathcal{N}=0$ we get trivially $\overset{t}{=\!=\!\!\blacktriangleleft}\overset{t_0}{}$. The results for every $\mathcal{N} \in \mathbb{N}_0$ are added together. This sum should be an approximation of the full propagator of the system. If this sum converges one gets the following result:

$$\begin{aligned} G_{(t,t_0)} &\approx \mathcal{G}_{(t,t_0)} + \textstyle\int_c d_{\tau_{1,2}} \mathcal{G}_{(t,\tau_1)} M_{(\tau_1,\tau_2)} \mathcal{G}_{(\tau_2,t_0)} + \\ &\quad + \textstyle\int_c d_{\tau_{1,2,3,4}} \mathcal{G}_{(t,\tau_1)} M_{(\tau_1,\tau_2)} \mathcal{G}_{(\tau_2,\tau_3)} M_{(\tau_3,\tau_4)} \mathcal{G}_{(\tau_4,t_0)} + \ldots \\ &= \mathcal{G}_{(t,t_0)} + \textstyle\int_c d_{\tau_{1,2}} \mathcal{G}_{(t,\tau_1)} M_{(\tau_1,\tau_2)} G_{(\tau_2,t_0)} \end{aligned} \tag{223}$$

which can be solved explicitly. The equation can be presented in the form (see App. FT):

$$\begin{aligned} \textstyle\int \frac{d_w}{2\pi} e^{-\imath w(t-t_0)} G_{(w)} &= \textstyle\int \frac{d_w}{2\pi} e^{-\imath w(t-t_0)} \mathcal{G}_{(w)} + \\ &\quad \textstyle\int \frac{d_w}{2\pi} e^{-\imath w(t-t_0)} \mathcal{G}_{(w)} \sigma_z \underbrace{\left[\int \frac{d_{w'} d_{w''}}{(2\pi)^2} M_{(w',w'',w'+w''-w)} \right]}_{\Sigma'_{(w)}} \sigma_z G_{(w)} \end{aligned} \tag{224}$$

with:

$$\begin{aligned} M^{--}_{(w',w'',w''')} &= (i\tfrac{U}{2})^2 8 \mathcal{G}^{--}_{(w')} \mathcal{G}^{--}_{(w'')} \mathcal{G}^{--}_{(w''')} \\ M^{-+}_{(w',w'',w''')} &= (i\tfrac{U}{2})^2 8 \mathcal{G}^{-+}_{(w')} \mathcal{G}^{-+}_{(w'')} \mathcal{G}^{+-}_{(w''')} \\ M^{+-}_{(w',w'',w''')} &= (i\tfrac{U}{2})^2 8 \mathcal{G}^{+-}_{(w')} \mathcal{G}^{+-}_{(w'')} \mathcal{G}^{-+}_{(w''')} \\ M^{++}_{(w',w'',w''')} &= (i\tfrac{U}{2})^2 8 \mathcal{G}^{++}_{(w')} \mathcal{G}^{++}_{(w'')} \mathcal{G}^{++}_{(w''')} \end{aligned} \tag{225}$$

The answer should be of the form:

$$G_{(w)} = \big[\mathcal{G}^{-1}_{(w)} - \underbrace{\sigma_z \Sigma'_{(w)} \sigma_z}_{\Sigma_{(w)}} \big]^{-1} \tag{226}$$

$\Sigma_{(w)}$ is the interaction contribution to the self-energy of the system.

9 Chain of two quantum dots coupled to two bosonic reservoirs. Self-energy approximation

The Hamiltonian of the system is given by [29]:

$$\begin{aligned} \hat{H} &= \textstyle\sum_k \varepsilon_k \hat{L}^\dagger_k \hat{L}_k + \sum_{k'} \varepsilon_{k'} \hat{R}^\dagger_{k'} \hat{R}_{k'} + \Delta_a \hat{a}^\dagger \hat{a} + \Delta_b \hat{b}^\dagger \hat{b} \\ &\quad + \textstyle\sum_k \left(\gamma_k \hat{L}^\dagger_k \hat{a} + \gamma^* \hat{a}^\dagger \hat{L}_k \right) + \left(\gamma' \hat{a}^\dagger \hat{b} + \gamma'^* \hat{b}^\dagger \hat{a} \right) + \sum_{k'} \left(\tilde{\gamma}_{k'} \hat{b}^\dagger \hat{R}_{k'} + \tilde{\gamma}^*_{k'} \hat{R}^\dagger_{k'} \hat{b} \right) \\ &\quad + \tfrac{U_a}{2} \hat{a}^\dagger \hat{a}^\dagger \hat{a} \hat{a} + \tfrac{U_b}{2} \hat{b}^\dagger \hat{b}^\dagger \hat{b} \hat{b} \end{aligned} \tag{227}$$

We use the following notation ($l_1, l_0 \in \{a, b\}$):

[29] In this section we have changed the sign of the tunneling terms . So we do not have to count the additional minus signs arising from these terms in the following approximations.

$$
\begin{aligned}
\langle \dots \rangle &\equiv \tfrac{1}{\mathcal{N}} \mathrm{tr}\big[\hat{\rho}_0 \dots e^{-\imath \int d_\tau \hat{H}^i_{H_0(\tau)}}\big] \\
\langle \dots \rangle_{\tilde{0}} &\equiv \tfrac{1}{\mathcal{N}} \mathrm{tr}\big[\hat{\rho}_0 \dots e^{-\imath \int_c d_\tau \hat{H}^i_{H_0(\tau)|_{U=0}}}\big] \\
\langle \dots \rangle_0 &\equiv \tfrac{1}{\mathcal{N}} \mathrm{tr}\big[\hat{\rho}_0 \dots e^{-\imath \int_c d_\tau \hat{H}^i_{H_0(\tau)|_{U,\gamma,\tilde{\gamma}=0}}}\big] \\
\overset{l,t \quad l_0,t_0}{\longleftarrow} &= (-\imath)\langle T_c \hat{l}_{H_0,(t)} \hat{l}^\dagger_{0,H_0(t_0)} \rangle_0 \equiv \delta_{ll_0} g_{ll_0(t,t_0)} \\
\overset{tk \quad t_0k'}{\dashleftarrow} &= (-\imath)\langle T_c \hat{R}_{H_0,k(t)} \hat{R}^\dagger_{H_0,k'(t_0)} \rangle_0 \equiv \delta_{kk'} g_{kk';R(t,t_0)} \\
\overset{tk \quad t_0k'}{\sim\!\!\leftarrow} &= (-\imath)\langle T_c \hat{L}_{H_0,k(t)} \hat{L}^\dagger_{H_0,k'(t_0)} \rangle_0 \equiv \delta_{kk'} g_{kk';L(t,t_0)} \\
\overset{l,t \quad l_0,t_0}{\Longleftarrow} &= (-\imath)\langle T_c \hat{l}_{H_0,(t)} \hat{l}^\dagger_{0,H_0(t_0)} \rangle_{\tilde{0}} \equiv \mathcal{G}_{ll_0(t,t_0)}
\end{aligned}
$$

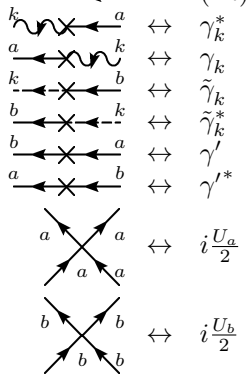

$$
\begin{aligned}
&\leftrightarrow \gamma^*_k \\
&\leftrightarrow \gamma_k \\
&\leftrightarrow \tilde{\gamma}_k \\
&\leftrightarrow \tilde{\gamma}^*_k \\
&\leftrightarrow \gamma' \\
&\leftrightarrow \gamma'^* \\
&\leftrightarrow i\tfrac{U_a}{2} \\
&\leftrightarrow i\tfrac{U_b}{2}
\end{aligned}
\tag{228}
$$

9.1 Symmetry factor of a diagram contributing to the full propagator for $U = 0$

We use a shorter notation for the operators in the Interaction picture $\hat{a}_1 \equiv \hat{a}_{H_0(\tau_1)}$ and the contour integration $\int_c d_{\tau_{1\dots n}} \equiv \int_c d_{\tau_1} \int_c d_{\tau_2} \dots \int_c d_{\tau_n}$. For simplicity we assume that the reservoir consists of only one mode ($\gamma_k = \gamma$, $\tilde{\gamma}_k = \tilde{\gamma}$, $\hat{R}_k = \hat{R}$, etc...) but the results can be generalised for many modes.
One can easily see that the symmetry factor of every graph contributing to $\mathcal{G}_{l,l_0(t,t_0)}$ has a symmetry factor equal to 1. In the **previous** section we have introduced the numbers n_i ($i = 1 \dots 4$) in order to count the number of different building blocks of the diagram. Now we have just to introduce n_i ($i = 1 \dots 6$) in order to count them. Everything else in the derivation of the symmetry factor is unchanged.

9.2 Expansion of the full propagator ($U_{a,b} \neq 0$) in diagrams

Expand the full propagator in diagrams in the same way given in eq. (214). First select the diagrams proportional to U^0 which begin with l_0 and end with l. They sum up to $\overset{l,t \quad l_0,t_0}{\Longleftarrow}$ which is already known. This is true for every combination of (l, l_0)

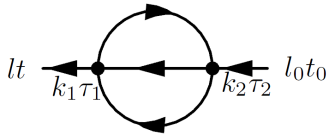

Figure 27: Sunset diagram, $l_1, l_2, k_1, k_2 \in \{a, b\}$, $t, t_0, \tau_1, \tau_2 \in \mathbb{R}$. Every line of the graph could be any contribution form the propagator $\mathcal{G}_{(t,t_0)}$.

Derivation of the symmetry factor of a Sunset diagram
Select for l, l_0 fixed one of the diagrams that looks like a Sunset-ring (see fig. (9.2)). On every one of the five lines there is a finite number of $n_{l,1}$ $\longleftarrow\!\!\times\!\!\sim$, $n_{l,2}$ $\sim\!\!\times\!\!\leftarrow$ etc. blocks ($l = L, U, M, B, R$). The total number of blocks of every type is $n_j = \sum_l n_{l,j}$ ($j = 1 \dots 6$). Let the left inner vertex of the

diagram be U_a and the right one be U_b From the expansion of $G_{a,b(t,t_0)}$ we get:

$$\begin{aligned} G_{l,l_2(t,t_0)} \quad \ni \quad & \tfrac{1}{1!1!n_1!\ldots n_6!}\gamma^{n_1}\gamma^{*n_2}\gamma'^{*n_3}\gamma^{n_4}\tilde{\gamma}^{n_5}\tilde{\gamma}^{*n_6}(i\tfrac{U_a}{2})(i\tfrac{U_b}{2})\int_c d_{\tau_{1\ldots n_1+\ldots+n_6+2}} \\ & \times(-\imath)^{5+n_1+\ldots+n_6}\langle \hat{T}_c\hat{l}_{(t)}\hat{l}^\dagger_{0(t_0)}\prod_{j=1}^{n_1}\left(\hat{L}_{(\tau_j)}\hat{a}^\dagger_{(\tau_j)}\right)\prod_{j=n_1+1}^{n_1+n_2}\left(\hat{a}_{(\tau_j)}\hat{L}^\dagger_{(\tau_j)}\right)\prod_{j=n_1+n_2+1}^{n_1+n_2+n_3}\left(\hat{a}_{(\tau_j)}\hat{b}^\dagger_{(\tau_j)}\right) \\ & \times\prod_{j=n_1+\ldots+n_3+1}^{n_1+\ldots+n_4}\left(\hat{b}_{(\tau_j)}\hat{a}^\dagger_{(\tau_j)}\right)\prod_{j=n_1+\ldots+n_4+1}^{n_1+\ldots+n_5}\left(\hat{R}_{(\tau_j)}\hat{b}^\dagger_{(\tau_j)}\right)\prod_{j=n_1+\ldots+n_5+1}^{n_1+\ldots+n_6}\left(\hat{b}_{(\tau_j)}\hat{R}^\dagger_{(\tau_j)}\right)\rangle_0 \end{aligned} \tag{229}$$

Except the addition of n_5, n_6 there are two other minor differences from the procedure of section 8.2. The first is in the step 2,5 where one has to choose a vertex. Since we have a U_a and U_b vertex one does not get a prefactor of 2! but 1!1! (for the case of two U_a or two U_b vertices we get again 2!). But this product cancels as before the denominator $\frac{1}{1!1!}$ and does not change the result. The second difference is that since $\hat{a}, \hat{b}$ are different operators the bare propagator $-\imath\langle T_c\hat{a}(t)\hat{b}^\dagger(t_0)\rangle_0$ is zero. The symmetry factor is again 8 and does not depend on l, l_0.
If one keeps l_1, l_0 and the two inner vertices fixed ($U_{k_1}, U_{k_2}; k_{1,2} \in \{a, b\}$) and sums over all Sunset-like diagrams which fulfill this constraint one gets:

$$(i\tfrac{U_{k_1}}{2})(i\tfrac{U_{k_2}}{2})8\int_c d_{\tau_{1,2}}\mathcal{G}_{l,k_1(t,\tau_1)}\mathcal{G}_{k_1,k_2(\tau_1,\tau_2)}\mathcal{G}_{k_1,k_2(\tau_1,\tau_2)}\mathcal{G}_{k_2,k_1(\tau_2,\tau_1)}\mathcal{G}_{k_2,l_0(\tau_2,t_0)} \tag{230}$$

We note again that one gets the same factor if one tears off the two external legs of the diagram. We substitute this result (without the external legs i.e. without $\mathcal{G}_{l,k_1(t,\tau_1)}\mathcal{G}_{k_2,l_0(\tau_2,t_0)}$ and without the time integration) with the 2×2 matrix $M_{k_1,k_2(\tau_1,\tau_2)}$ (see fig. (9.2)):

$$M_{k_1,k_2(\tau_1,\tau_2)} = 8\mathcal{G}_{k_1,k_2(\tau_1,\tau_2)}\mathcal{G}_{k_1,k_2(\tau_1,\tau_2)}\mathcal{G}_{k_2,k_1(\tau_2,\tau_1)} \tag{231}$$

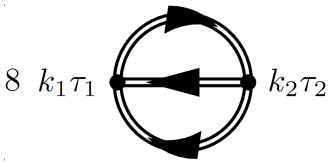

Figure 28: Feynman diagram of the matrix $M_{k_1,k_2(\tau_1,\tau_2)}$. $k_1, k_2 \in \{a, b\}$, $\tau_1, \tau_2 \in \mathbb{R}$.

Calculation of the symmetry factor of a diagram of the form of a chain of $\mathcal{N}$ Saturn rings

In addition to the constraint given in the title of the subsection we keep both ends l, l_0 fixed. We introduce a vector $\vec{k} = (k_1, \ldots, k_{2\mathcal{N}})$ $k_j \in \{a, b\}$ that takes into account the type and the order of the vertexes. This vector is also fixed. Let the number of U_a vertices be $\mathcal{M}$ and the number of U_b vertexes be $2\mathcal{N} - \mathcal{M}$. One repeats the steps from subsection 8.2 and takes into acount the following differences:

- the contribution from the vertexes in the expansion of the full propagator done more or less in the same way as in eq. (220) changes:

$$\frac{1}{(2\mathcal{N})!} \longrightarrow \frac{1}{(2\mathcal{N}-\mathcal{M})!(\mathcal{M})!}$$

- the contribution to the symmetry factor comnig from choosing one of the remained unselected $U_{a,b}$ vertices to take an empty place for a vertex in the diagram changes:

$$(2\mathcal{N})! \longrightarrow (2\mathcal{N}-\mathcal{M})!(\mathcal{M})!$$

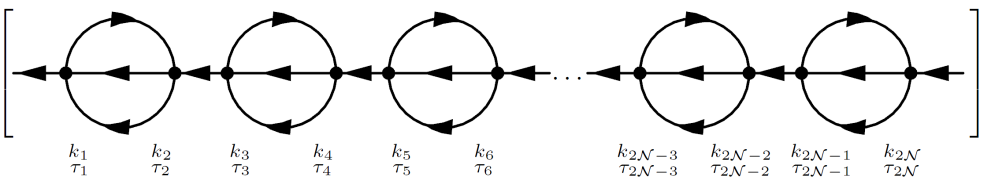

Figure 29: Feynman diagram of a chain of Sunset rings, $k_1, k_2 \ldots k_{\mathcal{N}} \in \{a, b\}$, $\tau_1, \tau_2 \ldots \tau_{\mathcal{N}} \in \mathbb{R}$. The number of the vertices given in the beginning of the subsection is arbitrary in every line of the diagram.

So the symmetry factor for the diagram factorizes in a product of the symmetry factors of the single Saturn rings i.e. it depends only on the vector $\vec{k}$ (position of the U_a, U_b vertices in the chain). It can be formally written as: $\Pi_{j=1}^{\mathcal{N}}(8)$.

If one adds all diagrams which have the form of a chain of $\mathcal{N}$ Saturn rings with l, l_0 and $\vec{k}$ fixed one gets that this sum is equal to:

$$\int_c d_{\tau_{1,2\ldots 2\mathcal{N}}} \mathcal{G}_{l,k_1(t,\tau_1)} M_{k_1,k_2(\tau_1,\tau_2)} \mathcal{G}_{k_2,k_3(\tau_2,\tau_3)} \ldots \mathcal{G}_{k_{2\mathcal{N}},l_0(\tau_{2\mathcal{N}},t_0)} \tag{232}$$

where an integration over the variables $t_1 \ldots t_{2\mathcal{N}}$ is applied. One can sum now over all possible realisations of the vector $\vec{k}$. The result is the (l, l_0) elementh of the matrix product:

$$\int_c d_{\tau_{1,2\ldots 2\mathcal{N}}} \mathcal{G}_{(t,\tau_1)} M_{(\tau_1,\tau_2)} \ldots \mathcal{G}_{(\tau_{2\mathcal{N}},t_0)} \tag{233}$$

Do the last three steps for every $\mathcal{N} \in \mathbb{N}$; for $\mathcal{N} = 0$ substitute the sum with $\mathcal{G}_{l,l_0}(t,t_0)$ and then add all these expressions together. Assume that this sum gives an approximation for the full propagator $G_{l,l_0}(t,t_0)$. One can repeat the same steps for all combinations of l, l_0. Then one gets the following equation:

$$\begin{array}{rcl} G_{(t,t_0)} & = & \mathcal{G}_{(t,t_0)} + \int_c d_{\tau_{1,2}} \mathcal{G}_{(t,\tau_1)} M_{(\tau_1,\tau_2)} \mathcal{G}_{(\tau_2,t_0)} + \ldots \\ & = & \mathcal{G}_{(t,t_0)} + \int_c d_{\tau_{1,2}} \mathcal{G}_{(t,\tau_1)} M_{(\tau_1,\tau_2)} G_{(\tau_2,t_0)} \end{array} \tag{234}$$

Here it is assumed that the infinite sum converges. This equation of motion can be solved and probably the solution should contain more information about the physics in the interacting case than the mean field approximation.

10 Flow equation for the interacting self-energy

This is an alternative approach to obtain the interacting self-energy of a system that can be directly implemented for a particular microscopic model (it is already implemented in [29], [30]). We begin with giving basic definitions of the effective action and its connection to the self-energy (sec. 10.1) followed by a short explanation of the idea of the method and derivation of the flow-equation for the self-energy from the flow equation for the effective action (sec. 10.2). The flow equations are simplified for the case of a system in steady state with the use of a particular cut-off function (sec. 10.3).

10.1 Basic definitions

We use again the Keldysh partition function $\mathcal{Z}$ used in the last subsection but now we add additional source fields which will be used to generate 2m-point functions ($m \in \mathbb{N}_0$). In the following the normalisation factor in front of $\mathcal{Z}$ is unimportant, we leave it undefined. One also defines the generating functional of connected Green's functions $\mathcal{W}_{[\vec{\eta}^*,\vec{\eta}]}$[30]:

$$\begin{array}{rcl} \mathcal{Z}_{[\vec{\eta},\vec{\eta}^*]} & = & \int D_{[\vec{\varphi}^\dagger,\varphi]} \exp\big[i\int_{\mathcal{C}} \vec{\varphi}^\dagger_{(\tau_1)} \mathcal{G}^{-1}_{(\tau_1-\tau_2)} \vec{\varphi}_{(\tau_2)} - i\frac{U}{2}\int_{\mathcal{C}} \varphi^*_{\beta(\tau)}\varphi^*_{\beta(\tau)}\varphi_{\beta(\tau)}\varphi_{\beta(t)} - i\int_{\mathcal{C}} (\vec{\eta}^\dagger_{(t)}\cdot\vec{\varphi}_{(\tau)} + \vec{\varphi}^\dagger_{(\tau)}\cdot\vec{\eta}_{(\tau)}) \big] \\ & = & \int D_{[\vec{\varphi}^\dagger,\varphi]} \exp\big[\int \frac{dw}{2\pi} \big(i\vec{\varphi}^\dagger_{(w)} \mathcal{G}^{-1}_{(w)} \vec{\varphi}_{(w)} - i\frac{U}{2}^{\beta} \varphi^*_{\beta(w)}\varphi^*_{\beta(w)}\varphi_{\beta(w)}\varphi_{\beta(w)} - i\vec{\eta}^\dagger_{(w)}\sigma_z\vec{\varphi}_{(w)} - i\vec{\varphi}^\dagger{}_{(w)}\sigma_z\vec{\eta}_{(w)} \big) \big] \\ & \overset{U=0}{=} & \exp\big[-i\int \frac{dw}{2\pi} \vec{\eta}^\dagger_{(w)}\sigma_z\mathcal{G}_{(w)}\sigma_z\vec{\eta}_{(w)} \big] \\ \mathcal{W}_{[\vec{\eta}^\dagger,\vec{\eta}]} & = & \ln\big[\mathcal{Z}_{[\vec{\eta}^\dagger,\vec{\eta}]}\big] \end{array} \tag{235}$$

Note that in the second line the length of the vectors $\vec{\varphi}_{(w)}$ is doubled because of the introduction of the additional integration contour index. $\mathcal{G}$ can be interpreted as the Green's function of the noninteracting system. For the case of a quantum dot coupled to two reservoirs it is a 2×2 matrix. Then the vector $\vec{\varphi}_{(w)}$ keeps only track of the position of the field on the time contour ($\vec{\varphi}_{(w)} = (\varphi_{-(w)}, \varphi_{+(w)})^T$). U is the interaction that as before has different sign on both contours ($U^- = U$; $U^+ = -U$). We absorb the factor $\frac{1}{2\pi}$ in the definition of $\mathcal{G}_{(w)}$, $\vec{\eta}_{(w)}$ and U. Later when we try to solve the flow equations for a

[30] The Keldysh partition function generates also connencted diagrams if the sources are swithed off.

particular problem this constant will be extracted from $\mathcal{G}_{(w)}$.

Let the subscript k describe the set of quantum numbers of interest. One defines also the new field $\vec{\zeta} = \sigma_z \vec{\eta}$. The Green's function $\mathcal{G}_{k,l(w)}$ is given by [31]:

$$\begin{array}{rcl}
\frac{\delta^2 \mathcal{W}}{\delta \eta^*_{-,k(w)} \delta \eta_{-,l(w)}}\big|_{U=0} &=& -i\mathcal{G}^{--}_{kl}(w) = (-i)^2 \langle \varphi_{-,k(w)} \varphi^*_{-,l(w)} \rangle_{\tilde{0}} = \frac{\delta^2 \mathcal{W}}{\delta \zeta^*_{-,k(w)} \delta \zeta_{-,l(w)}}\big|_{U=0} \\
\frac{\delta^2 \mathcal{W}}{\delta \eta^*_{-,k(w)} (-\delta \eta_{+,l(w)})}\big|_{U=0} &=& -i\mathcal{G}^{-+}_{kl}(w) = (-i)^2 \langle \varphi_{-,k(w)} \varphi^*_{+,l(w)} \rangle_{\tilde{0}} = \frac{\delta^2 \mathcal{W}}{\delta \zeta^*_{-,k(w)} \delta \zeta_{+,l(w)}}\big|_{U=0} \\
\frac{\delta^2 \mathcal{W}}{(-\delta \eta^*_{+,k(w)}) \delta \eta_{-,l(w)}}\big|_{U=0} &=& -i\mathcal{G}^{+-}_{kl}(w) = (-i)^2 \langle \varphi_{+,k(w)} \varphi^*_{-,l(w)} \rangle_{\tilde{0}} = \frac{\delta^2 \mathcal{W}}{\delta \zeta^*_{+,k(w)} \delta \zeta_{-,l(w)}}\big|_{U=0} \\
\frac{\delta^2 \mathcal{W}}{(-\delta \eta^*_{+,k(w)})(-\delta \eta_{+,l(w)})}\big|_{U=0} &=& -i\mathcal{G}^{++}_{kl}(w) = (-i)^2 \langle \varphi_{+,k(w)} \varphi^*_{+,l(w)} \rangle_{\tilde{0}} = \frac{\delta^2 \mathcal{W}}{\delta \zeta^*_{+,k(w)} \delta \zeta_{+,l(w)}}\big|_{U=0}
\end{array} \tag{236}$$

The Green's functions of an interacting system $G_{(w)}$ can be obtained in the same way without setting $U = 0$. With the new notation one does not have to take care about the minus signs coming from the position of the fields on the time contour and one can absorb the $\pm$ intex in the general index k. The expectation value of the fields is given by:

$$\begin{array}{rcl}
\frac{\delta \mathcal{W}}{\delta \zeta_{k(w)}} &=& -i\langle \psi^*_{k(w)} \rangle \equiv -i\phi^*_{k(w)} \\
\frac{\delta \mathcal{W}}{\delta \zeta^*_{k(w)}} &=& -i\langle \psi_{k(w)} \rangle \equiv -i\phi_{k(w)}
\end{array} \tag{237}$$

The definition of the one particle irreducible (1PI) effective action is:

$$\Gamma[\vec{\phi}^*, \vec{\phi}] = -\int \frac{\delta \mathcal{W}[\vec{\zeta}^*, \vec{\zeta}]}{\delta \zeta_k} \zeta_k - \int \frac{\delta \mathcal{W}[\vec{\zeta}^*, \vec{\zeta}]}{\delta \zeta^*_k} \zeta^*_k \tag{238}$$

One adds also the term $-i \int d_w \phi^*_{k(w)} \mathcal{G}_{kl(}w) \phi_{l(w)}$ to Γ. The new effective action Γ' is then:

$$\Gamma'[\vec{\phi}^*, \vec{\phi}] = -\int \frac{\delta \mathcal{W}[\vec{\zeta}^*, \vec{\zeta}]}{\delta \zeta_k} \zeta_k - \int \frac{\delta \mathcal{W}[\vec{\zeta}^*, \vec{\zeta}]}{\delta \zeta^*_k} \zeta^*_k - i \int \phi^*_k \mathcal{G}_{kl} \phi_l \tag{239}$$

One can use the derivatives of Γ' with respect to the expectation values of the fields ϕ, ϕ^*

$$\begin{array}{rclcrcl}
\frac{\delta \Gamma}{\delta \phi^*_l} &=& i\zeta_l - i\left(\mathcal{G}^{-1}\right)_{lm} \phi_m & & \frac{\delta \Gamma}{\delta \phi_l} &=& i\zeta^*_l - i\phi_m \left(\mathcal{G}^{-1}\right)_{ml} \\
\frac{\delta^2 \Gamma}{\delta \phi_k \delta \phi^*_l} &=& i\frac{\delta \zeta_l}{\delta \phi_k} - i\left(\mathcal{G}^{-1}\right)_{lk} & & \frac{\delta^2 \Gamma}{\delta \phi_k \delta \phi_l} &=& i\frac{\delta \zeta^*_l}{\delta \phi_k} \\
\frac{\delta^2 \Gamma}{\delta \phi^*_k \delta \phi^*_l} &=& i\frac{\delta \zeta_l}{\delta \phi^*_k} & & \frac{\delta^2 \Gamma}{\delta \phi^*_k \delta \phi_l} &=& i\frac{\delta \zeta^*_l}{\delta \phi^*_k} - i\left(\mathcal{G}^{-1}\right)_{kl}
\end{array} \tag{240}$$

to construct the following equation[32]:

$$\begin{bmatrix} \delta_{kk'} & 0 \\ 0 & \delta_{kk'} \end{bmatrix} = \begin{bmatrix} \frac{\delta \phi^*_{k'}}{\delta \phi^*_k} & \frac{\delta \phi_{k'}}{\delta \phi^*_k} \\ \frac{\delta \phi^*_{k'}}{\delta \phi_k} & \frac{\delta \phi_{k'}}{\delta \phi_k} \end{bmatrix} = \begin{bmatrix} \frac{\delta}{\delta \phi^*_k} \frac{i\delta \mathcal{W}}{\delta \zeta_{k'}} & \frac{\delta}{\delta \phi^*_k} \frac{i\delta \mathcal{W}}{\delta \zeta^*_{k'}} \\ \frac{\delta}{\delta \phi_k} \frac{i\delta \mathcal{W}}{\delta \zeta_{k'}} & \frac{\delta}{\delta \phi_k} \frac{i\delta \mathcal{W}}{\delta \zeta^*_{k'}} \end{bmatrix} = \begin{bmatrix} \frac{\delta^2 \Gamma'}{\delta \phi^* \delta \phi} + i\mathcal{G}^{-1} & \frac{\delta^2 \Gamma'}{\delta \phi^* \delta \phi^*} \\ \frac{\delta^2 \Gamma'}{\delta \phi \delta \phi} & \frac{\delta^2 \Gamma'}{\delta \phi \delta \phi^*} + i\left(\mathcal{G}^{-1}\right)^T \end{bmatrix} \begin{bmatrix} \frac{\delta^2 \mathcal{W}}{\delta \zeta^* \delta \zeta} & \frac{\delta^2 \mathcal{W}}{\delta \zeta^* \delta \zeta^*} \\ \frac{\delta^2 \mathcal{W}}{\delta \zeta \delta \zeta} & \frac{\delta^2 \mathcal{W}}{\delta \zeta \delta \zeta^*} \end{bmatrix} \tag{241}$$

Since:

$$\frac{\delta^2 \mathcal{W}}{\delta \zeta \delta \zeta}\big|_{\zeta = 0 = \zeta^*} = 0 = \frac{\delta^2 \mathcal{W}}{\delta \zeta^* \delta \zeta^*}\big|_{\zeta = 0 = \zeta^*}, \tag{242}$$

the upper left part of the matrix equation then reads:

$$\begin{array}{rcl}
 & \delta_{kk'} &= \left(\frac{\delta^2 \Gamma'}{\delta \phi^*_k \delta \phi_l} + i\mathcal{G}^{-1}_{kl}\right)\left(\frac{\delta^2 \mathcal{W}}{\delta \zeta^*_l \delta \zeta_{k'}}\right) \\
\iff & \delta_{kk'} &= \left(\frac{\delta^2 \Gamma'}{\delta \phi^*_k \delta \phi_l} + i\mathcal{G}^{-1}_{kl}\right)(-i)G_{lk'} \\
\iff & \delta_{kk'} &= \frac{-i\delta^2 \Gamma'}{\delta \phi^*_k \delta \phi_l} G_{lk'} + \mathcal{G}^{-1}_{kl} G_{lk'}
\end{array} \tag{243}$$

If we compare the last equation with the definition of the self-energy (eq. (226)):

$$\begin{array}{rcl}
\iff & G^{-1}_{kk'} &= \mathcal{G}^{-1}_{kk'} - \Sigma_{kk'} \\
 & \delta_{kk'} &= -\Sigma_{kl} G_{lk'} + \mathcal{G}^{-1}_{kl} G_{lk'}
\end{array} \tag{244}$$

[31] $\langle \ldots \rangle_{\tilde{0}} \equiv \mathrm{tr}\left[\hat{\rho}_0 \ldots e^{-i\int_c d_\tau \hat{H}^i_{H_0}(\tau)}\right]\big|_{U=0} \to \int D_{[\vec{\varphi}^\dagger, \varphi]} \ldots e^{i\mathcal{S}}\big|_{U=0}$
$\langle \ldots \rangle \equiv \mathrm{tr}\left[\hat{\rho}_0 \ldots e^{-i\int_c d_\tau \hat{H}^i_{H_0}(\tau)}\right] \to \int D_{[\vec{\varphi}^\dagger, \varphi]} \ldots e^{i\mathcal{S}}$

[32] We drop the internal indices for legibility: $\left(\frac{\delta^2 \Gamma'}{\delta \phi^* \delta \phi}\right)_{kk'} \equiv \frac{\delta^2 \Gamma'}{\delta \phi^*_k \delta \phi_{k'}}$.

one can identify the second derivative of the modified 1PI effective action with the self-energy:

$$\Sigma_{kl} = \tfrac{i\delta\Gamma'}{\delta\phi_k^*\delta\phi_l}\big|_{\phi=0=\phi^*} \tag{245}$$

The identity will be used in the construction of the flow equation for the self-energy. One can formally expand $\Gamma'[\vec{\phi}^*,\vec{\phi}]$ as a sum of the 1PI vertex functions γ_n ($n \in \mathbb{N}$) which legs are connected with the fields ϕ_k^*, ϕ_k:

$$\Gamma'_{[\vec{\phi}^*,\vec{\phi}]} = \gamma_0 + \tfrac{1}{(1!)^2}\gamma_{1(\alpha_1;\beta_1)}\phi^*_{\alpha_1}\phi_{\beta_1} + \tfrac{1}{(2!)^2}\gamma_{2(\alpha_1,\alpha_2;\beta_1,\beta_2)}\phi^*_{\alpha_1}\phi^*_{\alpha_2}\phi_{\beta_1}\phi_{\beta_2} + \dots \tag{246}$$

Here the subscripts $_{\alpha}$, $_{\beta}$ contain the information about all quantum numbers plus frequency.

10.2 Flow equation of the effective action

The main idea consists in making the bare propagator $\mathcal{G}_{(w)}$ dependent on a cut-off function $f_{(\Lambda)}$. For large Λ this function should switch off $\mathcal{G}_{(w)}$ and for $\Lambda \to 0$ turn it completely on. If the bare Green's function is zero one can not construct complicated 1PI-diagrams with n legs consisting of $\mathcal{G}_{(w)}$ and the bare vertices given in the definiton of the interaction part of the Hamiltonian. The effective action is then just given as a sum of the bare vertices. In this limit the (modified) effective action (Γ') Γ should be equal to the interaction part of the action $\mathcal{S}_{int}$. Decreasing, Λ high energy modes of $\mathcal{G}_{(w)}$ are switched on and for $\Lambda \to 0$ the full (modified) effective action should be obtained. In this context the flow equation interpolates the 1PI-vertices of Γ' from the bare interactions (which are known from H_{int}) of $\mathcal{S}_{int}$ to the full 1PI vertices of Γ' (which are unknown). From the 1PI vertex with two legs $\gamma_{1(kl)}$ we can obtain the effective action Σ_{kl} ($i\gamma_{1(kl)} = \Sigma_{kl}$) (see eq. (245)).
Without proof we give the general flow equation of the effective action plus the initial conditions:

$$\left|\begin{array}{lcl} \frac{d}{d\Lambda}\Gamma'_{[\vec{\phi}^*,\vec{\phi}]} & = & \mathrm{tr}\big[(\dot{\mathcal{G}_\Lambda^{-1}})\mathcal{G}_\Lambda\big] - i\,\mathrm{tr}\big[\frac{\delta^2\mathcal{W}^\Lambda}{\delta\zeta^*\delta\zeta}\mathcal{G}_\Lambda^{-1}\big] \\ \Gamma'^{\Lambda_0}_{[\vec{\phi}^*,\vec{\phi}]} & = & \mathcal{W}_{[\vec{\phi}^*,\vec{\phi}]} = i\mathcal{S}_{int\,[\vec{\phi}^*,\vec{\phi}]} \end{array}\right. \tag{247}$$

The dot denotes a derivative with respect to Λ. $\mathcal{G}_\Lambda$ is the bare Green's function $\mathcal{G}$ multiplied with the cut-off function $f_{(\Lambda)}$. The subscript $_\Lambda$ in all other expressions means that we have replaced $\mathcal{G}$ with $\mathcal{G}_\Lambda$ in their definiton. The equation of Γ' is equivalent to an infinite hierarchy of flow equations for the 1PI vertices. As in many other cases this hierarchy is cut off and the finite amount of equations is solved.
The components of $\frac{\delta^2\mathcal{W}}{\delta\zeta_l^*\delta\zeta_k}$ that appear in the first line of eq. (247) can be extracted from eq. (241) with $\mathcal{G}$ replaced by $\mathcal{G}_\Lambda$:

$$\begin{aligned}
\begin{bmatrix} \frac{\delta^2\mathcal{W}^\Lambda}{\delta\zeta^*\delta\zeta} & \frac{\delta^2\mathcal{W}^\Lambda}{\delta\zeta^*\delta\zeta^*} \\ \frac{\delta^2\mathcal{W}^\Lambda}{\delta\zeta\delta\zeta} & \frac{\delta^2\mathcal{W}^\Lambda}{\delta\zeta\delta\zeta^*} \end{bmatrix} &= \begin{bmatrix} \frac{\delta^2\Gamma'^\Lambda}{\delta\phi^*\delta\phi} + i\mathcal{G}_\Lambda^{-1} & \frac{\delta^2\Gamma'^\Lambda}{\delta\phi^*\delta\phi^*} \\ \frac{\delta^2\Gamma'^\Lambda}{\delta\phi\delta\phi} & \frac{\delta^2\Gamma'^\Lambda}{\delta\phi\delta\phi^*} + i\big(\mathcal{G}_\Lambda^{-1}\big)^T \end{bmatrix}^{-1} \\
&= \left[\begin{bmatrix} iG_\Lambda^{-1} & 0 \\ 0 & i\big(G_\Lambda^{-1}\big)^T \end{bmatrix} + \begin{bmatrix} \mathcal{U}_{\phi^*\phi} & \frac{\delta^2\Gamma'}{\delta\phi^*\delta\phi^*} \\ \frac{\delta^2\Gamma'}{\delta\phi\delta\phi} & \mathcal{U}^T_{\phi^*\phi} \end{bmatrix}\right]^{-1} \\
&= \left[\begin{bmatrix} iG_\Lambda^{-1} & 0 \\ 0 & i\big(G_\Lambda^{-1}\big)^T \end{bmatrix}\left[\hat{1} - \begin{bmatrix} iG_\Lambda & 0 \\ 0 & iG_\Lambda^T \end{bmatrix}\begin{bmatrix} \mathcal{U}_{\phi^*\phi} & \frac{\delta^2\Gamma'}{\delta\phi^*\delta\phi^*} \\ \frac{\delta^2\Gamma'}{\delta\phi\delta\phi} & \mathcal{U}^T_{\phi^*\phi} \end{bmatrix}\right]\right]^{-1} \\
&= \left[\hat{1} - \begin{bmatrix} iG_\Lambda & 0 \\ 0 & iG_\Lambda^T \end{bmatrix}\begin{bmatrix} \mathcal{U}_{\phi^*\phi} & \frac{\delta^2\Gamma'}{\delta\phi^*\delta\phi^*} \\ \frac{\delta^2\Gamma'}{\delta\phi\delta\phi} & \mathcal{U}^T_{\phi^*\phi} \end{bmatrix}\right]^{-1}\begin{bmatrix} -iG_\Lambda & 0 \\ 0 & -iG_\Lambda^T \end{bmatrix} \\
&= -i\Xi_{\phi^*\phi}\cdot\begin{bmatrix} G_\Lambda & 0 \\ 0 & G_\Lambda^T \end{bmatrix}
\end{aligned} \tag{248}$$

In the second line we have used:

$$\tfrac{\delta^2\Gamma'}{\delta\phi^*\delta\phi} + i\mathcal{G}_\Lambda^{-1} = \big(i\mathcal{G}_\Lambda^{-1} + \gamma_1\big) + \big(\tfrac{\delta^2\Gamma'}{\delta\phi^*\delta\phi} - \gamma_1\big) = i\big(\mathcal{G}_\Lambda^{-1} - \Sigma\big) + \mathcal{U}_{\phi^*\phi} = iG_\Lambda^{-1} + \mathcal{U}_{\phi^*\phi} \tag{249}$$

The expression in the beginning of the equation is redistributed such that $\mathcal{U}_{\phi^*\phi}$ is at least quadtratic in the fields ϕ, ϕ^*. The matrix $\Xi_{\phi^*\phi}$ is of the form $(1-M)^{-1}$ and we assume that we can do the expansion

$(1-M)^{-1} = \sum_{m=0}^{\infty} M^m$. Then for every $N \in \mathbb{N}$ only the first few terms of the upper left part of $\Xi_{\phi^*\phi}$ contain fields $\phi^m \phi^{*n}$ with $m+n < N$.

The flow equation for the 1PI vertex with two external legs $\gamma_{1\,(\alpha_1;\beta_1)}^{\Lambda}$ one gets by applying on both sides of equation (247) the operator $\big(\frac{\delta^2}{\delta\phi^*_{\alpha_1}\delta\phi_{\beta_1}}\dots\big|_{\phi=0=\phi^*}\big)$. In the same way one gets the equation for the 1PI vertex function with four or more legs. So the equations for $\gamma_{1(\alpha_1;\beta_1)}$ and $\gamma_{2(\alpha_1,\alpha_2;\beta_1,\beta_2)}$ are:

$$\begin{aligned}
\partial_\Lambda \gamma_{1(\alpha_1;\beta_1)} &= i\,\mathrm{tr}\big[G_\Lambda \dot{(\mathcal{G}_\Lambda^{-1})} G_\Lambda \tfrac{\delta^2}{\delta\phi^*_{\alpha_1}\delta\phi_{\beta_1}} \mathcal{U}_{\phi^*\phi}\big]\big|_{\phi^*=0=\phi} \\
\partial_\Lambda \gamma_{2(\alpha_1,\alpha_2;\beta_1,\beta_2)} &= -\mathrm{tr}\big[G_\Lambda \dot{(\mathcal{G}_\Lambda^{-1})} G_\Lambda \tfrac{\delta^4}{\delta\phi^*_{\alpha_1}\delta\phi^*_{\alpha_2}\delta\phi_{\beta_1}\delta\phi_{\beta_2}}\big(-i\mathcal{U}_{\phi^*\phi} - \mathcal{U}_{\phi^*\phi} G_\Lambda \mathcal{U}_{\phi^*\phi} - \tfrac{\delta^2\Gamma'}{\delta\phi^*\delta\phi^*} G_\Lambda^T \tfrac{\delta^2\Gamma'}{\delta\phi\delta\phi}\big)\big]
\end{aligned} \tag{250}$$

We use the fact that we deal with bosons and because of the bosonic properties of the fields every permutation of the first m or/and the last m indices of γ_m does not change the vertex (e.g. $\gamma_{2(\alpha_1,\alpha_2;\beta_1,\beta_2)} = \gamma_{2(\alpha_2,\alpha_1;\beta_1,\beta_2)} = \gamma_{2(\alpha_1,\alpha_2;\beta_2,\beta_1)} = \gamma_{2(\alpha_2,\alpha_1;\beta_2,\beta_1)}$). This means that:

$$\begin{aligned}
\big(\mathcal{U}_{\phi^*\phi}\big)_{kl} &= \tfrac{\delta^2}{\delta\phi^*_k\delta\phi_l}\big[\sum_{n_1,n_2,m_1,m_2} \tfrac{1}{(2!)^2}\gamma_{2(n_1,n_2;m_1,m_2)}\phi^*_{n_1}\phi^*_{n_2}\phi_{m_1}\phi_{m_2} + \phi^{*n}\phi^m|_{n+m\geq 6}\text{ terms}\big] \\
&= \sum_{n_1,m_1} \gamma_{2(k,n_1;l,m_1)}\phi^*_{n_1}\phi_{m_1} + \phi^{*n}\phi^m|_{n+m\geq 4}\text{ terms} \\
\tfrac{\delta^2}{\delta\phi^*_{\alpha_1}\delta\phi_{\beta_1}}\big(\mathcal{U}_{\phi^*\phi}\big)_{kl}\Big|_{\phi^*=0=\phi} &= \gamma_{2(k,\alpha_1;l,\beta_1)}
\end{aligned} \tag{251}$$

10.3 Special case. Steady-state GF.

The equation can be further simplified if one takes into account that we work with steady-state Green's functions $G_{(w,w')} \equiv 2\pi\delta_{(w-w')}G_{(w)}$ and $G^{-1}_{(w,w')} = \frac{1}{2\pi}\delta_{(w-w')}G^{-1}_{(w)}$. The 2π-factor is cancelled if we take into account that in the beginning of the subsection we have absorbed a factor of $\frac{1}{2\pi}$ in the definition of G and the source fields. From now on we separate the frequency from the multiindex k. The frequency w appears as an argument of the function and the rest of the index k appears as a superscript. Both w and k should be moved together if one applies the bosonic properties of some vertex function γ (e.g. $\gamma_{2\,(w_1,w_2,w_3,w_4)}^{k_1,k_2,k_3,k_4} = \gamma_{2\,(w_2,w_1,w_3,w_4)}^{k_2,k_1,k_3,k_4}$). The product of three Green's functions in eq. (250) now reads:

$$\begin{aligned}
\big[G_\Lambda \dot{(\mathcal{G}_\Lambda^{-1})} G_\Lambda\big]^{k_1k_4}_{(w_1,w_4)} &\equiv \sum_{k_2,k_3}\int d_{w_2}\int d_{w_3}\tfrac{1}{2\pi}G^{k_1,k_2}_{\Lambda\,(w_1,w_2)}\big(2\pi\dot{\mathcal{G}}^{-1}_\Lambda\big)^{k_2,k_3}_{(w_2,w_3)}\tfrac{1}{2\pi}G^{k_3,k_4}_{\Lambda\,(w_3,w_4)} \\
&= \sum_{k_2,k_3} G^{k_1,k_2}_{\Lambda\,(w_1)}\big(\dot{\mathcal{G}^{-1}_\Lambda}\big)^{k_2,k_3}_{(w_1)}G^{k_3,k_4}_{\Lambda\,(w_1)}\delta_{(w_1-w_4)} \\
&\equiv \big[G_\Lambda \dot{(\mathcal{G}_\Lambda^{-1})} G_\Lambda\big]^{k_1,k_4}_{(w_1)}\delta_{(w_1-w_4)}
\end{aligned} \tag{252}$$

The flow equations for the two-leg 1PI vertex function is given by:

$$\partial_\Lambda \gamma_{1\,(w';w'')}^{\Lambda\,(\alpha_1\beta_1)} = i\sum_{k,l}\int d_{w_l}\big[G_\Lambda \dot{(\mathcal{G}_\Lambda^{-1})} G_\Lambda\big]^{lk}_{(w_l)}\gamma_{2\,(w',w_l;w'',w_l)}^{\Lambda\,\alpha_1k\beta_1l} \tag{253}$$

10.4 Lowest order flow equation for a quantum dot coupled to two bosonic reservoirs.

In the lowest order approximation we assume that the four leg vertex does not change during the flow, i.e. it is equal to the interaction term of the action $\mathcal{S}$:

$$\gamma_{2\,(w_1,w_2;w_1',w_2')}^{\Lambda\,\alpha_1\alpha_2\beta_1\beta_2} = \gamma_{2\,(w_1,w_2;w_1',w_2')}^{\Lambda_0\,\alpha_1\alpha_2\beta_1\beta_2} = -\tfrac{1}{2\pi}\big(i\tfrac{U}{2}\big)^{\alpha_1}\delta_{\alpha_1\alpha_2\beta_1\beta_2}\delta_{(w_1+w_2-w_1'-w_2')} \tag{254}$$

The upper indices of the interaction, the 1PI n-leg vertices and the GF's now denote only the position on the time contour. The interaction U^{α_1} is given by $U^- = U$, $U^+ = -U$, $\delta_{\alpha_1,\alpha_2,\beta_1,\beta_2} \equiv \delta_{\alpha_1\alpha_2}\delta_{\alpha_2\beta_1}\delta_{\beta_1\beta_2}$. All 1PI n-leg vertices with $n > 4$ are equal to zero. The flow equation for the self-energy $\Sigma^{\alpha_1\beta_1}_{(w';w'')} =$

$i\gamma_{1\ (w';w'')}^{\alpha_1,\beta_1}$ is then:

$$\begin{array}{lcl} \partial_\Lambda \Sigma^{\Lambda\ --}_{(w';w'')} &=& +\frac{iU}{4\pi}\delta_{(w'-w'')}\int d_w \left[G_\Lambda \left(\dot{\mathcal{G}_\Lambda^{-1}}\right) G_\Lambda\right]^{--}_{(w)} \\ \partial_\Lambda \Sigma^{\Lambda\ ++}_{(w';w'')} &=& -\frac{iU}{4\pi}\delta_{(w'-w'')}\int d_w \left[G_\Lambda \left(\dot{\mathcal{G}_\Lambda^{-1}}\right) G_\Lambda\right]^{++}_{(w)} \\ \partial_\Lambda \Sigma^{\Lambda\ -+}_{(w';w'')} &=& 0 \\ \partial_\Lambda \Sigma^{\Lambda\ +-}_{(w';w'')} &=& 0 \end{array} \tag{255}$$

It follows that in the lowest order approximation Σ gives just a correction to the energy level of the quantum dot:

$$\partial_\Lambda \Sigma^{\Lambda\ \alpha_1\alpha_2}_{(w';w'')} = \tfrac{1}{2\pi}\delta_{(w'-w'')}\Sigma^{\Lambda\ \alpha_1\alpha_2}_{(w')} = \tfrac{1}{2\pi}\delta_{(w'-w'')}\partial_\Lambda \Sigma^{\Lambda\ \alpha_1\alpha_2} \tag{256}$$

We specify the cut-off function to be $f_{(\Lambda,w)} = \theta_{(|w|-\Lambda)}$ and $\mathcal{G}_{\Lambda(w)} \equiv f_{(\Lambda,w)}\mathcal{G}_{(w)}$. We also define the GF $\tilde{G}_{\Lambda\ (w)}$ and give again the definition of $G_{\Lambda(w)}$:

$$\begin{array}{lcl} G_{\Lambda(w)} &\equiv& \left[\mathcal{G}^{-1}_{\Lambda\ (w)} - \Sigma^\Lambda\right]^{-1} \\ \tilde{G}_{\Lambda(w)} &\equiv& \left[\mathcal{G}^{-1}_{\ (w)} - \Sigma^\Lambda\right]^{-1} \end{array} \tag{257}$$

In order to overcome the ambiguity arising by having an integral over an expression that contains two functions with discontinuity at the same point (like $\delta_{(|w|-\Lambda)}$ and $\theta_{(|w|-\Lambda)}$) we apply the Morris lemma[33]. The lemma stays that for every function $\mathcal{F}_{(\theta_{(w)},w)}$, continuous in its second argument at $w = 0$, we can apply the following transformation:

$$\delta_{(w)}\mathcal{F}_{(\theta(w),w)} \to \delta_{(w)}\int_0^1 d_u \mathcal{F}_{(u,0)} \tag{258}$$

By performing a partial integration (see appendix sec. 12) one gets the following set of equiations:

$$\partial_\Lambda \Sigma^{\Lambda\ --} = \frac{iU}{2}\sum_{w=\pm\Lambda}\tilde{G}^{--}_{\Lambda\ (w)} \qquad \partial_\Lambda \Sigma^{\Lambda\ ++} = -\frac{iU}{2}\sum_{w=\pm\Lambda}\tilde{G}^{++}_{\Lambda\ (w)} \tag{259}$$

The initial condition is $\Sigma^{\Lambda_0\ ll'} = 0$ for $l, l' \in \{-,+\}$. The matrix $\mathcal{G}_{(w)}$ given in eq. (33) fulfills the relations $\left(\Re\mathcal{G}^{-+}_{(w)} = 0 = \Re\mathcal{G}^{+-}_{(w)}\right)$, $\left(\mathcal{G}^{--}_{(w)} = -\left(\mathcal{G}^{++}_{(w)}\right)^*\right)$. Using this one can show (see appendix sec. 11) that this equation conserves the relation $\Sigma^{--} = -\left(\Sigma^{++}\right)^*$. It follows that $\tilde{G}^{--}_{(w)} = -\left(\tilde{G}^{++}_{(w)}\right)^*$. This proof reduces the number of differential equations from two to one.

10.5 Lowest order flow equation for a chain of quantum dots coupled to two bosonic reservoirs

Taking again $\partial_\Lambda \Sigma^\Lambda_{(w';w'')} = \frac{1}{2\pi}\delta_{(w'-w'')}\partial_\Lambda \Sigma^\Lambda$ into account one obtains the following set of differential equations:

$$\begin{array}{lcllcl} \partial_\Lambda \Sigma^{\Lambda\ --}_{11} &=& \frac{iU}{2}\sum_{w=\pm\Lambda}\tilde{G}^{--}_{\Lambda\ 11(w)} & \partial_\Lambda \Sigma^{\Lambda\ ++}_{11} &=& -\frac{iU}{2}\sum_{w=\pm\Lambda}\tilde{G}^{++}_{\Lambda\ 11(w)} \\ \partial_\Lambda \Sigma^{\Lambda\ --}_{22} &=& \frac{iU}{2}\sum_{w=\pm\Lambda}\tilde{G}^{--}_{\Lambda\ 22(w)} & \partial_\Lambda \Sigma^{\Lambda\ ++}_{22} &=& -\frac{iU}{2}\sum_{w=\pm\Lambda}\tilde{G}^{++}_{\Lambda\ 22(w)} \end{array} \tag{260}$$

The initial condition is $\Sigma^{\Lambda_0\ ll'}_{jj'} = 0$ for $l, l' \in \{-,+\}$ and $j, j' \in \{1,2\}$. For all other components of the self-energy the flow on the RHS of the equation is zero. The matrices $\tilde{G}_{\Lambda\ (w)}$ and $\mathcal{G}_{(w)}$ are defined in eq. (257) and (36) respectively. One can show again in analogy to the proof for one quantum dot that $\Sigma^{\Lambda\ --}_{jj} = -\left(\Sigma^{\Lambda\ ++}_{jj}\right)^*$ and $\tilde{G}^{--}_{\Lambda\ jj(w)} = -\left(\tilde{G}^{++}_{\Lambda\ jj(w)}\right)^*$ for $(jj) \in \{(11),(22)\}$. So instead of four one has to solve just the first column of equations in eq. (260).

10.6 Properties of the approximation

Since we do not solve the infinite set of flow equations but truncate them we can not expect that the approximated Σ has all symmetries that the true Σ has. We can show that the causality condition is not fulfilled but the current is conserved. The results for the case of one quantum dot can be easily

[33]The precise definition is given in the Appendix sec 12.

derived by taking the results from sec. 4.1 and setting $\left(\Sigma^{-+}=0=\Sigma^{+-}\right)$ [34]. The causality condition is not fulfilled since in general $\Im\Sigma^{--}\neq 0$ and eq. (56) is not fulfilled. The current is conserved and it is given by (see eq. (59)):

$$\langle\hat{I}\rangle \;=\; \int \tfrac{dw}{2\pi}\tfrac{4\Gamma_{L\,(w)}\Gamma_{R(w)}}{-\mathrm{Det}_{(w)}}(n_L-n_R) \tag{261}$$

with $\mathrm{Det}_{(w)}$ equal to (see eq. (57)):

$$\begin{array}{rcl}\mathrm{Det}_{(w)} & = & -\left[\left(w-\Delta-\tilde{\Lambda}_{L\,(w)}-\tilde{\Lambda}_{R\,(w)}-\Re\Sigma^{--}\right)^2+\left(\Gamma_{L(w)}+\Gamma_{R(w)}+\Im\Sigma^{--}\right)^2\right]\\ & & +4\Im\Sigma^{--}\left[\Gamma_{L\,(w)}(n_L+1)+\Gamma_{R\,(w)}(n_R+1)\right]\end{array} \tag{262}$$

As in the previous approximation one can argue that the last line from the determinat origins from the fact that the causality condition (eq. (56)) is not fulfilled and this term can be neglected.

11 Reduction of the number of flow equations for a system of a quantum dot coupled to two bosonic resrevoirs

Proposition
First note that if $\left(\Re g^{-+}_{(w)}=0=\Re g^{+-}_{(w)}\right)$ and $\left(g^{--}_{(w)}=-\left(g^{++}_{(w)}\right)^*\right)$ for an arbitrary 2x2 matrix g by direct calculation it follows that:

$$\begin{array}{rcl}\left(g^{-1}_{(w)}\right)^{--} & = & -\left[\left(g^{-1}_{(w)}\right)^{++}\right]^*\\ \Re\left(g^{-1}_{(w)}\right)^{-+} & =0= & \Re\left(g^{-1}_{(w)}\right)^{+-}\qquad\square.\end{array} \tag{263}$$

For the 2x2 matrices $\mathcal{G}$ and Σ_Λ it is given that:

$$\begin{array}{rclcrcl}\Re\mathcal{G}^{-+}_{(w)} & = & 0 & & \Sigma^{-+}_{\Lambda} & = & 0\quad\forall\Lambda\in\mathbb{R}\\ \Re\mathcal{G}^{+-}_{(w)} & = & 0 & & \Sigma^{+-}_{\Lambda} & = & 0\quad\forall\Lambda\in\mathbb{R}\\ \mathcal{G}^{--}_{(w)} & = & -\left(\mathcal{G}^{++}_{(w)}\right)^* & & \Sigma^{--}_{\Lambda_0} & = & -\left(\Sigma^{++}_{\Lambda_0}\right)^*\end{array} \tag{264}$$

The flow equation for the self-energy is:

$$\partial_\Lambda\Sigma^\Lambda \;=\; \left[\begin{array}{cc}\partial_\Lambda\Sigma^{--}_\Lambda & 0\\ 0 & \partial_\Lambda\Sigma^{++}_\Lambda\end{array}\right] \;=\; \left[\begin{array}{cc}\frac{iU}{2}\sum\limits_{w=\pm\Lambda}\tilde{G}^{--}_{\Lambda\;(w)} & 0\\ 0 & -\frac{iU}{2}\sum\limits_{w=\pm\Lambda}\tilde{G}^{++}_{\Lambda\;(w)}\end{array}\right] \tag{265}$$

The matrices $\mathcal{G}^\Lambda, G^\Lambda, \tilde{G}^\Lambda$ depend on the flow parameter Λ and the cut-off function $f(\Lambda)$, and are defined as:

$$\begin{array}{rcl}\mathcal{G}_{\Lambda(w)} & = & \mathcal{G}_{(w)}f(\Lambda)\\ G_{\Lambda(w)} & = & \left[\mathcal{G}^{-1}_{\Lambda\;(w)}-\Sigma_\Lambda\right]^{-1}\\ \tilde{G}_{\Lambda(w)} & = & \left[\mathcal{G}^{-1}_{(w)}-\Sigma_\Lambda\right]^{-1}.\end{array} \tag{266}$$

For $\Lambda=0$ the cut-off function is equal to one and $\mathcal{G}_\Lambda=\mathcal{G}, G_\Lambda=G, \Sigma_\Lambda=\Sigma$.

One has to show that $G^{--}_{(w)}=-\left(G^{++}_{(w)}\right)^*$. This condition is always fulfilled for [35]:

$$\Sigma^{--} \;=\; -\left(\Sigma^{++}\right)^* \qquad\qquad \Sigma^{-+}=0=\Sigma^{+-}. \qquad\qquad \diamondsuit$$

So we have to show only that the differential eq. (265) with the given initial conditions (right column of eq. (264)) fulfills ($\diamondsuit$) for $\Lambda=0$.
In practice we use the Euler method to integrate eq. (265):

$$\Sigma_{\Lambda_0+\Delta(n+1)} \;=\; \Sigma_{\Lambda_0+\Delta n}+\Delta\partial_\Lambda\Sigma_\Lambda\big|_{\Lambda=\Lambda_0+n\Delta} \tag{267}$$

[34] In the approximation of sec. 4.1 we had again that $\Sigma^{--}_{(w)}=-\left(\Sigma^{++}\right)^*$ and $\Re\Sigma^{-+}=0=\Re\Sigma^{+-}$.

[35] Just calculate directly $G=\left[\mathcal{G}-\Sigma\right]^{-1}$.

The finite integration step is Δ. The condition $\diamondsuit$ can be fulfilled if for $\Sigma_{\Lambda_0+\Delta(n+1)}$ it is partially fulfilled for both summands in the RHS of the last equation and for all $n \in \mathbb{N}$ (n is the integration step number). One can proove this by iduction. So the statement we have to proove for every $n \in \mathbb{N}_0$ is:

$$\Sigma^{--}_{\Lambda_0+n\Delta} = -\big(\Sigma^{++}_{\Lambda_0+n\Delta}\big)^* \tag{268a}$$

$$\partial_\Lambda \Sigma^{--}_\Lambda\big|_{\Lambda=\Lambda_0+n\Delta} = -\big(\partial_\Lambda \Sigma^{++}_\Lambda\big)^*\big|_{\Lambda=\Lambda_0+n\Delta} \tag{268b}$$

For $n = 0$ it follows $\Sigma^{--}_{\Lambda_0} = -\big(\Sigma^{++}_{\Lambda_0}\big)^*$ because of the assumption in the beginning of the section. The second condition - eq. (268b), is also fulfilled since $\Sigma_{\Lambda_0} = 0$:

$$\begin{aligned}
\partial_\Lambda \Sigma_\Lambda\big|_{\Lambda=0=\Lambda_0} &= \sum_{w=\pm\Lambda_0} \begin{bmatrix} \frac{iU}{2}\big(\Re\tilde{G}^{--}_{\Lambda_0}(w) + i\Im\tilde{G}^{--}_{\Lambda_0}(w)\big) & 0 \\ 0 & -\frac{iU}{2}\big(\Re\tilde{G}^{++}_{\Lambda_0}(w) + i\Im\tilde{G}^{++}_{\Lambda_0}(w)\big) \end{bmatrix} \\
&= \sum_{w=\pm\Lambda_0} \begin{bmatrix} \frac{iU}{2}\big(\Re\mathcal{G}^{--}(w) + i\Im\mathcal{G}^{--}(w)\big) & 0 \\ 0 & -\frac{iU}{2}\big(\Re\mathcal{G}^{++}(w) + i\Im\mathcal{G}^{++}(w)\big) \end{bmatrix} \\
&= \sum_{w=\pm\Lambda_0} \begin{bmatrix} -\frac{U}{2}\Im\mathcal{G}^{--}(w) + \frac{iU}{2}\Re\mathcal{G}^{--}(w) & 0 \\ 0 & \frac{U}{2}\Im\mathcal{G}^{--}(w) + \frac{iU}{2}\Re\mathcal{G}^{--}(w) \end{bmatrix}
\end{aligned} \tag{269}$$

Now assume that eq. (268a),(268b) are fulfilled for some $n \in \mathbb{N}$. One has to show that they are fulfilled for $(n+1)$.
Proof: Since

$$\begin{bmatrix} \Sigma^{--}_{\Lambda_0+(n+1)\Delta} & 0 \\ 0 & \Sigma^{++}_{\Lambda_0+(n+1)\Delta} \end{bmatrix} = \begin{bmatrix} \Sigma^{--}_{\Lambda_0+n\Delta} & 0 \\ 0 & \Sigma^{++}_{\Lambda_0+n\Delta} \end{bmatrix} + \Delta \begin{bmatrix} \partial_\Lambda\Sigma^{--}_\Lambda & 0 \\ 0 & \partial_\Lambda\Sigma^{++}_\Lambda \end{bmatrix}\Big|_{\Lambda=\Lambda_0+n\Delta} \tag{270}$$

and both summands fulfill partially the condition $f^{--} = -\big(f^{++}\big)^*$ by assumption, it follows that eq. (268a) is fulfilled for $(n+1)$.
To show eq. (268b) we calculate:

$$\begin{aligned}
\begin{bmatrix} \partial_\Lambda\Sigma^{--}_\Lambda & 0 \\ 0 & \partial_\Lambda\Sigma^{++}_\Lambda \end{bmatrix}\Big|_{\substack{\Lambda=\Lambda_0 \\ +(n+1)\Delta}} &= \tfrac{iU}{2} \sum_{\substack{w=\pm\Lambda_0 \\ +(n+1)\Delta}} \begin{bmatrix} \tilde{G}^{--}_{\Lambda+n\Delta(w)} & 0 \\ 0 & -\tilde{G}^{++}_{\Lambda+n\Delta(w)} \end{bmatrix} \\
&= \tfrac{iU}{2} \sum_{\substack{w=\pm\Lambda_0 \\ +(n+1)\Delta}} \begin{bmatrix} \big[\big(\mathcal{G}^{-1}(w) - \Sigma_{\Lambda_0+n\Delta}\big)^{-1}\big]^{--} & 0 \\ 0 & -\big[\big(\mathcal{G}^{-1}_{(w)} - \Sigma_{\Lambda_0+n\Delta}\big)^{-1}\big]^{++} \end{bmatrix}
\end{aligned} \tag{271}$$

Use the Proposition for $g = \mathcal{G}$. Because of the assumption for a given $n \in \mathbb{N}$ (eq. (268a)) it follows that the Proposition is fulfilled also for $\Sigma^{\Lambda_0+n\Delta}$ and for the sum $\mathcal{G}^{-1} - \Sigma_{\Lambda_0+n\Delta}$. Using these relations we get:

$$\big[(\mathcal{G}^{-1}_{(w)} - \Sigma_{\Lambda_0+n\Delta})^{-1}\big]^{--} = -\Big(\big[(\mathcal{G}^{-1}_{(w)} - \Sigma_{\Lambda_0+n\Delta})^{-1}\big]^{++}\Big)^* \tag{272a}$$

$$\Re\big[(\mathcal{G}^{-1}_{(w)} - \Sigma_{\Lambda_0+n\Delta})^{-1}\big]^{-+} = 0 = \Re\big[(\mathcal{G}^{-1}_{(w)} - \Sigma_{\Lambda_0+n\Delta})^{-1}\big]^{+-} \tag{272b}$$

From eq. (272a) and eq. (271) it follows that eq. (268b) is fulfilled for $n+1$ $\square$.

12 Morris lemma. Application for lowest order flow equation

Let $\theta_{\varepsilon(w,\Lambda)}$ be a smooth cutoff function with $\theta_{\varepsilon(w,\Lambda)} \to 0$ for $w < \Lambda - \varepsilon$ and $\theta_{\varepsilon(w,\Lambda)} \to 1$ for $w > \Lambda + \varepsilon$. Define also $\delta_{\varepsilon(w,\Lambda)}$ which is equal to zero for $|w - \Lambda| > \varepsilon$ and fulfills the equaiton $\big(\int dw \delta_{\varepsilon(w,\Lambda)} = 1\big)$. In the limit $\varepsilon \to 0$ both functions should converge to the usual theta- and delta-functions:

$$\begin{aligned}
\theta_{\varepsilon(w,\Lambda)} &\xrightarrow[\varepsilon\to 0]{} \theta_{(w-\Lambda)} \\
\delta_{\varepsilon(w,\Lambda)} &\xrightarrow[\varepsilon\to 0]{} \delta_{(w-\Lambda)}
\end{aligned} \tag{273}$$

Let $f_{(\theta_{\varepsilon(w,\Lambda)},\Lambda)}$ be a function whoose dependence on the second argument remains continuous at $\Lambda \to w$ in the limit $\varepsilon \to 0$. The Morris lemma [28] stays that:

$$\delta_{\varepsilon(w,\Lambda)} f_{(\theta_{\varepsilon(w,\Lambda)},\Lambda)} \xrightarrow[\varepsilon\to 0]{} \delta_{(w-\Lambda)} \int_0^1 du f_{(u,w)} \tag{274}$$

For the matrix $\big[\mathcal{G}^{-1}_{\Lambda\,(w)}-\Sigma\big]^{-1}\big(\partial_\Lambda\mathcal{G}_{\Lambda(w)}\big)\big[\mathcal{G}^{-1}_{\Lambda\,(w)}-\Sigma\big]^{-1}=-\partial_\Lambda G_{\Lambda\,(w)}$ with the cutoff function $\theta_{(|w|-\Lambda)}$ this means:

$$\begin{aligned}
-\partial_\Lambda G_{\Lambda(w)} &= -\partial_\Lambda\big[\mathcal{G}^{-1}_{\Lambda\,(w)}-\Sigma\big]^{-1}\\
&= -\partial_\Lambda\big[\big(\theta_{(|w|-\Lambda)}\mathcal{G}_{(w)}\big)^{-1}-\Sigma\big]^{-1}\\
&= -\partial_\Lambda\theta_{(|w|-\Lambda)}\big[\mathcal{G}^{-1}_{(w)}-\theta_{(|w|-\Lambda)}\Sigma\big]^{-1}\\
&= -\partial_\Lambda\big(\theta_{(|w|-\Lambda)}\big)\int_0^1 du\big[\mathcal{G}^{-1}_{(w)}-u\Sigma\big]^{-1}\\
&\quad -\theta_{(|w|-\Lambda)}\big[\mathcal{G}^{-1}_{(w)}-\theta_{(|w|-\Lambda)}\Sigma\big]^{-1}\big(\partial_\Lambda\theta_{(|w|-\Lambda)}\Sigma\big)\big[\mathcal{G}^{-1}_{(w)}-\theta_{(|w|-\Lambda)}\Sigma\big]^{-1}\\
&= \delta_{(|w|-\Lambda)}\int_0^1 du\big[\mathcal{G}^{-1}_{(w)}-u\Sigma\big]^{-1}+\delta_{(|w|-\Lambda)}\int_0^1 du\,u\big[\mathcal{G}^{-1}_{(w)}-u\Sigma\big]^{-1}\Sigma\big[\mathcal{G}-u\Sigma\big]^{-1}\\
&= \delta_{(|w|-\Lambda)}\int_0^1 du\big[\mathcal{G}^{-1}_{(w)}-u\Sigma\big]^{-1}+\delta_{(|w|-\Lambda)}\int_0^1 du\,u\partial_u\big(\big[\mathcal{G}^{-1}_{(w)}-u\Sigma\big]^{-1}\big)\\
&= \delta_{(|w|-\Lambda)}\int_0^1 du\big[\mathcal{G}^{-1}_{(w)}-u\Sigma\big]^{-1}+\delta_{(|w|-\Lambda)}u\big[\mathcal{G}^{-1}_{(w)}-u\Sigma\big]^{-1}\big|_0^1-\delta_{(|w|-\Lambda)}\int_0^1 du\big[\mathcal{G}^{-1}_{(w)}-u\Sigma\big]^{-1}\\
&= \delta_{(|w|-\Lambda)}\big[\mathcal{G}^{-1}_{(w)}-\Sigma\big]^{-1}\\
&= \delta_{(|w|-\Lambda)}\tilde{G}_{(w)}
\end{aligned}\tag{275}$$

The partial derivative ∂_Λ is with respect to the arguments of the function $\mathcal{G}_{\Lambda\,(w)}$, $\Sigma_{(w)}$ (here $\Sigma_{(w)}=const$) but not with respect to the superscript of Λ of the self-energy (we have omitted it in the last calculation).

13 Notation

$\hat{H}_0$	Hamiltonian quadratic in its operators
$\hat{H}^i$	Interaction part of a Hamiltonian
$\hat{\mathcal{O}}_{H_0}$	Operator in the Interaction picture representation
$\hat{\mathcal{O}}_H$	Operator in the Heisenberg picture representation
$\hat{T}$	Time ordering operator
$\hat{\tilde{T}}$	Anti-time ordering operator
$\hat{T}_c$	Contour ordering operator
U	Interaction parameter in the Hamiltonian
γ	Coupling between reservoir and the nearest quantum dot. Subscript $_{L/R}$ refers to the left/right reservoir
$D_{(w)}$	Density of states of a bosonic reservoir. Subscript $_{L/R}$ refers to the left/right reservoir.
Γ	Short notation for $\Gamma_{(w)}=\pi\gamma^2 D_{(w)}$. Subscript $_{L/R}$ refers to the case when $\gamma_{L/R}$ and $D_{L/R(w)}$ are used.
$\tilde{\Lambda}_{L/R}$	Short notation for $\tilde{\Lambda}_{L/R(w)}=\lim\limits_{\delta\to0^+}\int\limits_{\lvert w-\varepsilon\rvert>\delta}d_\varepsilon\frac{D_{(\varepsilon)\,L/R}\lvert\gamma_{L/R}\rvert^2}{w-\varepsilon}$. Subscript $_{L/R}$ refers to the case when $\gamma_{L/R}$ and $D_{L/R(w)}$ are used.
$\tilde{\Lambda}$	Short notation for $\tilde{\Lambda}_{(w)}=\tilde{\Lambda}_{L(w)}+\tilde{\Lambda}_{R(w)}$
$n_{L/R}$	Short notation for $n_{(w-\mu_{L/R})}=\big[\exp(\beta(w-\mu_L))-1\big]^{-1}$. The chemical potentials of the left/right reservoirs are denoted by $\mu_{L/R}$.
$\langle\ldots\rangle$	$=\mathrm{tr}\big[\hat{\rho}\ldots e^{-i\int_c d_\tau\hat{H}^i_{H_0(\tau)}}\big]$
$\langle\ldots\rangle_{\tilde{0}}$	$=\mathrm{tr}\big[\hat{\rho}\ldots e^{-i\int_c d_\tau\hat{H}^i_{H_0(\tau)\lvert U=0}}\big]$
$\langle\ldots\rangle_0$	$=\mathrm{tr}\big[\hat{\rho}\ldots e^{-i\int_c d_\tau\hat{H}^i_{H_0(\tau)\lvert U,\gamma=0}}\big]=\mathrm{tr}\big[\hat{\rho}\ldots\big]$

Acknowledgements

First of all, I want to thank Georgios Kordas and Stepnan Burkhard for helping me to understand some aspects of the theory and correcting my Master Thesis. Stephan was also patient enough to answer all my bash-, C-, Latex-related questions for which I am very grateful. Further thanks go to Carlos Parra-Murillo, Matthias Kraft, Felix Ziegler and Julia Link for providing a hospitable atmosphere and allowing me to use their institute accounts for some numerical calculations.
I am also very grateful to my supervisor Sandro Wimberger for giving me the opportunity to work on this topic and Andreas Komnik for the helpful discussions.
Finally, I want to thank my family for their lifelong support. Without them I would have never had the chance to study physics at Heidelberg.

References

[1] M. Fuechsle, J. A. Miwa, S. Mahapatra, H. Ryu, S. Lee, O. Warschkolow, L. C. L. Hollenberg, G. Klimeck, M. Y. Simmons, Nature Nan. **7**, 242 (2012).

[2] K. B. Davis, M. O. Mewes, M. R. Andrews, N. J. van Druten, D. S. Durfee, D. M. Kurn, W. Ketterle, Phys. Rev. Lett. **75**, 3969 (1995).

[3] P. A. Lee, D. A. Fisher, Phys. Rev. Lett. **47**, 882 (1981).

[4] P. Schmitteckert, T. Schulze, C. Schuster, P. Schwab, U. Eckern, Phys. Rev. Lett. **80**, 560 (1998).

[5] Q. Beaufils, G. Tackmann, X. Wang, B. Pelle, S. Pellison, P. Wolf, F. Pereira dos Santos, Phys. Rev. Lett. **106**, 213002 (2011).

[6] M. Raizen, C. Solomon, Qian Niu, Phys. Today **50**, 30 (1997).

[7] E. Peik, M. B. Dahan, I. Bouchoule, Y. Castin, C. Salomon, Phys. Rev. A. **55**, 2989 (1997).

[8] S. R. Wilkinson, C. F. Bharucha, K. W. Madison, Q. Niu, M. G. Raizen, Phys. Rev. Lett. **76**, 4512 (1996).

[9] J. R. Anglin, W. Ketterle, Nature **416**, 211 (2002).

[10] O. Morsch, M. Oberthaler, Rev. Mod. Phys. **78**, 179 (2006).

[11] J. Reichel, W. Hänsel, T. W. Hänsch, Phys. Rev. Lett. **83**, 3398 (1999).

[12] J. H. Thywissen, R. M. Westervelt, M. Prentiss, Phys. Rev. Lett. **83**, 3762 (1999).

[13] Artem Dudarev, "Dynamics of ultracold atoms in optical potentials", Ph.D. Thesis, University of Texas at Austin (2005).

[14] T Gericke, P. Würtz, D. Reitz, T. Langen, H. Ott, Nature. Phys. **4**, 949 (2008).

[15] J. Sherson, C. Weitenberg, M. Endres, M. Cheneau, I. Bloch, S Kuhr, Nature **467**, 68, (2010).

[16] D B. Gutman, Y. Gefen, A. D. Mirlin, Phys. Rev. B **85**, 125102 (2012).

[17] J. H. Thywissen, R. M. Westervelt, M. Prentiss, Phys. Rev. Lett. **83**, 19, (1999).

[18] Kunal K. Das, Seth Aubin, Phys. Rev. Lett. **103**, 123007 (2009).

[19] R. A. Pepino, J. Cooper, D. Meiser, D. Z. Anderson, M. J. Holland, Phys. Rev. A **82**, 013640 (2010).

[20] P. Schlagheck, F. Malet, J. C. Cremon, S. M. Reimann, New J. Phys. **12**, 065020, (2010).

[21] C. Chien, M. Zwolak, M. Ventra, Phys. Rev. A **85**, 041601 (2012).

[22] J. G. E. Harris, R. A. Michniak, S. V. Nguyen, N. Brahms, W. Ketterle, J. M. Doyle, Europhys. Lett. **67**, 198 (2004).

[23] M. Gell-Mann, F. Low, Phys. Rev. **84**, 350 (1951).

[24] Victor Galitski, Lecture notes on "Non-relativistic Quantum Mechanics", (2010).

[25] Jorgen Rammer, "Quantum Field Theory of Non-Equilibrium States", Cambridge University Press, Cambridge (2007).

[26] Alex Kamenev, "Field Theory of Non-Equilibrium Systems", Cambridge University Press, Cambridge (2011).

[27] C. Caroli, R. Combescot, P. Nozieres J. Phys. C **4**, 916 (1971).

[28] T. R. Morris, Int. J. Mod. Phys. A. **9**, 2411 (1994).

[29] D. M. Kennes, S. G. Jakobs, C. Karrasch, V. Meden, Phys. Rev. B **85**, 085113 (2012).

[30] C. Karrasch, M. Pletyukhov, L. Borda, V. Meden, Phys. Rev. B **81**, 125122 (2010).

[31] C. J. Pethick, H. Smith "Bose-Einstein condensation in dilute gases", Cambridge University Press, Cambridge (2008).

[32] A. Polkovnikov, Phys. Rev. A **68**, 053604 (2003).

[33] A. Polkovnikov, Phys. Rev A **68**, 033609 (2003).

[34] C.W. Gardiner, "Handbook of Stochastic Methods", Springer-Verlag, Heidelberg, (1985).

[35] S. Habib, K. Shizume, W. Zurek, Phys. Rev. Let. **80**, 4361 (1998).

[36] M. Naraschewski, Phys. Rev. A **59**, 4595 (1999).

[37] J. A. Stickney, D. Z. Anderson, A. A. Zozulya, Phys. Rev. A **75**, 013608 (2007).

[38] H. Breuer, B. Vacchini, Phys. Rev. E **79**, 041147 (2009).

[39] H. Breuer, Phys. Rev. A **75**, 022103 (2007).

[40] H. Breuer, F. Petruccione, "The Theory of Open Quantum Systems", Oxford University Press, Oxford (2003).

[41] H. Breuer, F. Petruccione, Phys. Rev. E **51**, 4041 (1995).

[42] A. Polkovnikov, Ann. Phys. **325**, 1790 (2003).

[43] K. Mølmer, J. Opt. Soc. Am. B **10**, 524 (1993).

[44] D. B. Percival, Computer Science and Statistics, **10**, 534 (1992).

[45] S. M. Kay, "Efficient Geneartion of Colored Noise". Proc. IEEE, **69**, 480 (1981).

[46] J. N. Franklin, "Numerical Simulation of Stationary and Nonstationary Gaussian Random Processes", SIAM Review, **7**, 68

[47] S. Tomsovic, E. Heller, Phys. Rev. Lett. **67**, 664 (1991).

[48] P. C. Martin, E. D. Sigga, H. A. Rose, Phys. Rev. A **8**, 423 (1973).

[49] J. Kim, B. Friedrich, D.P. Katz, D. Patterson, J. D. Weinstein, R. DeCarvalho, J. M Doyle, Phys. Rev. Lett. **78**, 3665 (1997).

[50] R. B. Diener, Biau Wu, Mark. G. Raizen, Qiau Niu, Phys. Rev. Lett. **89**, 070401 (2002).

[51] T. Karpink, B. Gremand, C. Miniatura, M. Gajda, Phys. Rev. A **86**, 033619 (2012).

[52] D. F. Walls, G. J. Milburn, "Quantum Optics", Springer (2010).

Erklärung:

Ich versichere, dass ich diese Arbeit selbstständig verfasst habe und keine anderen als die angegebenen Quellen und Hilfsmittel benutzt habe.

Heidelberg, den (Datum) .....